NASA Technical Memorandum 104566, Vol. 5

SeaWiFS Technical Report Series

Stanford B. Hooker and
Elaine R. Firestone, Editors

Volume 5, Ocean Optics Protocols for SeaWiFS Validation

James L. Mueller
and Roswell W. Austin

July 1992

NASA

NASA Technical Memorandum 104566, Vol. 5

SeaWiFS Technical Report Series

Stanford B. Hooker, Editor
NASA Goddard Space Flight Center
Greenbelt, Maryland

Elaine R. Firestone, Technical Editor
General Sciences Corporation
Laurel, Maryland

Volume 5, Ocean Optics Protocols for SeaWiFS Validation

James L. Mueller
and Roswell W. Austin
Center for Hydro-Optics and Remote Sensing
San Diego State University
San Diego, California

NASA
National Aeronautics and
Space Administration

Goddard Space Flight Center
Greenbelt, Maryland 20771

1992

PREFACE

The Nimbus-7 Coastal Zone Color Scanner (CZCS) introduced remotely sensed ocean color as a powerful new tool for observing ocean bio-optical properties. Through the early 1980s, CZCS data were exploited by a growing number of scientists studying marine phytoplankton, ocean productivity, and ocean optical properties. Practical applications to marine fisheries were also demonstrated. Unfortunately, a successor ocean color imaging system was not developed before the CZCS ceased operating in mid-1986. At present, therefore, research in these areas is limited to retrospective, albeit productive, investigations of the CZCS historical database. In late 1993, the launch of the Sea-viewing Wide Field-of-view Sensor (SeaWiFS), the next generation ocean color sensor, will bring to the ocean community a welcomed and improved renewal of ocean color time series observations.

The CZCS experiment was unquestionably a scientific success, but it also taught the participants that the satisfactory performance of a satellite remote sensing system cannot be taken for granted. Initially, after launch and periodically throughout its five-year mission, the SeaWiFS system performance, including algorithms, must be independently verified using *in situ* optical measurements of the ocean and atmosphere. It is imperative that these supporting optical measurements meet a uniform standard of quality and accuracy if the primary SeaWiFS goals of 5% accuracy in water-leaving radiance and 35% accuracy in chlorophyll *a* concentration are to be met, or even closely approached. To that end, the National Atmospheric and Space Administration's (NASA) Goddard Space Flight Center (GSFC) SeaWiFS Project convened a workshop to draft protocols and define standards for optical measurements to be used in SeaWiFS radiometric validation and algorithm development, and validation. This document reports the protocols agreed to by the participants, as expanded by the authors, in consultation with the participants and others in the ocean bio-optics community.

The Ocean Optics Protocols for SeaWiFS Validation are intended to provide standards, which if followed carefully and documented appropriately, will assure that any particular set of optical measurements will be acceptable for SeaWiFS validation and algorithm development. It is true that in the case of ship shadow avoidance, for example, there are some circumstances in which acceptable radiometric profiles may be acquired considerably closer to a ship than is specified here (section 5.1.1). When the protocols are not followed in such cases, however, it is incumbent upon the investigator to explicitly demonstrate that the actual error levels are within tolerance. The most straightforward way for an investigator to establish a measurement that is accurate enough to meet the SeaWiFS standards, and is uncontaminated by artifacts such as ship shadow, will be to adhere closely to the protocols.

In general, the specifications and protocols set forth here simply describe and adapt instrument specifications and procedures that are common practice in the ocean optics community. However, protocols in several areas call for significant improvements over today's instruments and practices; these very challenging protocols should, at least for the present, be regarded more as goals than as strict requirements. The motives for adopting these goals as protocols are that the improvements called for are necessary to meet the extremely challenging SeaWiFS accuracy goals, and that the community feels that we can closely approach these standards with a significant but affordable effort. Areas in which new research and development must be done to satisfy challenging protocols are summarized below.

1. Model sensitivity studies and experimental verifications are needed to develop methods for adjusting *in situ* radiometric measurements at a given wavelength to correspond to SeaWiFS measurements at a wavelength as much as 4 nm away, and with a different spectral response function (sections 3.1.1 and 6.1.7).
2. Laboratory research is needed to improve absolute standards of radiance, irradiance, and associated absolute calibration procedures, to achieve or approach 1% internal consistency in the responsivity calibrations of radiometers to be used in SeaWiFS validation experiments (sections 4.2.2 and 4.2.3).
3. Radiometric linearity test procedures must be improved to extend linearity characterizations over the full operating dynamic ranges (Table 4) of the various irradiance and radiance sensors (section 4.1.7). This is especially critical for downwelling irradiance measurements at the sea surface, where

irradiances of laboratory irradiance standards are only 2–15%, depending on wavelength, of saturation irradiance.

4. Instrument self-shading effects are a significant, but probably correctable, source of error (sections 3.1.8 and 5.1.6). The maximum diameter of a radiometer for which self-shading error can be corrected to within less than 5% varies with the absorption coefficient and, therefore, as a function of wavelength and water mass, and of solar zenith angle. For oligotrophic to moderately turbid coastal water masses, wavelengths less than 600 nm and solar zenith angles greater than 30°, upwelled irradiance and radiance data from many of the currently popular radiometers, having diameters of 20–40 cm, can be adequately corrected. In more general conditions, however, new instruments must be developed to minimize self-shading effects, particularly for near-infrared wavelengths and in Case 2 waters. Furthermore, candidate correction models must be verified experimentally.
5. Measurements following the stringent protocols for avoiding ship shadows and reflections will require exclusive use of profiling radiometer configurations which are not in wide use today (section 5.1.1). Tethered free-fall systems appear to offer the most economical approach to meeting these requirements. More sophisticated and expensive approaches include optical systems on either remotely operated vehicles (ROV), or on small surface platforms with self-contained winches.
6. Quantitative characterization of polarization sensitivity is critical for any airborne radiometer to be used for SeaWiFS radiometric validation, or algorithm development and validation. Protocols and procedures for polarization sensitivity characterization must be developed in more specific detail than we were able to do here because of time constraints (sections 3.3 and 4.3).
7. The accuracies specified here for cosine responses of irradiance collectors are significantly better than is typically realized in commercially available radiometers (section 3.1.5). Moreover, the specified accuracies may challenge the precision of the laboratory procedures used to characterize an instrument's cosine response (section 4.1.5). Error in cosine response almost directly translates to an equivalent error in downwelling irradiance for the clear-skies case so critical to SeaWiFS validation. Therefore, a significant effort to carefully characterize the effect, and to work with instrument manufacturers to approach or achieve the specified accuracies, is an important factor in our strategy for reducing the overall error budget for water-leaving radiance measurements to less than 5%.
8. The use of a portable standard to trace a radiometer's performance stability during the course of a field deployment is called for in the present protocols (section 4.2.5). Several manufacturers offer reasonably portable radiometric sources, which may be suitable for this purpose, but laboratory and field evaluations must be carried out to prove their suitability and develop detailed procedures for their use in the field.
9. The present protocols for deploying and analyzing data from moored and free-drifting optical systems are tentative, preliminary, and incomplete. Although moored and drifting optical systems have been used successfully in several oceanographic experiments, there are no previous examples of their use for ocean color remote sensing algorithm development, or for radiometric validation of airborne or satellite radiometers. New moored and drifting optical systems are currently being developed and tested, in preparation for applications to SeaWiFS validation. As results from these efforts become available, new and detailed protocols for making these measurements will be developed and distributed.

The protocols and recommendations in this document attempt to represent and consolidate the contributions of the workshop participants, and of many others who participated in the review process. The final document has, by necessity however, been interpreted and written by us and we accept full responsibility for any remaining mistakes and misrepresentations. As can be readily deduced from the above list of critically needed improvements, this document represents only a first attempt to establish protocols for ocean optical measurements. It will be appropriate to develop and issue a revised set of protocols, reflecting our collective experience in pre-launch algorithm development activity, just prior to the scheduled SeaWiFS launch.

San Diego, California
March 1992

—J. L. M. and R. W. A.

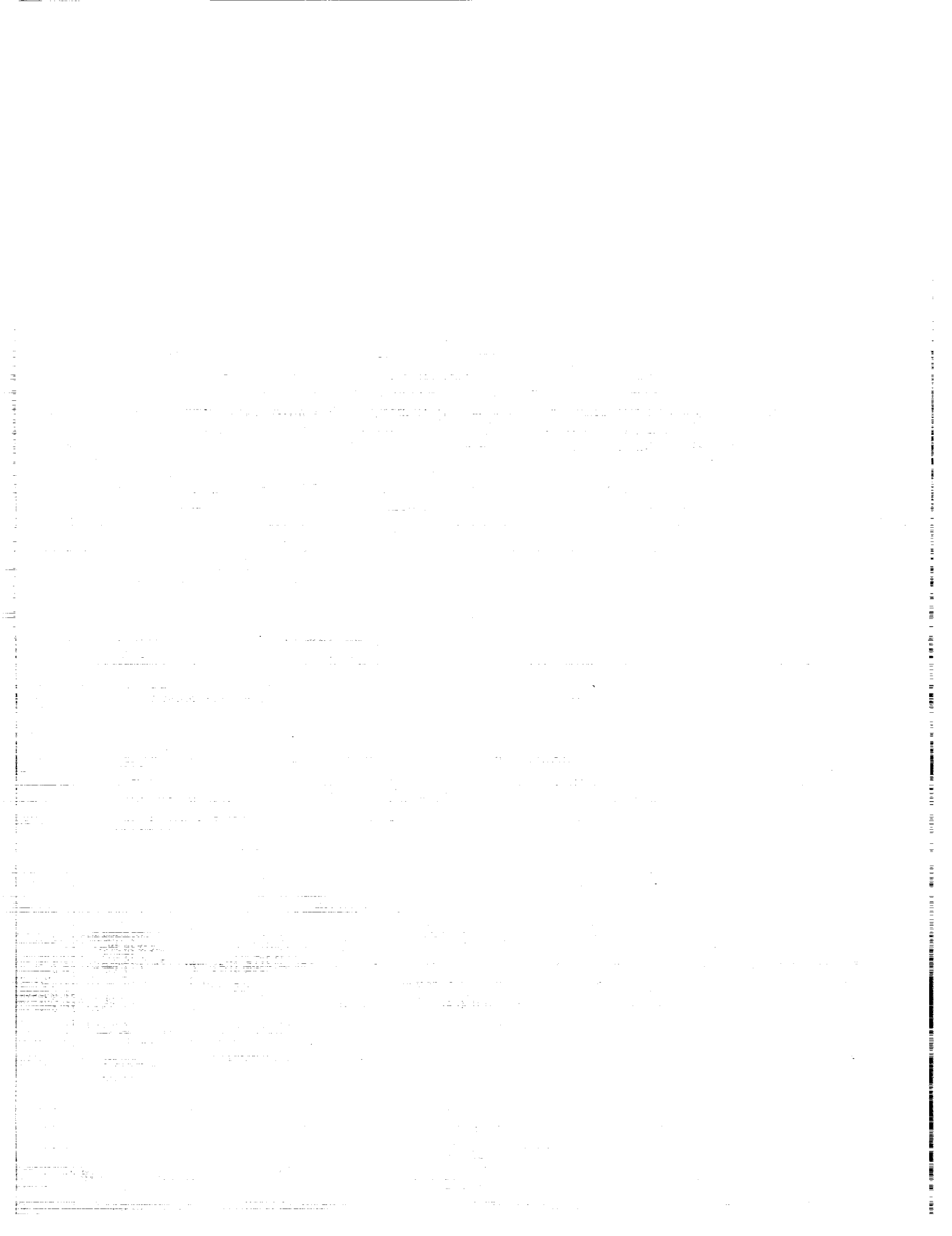

ABSTRACT

This report presents protocols for measuring optical properties, and other environmental variables, to validate the radiometric performance of the Sea-viewing Wide Field-of-view Sensor (SeaWiFS), and to develop and validate bio-optical algorithms for use with SeaWiFS data. The protocols are intended to establish foundations for a measurement strategy to verify the challenging SeaWiFS accuracy goals of 5% in water-leaving radiances and 35% in chlorophyll *a* concentration. The protocols first specify the variables which must be measured, and briefly review rationale. Subsequent chapters cover detailed protocols for instrument performance specifications, characterizing and calibrating instruments, methods of making measurements in the field, and methods of data analysis. These protocols were developed at a workshop sponsored by the SeaWiFS Project Office (SPO) and held at the Naval Postgraduate School in Monterey, California (9–12 April, 1991). This report is the proceedings of that workshop, as interpreted and expanded by the authors and reviewed by workshop participants and other members of the bio-optical research community. The protocols are a first prescription to approach unprecedented measurement accuracies implied by the SeaWiFS goals, and research and development are needed to improve the state-of-the-art in specific areas. The protocols should be periodically revised to reflect technical advances during the SeaWiFS Project cycle.

1. INTRODUCTION

The National Aeronautics and Space Administration's (NASA) SeaWiFS Prelaunch Science Working Group (SPSWG) has recommended baseline satellite ocean color products consisting of normalized water-leaving radiance (L_{WN}) at five wavelengths, aerosol radiance at three wavelengths, chlorophyll *a* concentration, chlorophyll-like pigment (chlorophyll *a* plus phaeopigment *a*) concentration, the diffuse attenuation coefficient at 490 nm, $K(490)$, and calibrated radiances observed at the satellite. The primary SPSWG goals for product accuracy are derived water-leaving radiances to within 5% and chlorophyll *a* concentration to within 35% in Case 1 waters, both globally and throughout a five-year mission. These goals have been accepted by NASA, who has the responsibility to lead a product assurance, calibration, and validation program which will determine how well the commercially procured ocean color data fulfills the contractually stated NASA requirements.

This report specifies the type and quality of supporting *in situ* optical measurements and analytical protocols needed to develop bio-optical algorithms and validate the SeaWiFS calibration. The observations and data will necessarily accrue over several years from a variety of sources, using different instruments and techniques. To be useful, the data must be internally consistent, of known and documented accuracy, and in a readily accessible form.

A workshop was conducted to draft protocols, standards, and sampling strategies for optical measurements to be used for SeaWiFS algorithm development and system validation. Also addressed were procedures for obtaining biogeochemical observations to validate chlorophyll *a* concentrations derived from SeaWiFS data. The findings and recommendations of the workshop are presented here. Although immediate concerns have focused this document on preparations for the SeaWiFS mission, the capabilities of the Japanese Ocean Color Temperature Sensor (OCTS), the Moderate Resolution Imaging Spectrometer (MODIS), Medium Resolution Imaging Spectrometer (MERIS), the German Reflecting Optics System Imaging Spectrometer (ROSIS), and other potential ocean color sensors are also recognized, with the intent of developing databases relevant to future needs.

The key objective of the working group was to recommend protocols and standards for supporting *in situ* optical measurements that will define:

1. The required and useful optical parameters for validation of SeaWiFS normalized water-leaving radiances and atmospheric correction algorithms, and for monitoring the satellite sensor's calibration and stability.
2. The measurement requirements and standards, including definitions of quantities, wavelengths, sensitivity, accuracy and stability, field-of-view (FOV) and band specifications.
3. The instrument characterization, intercalibration, and related protocols, including:

   a) laboratory calibration and characterization measurements, accuracies and procedures to be applied to instruments used in SeaWiFS validation and algorithm development activities;

   b) pre- and post-deployment measurements and procedures for moored instruments; and

   c) procedures for instrument calibration and characterization, and requirements for record keeping and traceability, including intercalibrations of radiometric and optical standards between participating laboratories.

4. The at-sea optical sampling strategy and protocols, including such considerations as:

   a) the rationale and justifications for moored, underway, drifting, shipboard, and airborne measurements;

   b) depth resolution in optical profiles, total sampling depths, and ship shadow avoidance; and

   c) time of day, sky conditions, season, and geographic considerations.

5. The analysis approaches to be used, including the procedures and methodologies recommended for generating variables from the *in situ* observations, e.g., $L_{WN}(z)$ from $L_u(z)$, $K(z)$, remote sensing reflectance, etc., and error analysis.
6. The protocols for obtaining ancillary measurements, data archiving, database population, and access to the data.
7. The atmospheric measurements and the degree to which standard methodologies are available.

Development and validation of bio-optical algorithms for SeaWiFS will be addressed by a separate working group, thus, these topics are briefly examined in this report. Nonetheless, the SPSWG was charged with identifying data requirements and sampling strategies for bio-optical support measurements in the context of the optical and radiometric measurements, including:

1. Discrete chlorophyll a and pigment concentrations will be measured using the U.S. Joint Global Ocean Flux Study (JGOFS) program's protocols and standards for high performance liquid chromatography (HPLC) pigment sampling and analysis, which are adopted by reference to *JGOFS Core Measurement Protocols*, Chapter 9, "Pigments and Chlorophyll."
2. The roles of underway, moored, and discrete chlorophyll a fluorescence, and its calibration for satellite data product validation.
3. Other biogeochemical quantities, e.g., coccoliths, detritus, suspended sediment, and colored dissolved organic material (CDOM), needed for the baseline products and the extent to which standards and protocols have been defined for them.

This report is complementary to anticipated reports of U.S. and International JGOFS working groups, which are concurrently evaluating bio-optical needs and sampling strategies for their respective science programs.

1.1 Sensor Calibration

The SPO must make every effort to track the sensor's performance throughout the duration of the mission. Since the instrument will be designed for a five-year mission, it is certain that the sensor calibration at each wavelength will change in some unpredictable manner as a function of time. Experience with the CZCS has shown it is very difficult to determine a sensor's calibration once it has been launched (Viollier 1982, Gordon et al. 1983, Hovis et al. 1985, Mueller 1985, and Gordon 1987). Similar problems have been encountered with other Earth observing systems, such as, the National Oceanic and Atmospheric Administration's (NOAA) Advanced Very High Resolution Radiometer (AVHRR) (Brown and Evans 1985, Weinreb et al. 1990). Because of the large atmospheric contribution to the total observed radiances (Gordon 1981) and the great sensitivity of the bio-optical algorithms to the estimated water-leaving radiances (Clark 1981), small errors in the calibration can induce sizable errors in derived geophysical products, rendering them useless for many applications.

By processing large quantities of so-called "clear water" imagery, pigment concentrations less than 0.25 mg m^{-3}, (Gordon and Clark 1981), Evans (unpub.) was able to develop a *vicarious* calibration that was used in the global processing of the entire CZCS data set (Esaias et al. 1986, Feldman et al. 1989). However, the approach requires assumptions that may limit the scientific utility of ocean color imagery. Specifically, the normalized clear water-leaving radiances, $L_{WN}(443)$, $L_{WN}(520)$, and $L_{WN}(550)$, were assumed to be 1.40, 0.48, and 0.30 mW cm^{-2} μm^{-1} sr^{-1}, respectively. The Ångström exponents were assumed to be zero and certain geographical regions such as the Sargasso Sea were assumed to be clear water sites at all times. Under these assumptions, analyses of the derived (L_{WN}) values were used to calculate calibration adjustment coefficients to bring CZCS derived (L_{WN}) values into agreement for these regions. The vicarious calibration of the 443 nm band is tenuous because of the great variability in $L_{WN}(443)$ even in clear water. Additionally, certain command and engineering data from the Nimbus-7 platform were not archived, so that a detailed analysis of possible effects related to the spacecraft environment and operation on the calibration could not be performed.

Unlike the CZCS, SeaWiFS will routinely produce geophysical fields in a near real-time, operational mode for distribution to the science community. This aspect of the mission necessitates constant evaluation of the sensor performance and the derived products. Therefore, a multifaceted approach to address the problem of sensitivity degradation and sensor characterization is required during both the prelaunch and post-launch phases. The goal is to ensure that SeaWiFS level-1 radiances are accurately known and meet the specifications of the SPSWG.

The plan includes both onboard and vicarious calibration approaches. SeaWiFS will have a solar measuring diffuser plate to reference the response to the sun (Gordon 1981) and also will be capable of periodically imaging the moon by maneuvering the spacecraft. The vicarious calibration program will incorporate measurements of water-leaving radiances and other related quantities, from ships, drifting buoys, and fixed moorings, to develop time

series and geographically diverse samples of oceanic and atmospheric data sets. Each approach has advantages and disadvantages, but when combined, provide a complementary and comprehensive data set that will be sufficient to monitor short-term changes and long-term trends in the sensor's performance.

1.2 Bio-Optical Algorithms

The SPO will be responsible for producing a standard set of derived products and will produce both *CZCS-type* products and *baseline* products. The CZCS-type products will consist of pigment concentration, $K(490)$, five normalized water-leaving radiances, and three aerosol radiances based on constant default wavelength dependence (epsilon) coefficients in aerosol corrections. The proposed baseline products will include five normalized water-leaving radiances, $K(490)$, chlorophyll *a* concentration, three aerosol radiances, and one or more error analysis products.

The basic quantities to be computed from the sensor radiances are the water-leaving radiances, from which all other derived products, except the aerosol radiances, are computed. Every effort must be made to ensure these radiances meet the specifications of the SPSWG, i.e., ±5% in Case 1 waters. This requires the atmospheric correction algorithms be considerably more sophisticated than the current CZCS algorithms.

The baseline bio-optical products must meet the accuracy requirements established by the SPSWG over a variety of water masses. The current CZCS algorithms were based on a data set consisting of fewer than 50 data points (only 14 observations were available for the band-2-to-band-3 ratio algorithm) and performed poorly in regions of high chlorophyll *a* concentration, high suspended sediment concentration, high colored dissolved organic material concentration, and coccolithophorid blooms (Groom and Holligan 1987). Accurate estimates of the baseline products are essential if SeaWiFS is to be useful in programs such as the Global Ocean Flux program [National Academy of Science (NAS) 1984]. SeaWiFS will have the capability, due to improvements in the signal-to-noise ratio (SNR), digitization, dynamic range, and wavelength selection, to increase the accuracy of these products and to flag areas where anomalies or low confidence conditions exist. Clearly, a much larger database will be needed for developing a broader variety of bio-optical algorithms, some of which will be region specific. Therefore, the radiometric, optical, and chemical field observations used in deriving the bio-optical algorithms and for the satellite vicarious calibration must conform to stringent requirements with respect to instrument calibration and characterization, and to observation protocols specified to take advantage of SeaWiFS capabilities.

The SPO will manage a program to compare the various atmospheric correction and bio-optical algorithms proposed by the science community. The purpose of this program is to independently evaluate suggested improvements or additions to the SeaWiFS products. This component of the calibration and algorithm development program will run in parallel with, but off-line from, operational processing and will provide an essential mechanism for incorporating data and analyses from the community at large.

1.3 Community Participation

The SPO will rely on the oceanographic community to perform field research for atmospheric and bio-optical algorithm development, and for all of the *in situ* data collection for the vicarious sensor calibration. A minimal subset of these observations will be sponsored by the SPO, but many projects sponsored by NASA's Research and Application Program and other agencies are expected to make major contributions to the global five-year effort. This requires close coordination of these programs and a clear definition of the observations, accuracies, and data collection protocols that are required for each type of activity. The purpose of this document is to clarify these requirements.

1.4 Vicarious Calibration

For ocean observations, it is easy to show (Gordon 1987 and 1988) that satellite sensor calibration requirements based on the quality of the existing CZCS pigment algorithms exceed currently available capabilities. In addition, the sensor calibration is unlikely to remain unchanged through launch and five years of operation in orbit. The only foreseeable way of approaching the ocean calibration needs is through vicarious calibration, i.e., fine tuning the calibration in orbit.

The methodology used to achieve vicarious calibration for CZCS was described in detail by Gordon (1987). First, the calibration was initialized after launch by forcing agreement between the sensor determined radiance and the expected radiance based on radiometric measurements made at the surface under clear atmospheric conditions. Next, since the CZCS responsivity was observed to be time dependent, the algorithms were applied to other scenes characterized by bio-optical surface measurements and more typical atmospheres, and the calibration was adjusted until the measured water-leaving radiances were reproduced. Finally, the surface measurements of pigments were combined with satellite pigment estimates for a wide variety of atmospheric conditions, and the radiance calibration fine tuned until the best agreement was obtained between the retrieved and true pigments.

The CZCS vicarious calibration was not radiometric. Rather, it was a calibration of the entire system—sensor plus algorithms. To predict the radiance measured at the satellite, L_t, the water-leaving radiance, the aerosol optical thickness, and the aerosol phase function are all required. Also needed are ancillary data such as the surface pressure, the wind speed, and the ozone optical thickness.

These data for vicarious calibration and validation are to be obtained by measuring the upwelling radiance distribution just beneath the surface, along with the aerosol optical thickness and the sky radiance, at the time of the satellite overpass. The sky radiance will be used to deduce the required information about the aerosol phase function (Voss and Zibordi 1989). The data set will be used to deduce L_t, at the top of the atmosphere, coincident with a SeaWiFS overpass from which the calibration will be initialized. This exercise is essential for calibrating the SeaWiFS system, i.e., sensor plus algorithms, and cannot be effected without a high quality surface data set obtained simultaneously with the satellite imagery.

2. DATA REQUIREMENTS

The prime objective of in-water optical measurements for SeaWiFS is to derive accurate normalized water-leaving radiances that will be used both for direct validation comparisons with those derived from SeaWiFS data, and to develop and validate in-water bio-optical algorithms. Therefore, a comprehensive field program to measure optical and biogeochemical state variables will be required.

The required and useful variables to be measured for SeaWiFS validation are listed in Table 1 for radiometric initialization and ongoing validation, and for bio-optical algorithm development and validation.

2.1 Initialization and Calibration

Surface incident spectral irradiance $E_d(0^-, \lambda)$, downwelled spectral irradiance $E_d(z, \lambda)$, and upwelled spectral radiance $L_u(z, \lambda)$ are the fundamental measurables needed to derive normalized water-leaving radiances in most circumstances. Other ambient properties, like sky radiance, sea state, wind velocity, etc., are also useful initialization and calibration measurements and are discussed below.

Surface incident spectral irradiance $E_d(0^-, \lambda)$ is usually derived from surface irradiance, $E_s(\lambda)$, measured on a ship well above the water, but use of a radiometer floated just beneath the surface ($z = 0^-$) may provide a better approach (sections 3.2.1 and 5.1.4). $E_d(0^-, \lambda)$ varies due to fluctuations in cloud cover and aerosols, and with time of day, i.e., solar zenith angle. Profiles of $E_d(z, \lambda)$ and $L_u(z, \lambda)$ must be normalized to account for such variabilities during a cast.

Downwelled spectral irradiance $E_d(z, \lambda)$ is required to compute the diffuse attenuation coefficient, $K(z, \lambda)$, which in turn, is needed for diffuse attenuation coefficient algorithm development (Austin and Petzold 1981), and for optically weighting the pigment concentrations to be estimated from remotely sensed ocean color (Gordon and Clark 1981). $E_d(z, \lambda)$ is also required to compute remote sensing reflectance $R_L(z, \lambda)$, which is used to normalize $L_u(z, \lambda)$ when developing and validating bio-optical algorithms. The need for this normalization arises because the spectrum of incident irradiance varies with changing solar zenith angle and atmospheric conditions. $E_d(0^-, \lambda)$ can then be used, through $R_L(z, \lambda)$, to convert $L_u(0^-, \lambda)$ measured under a given set of illumination conditions, e.g., overcast to normalized water-leaving radiance $L_{WN}(\lambda)$ that will be measured under the restricted illumination and viewing conditions which are associated with SeaWiFS measurements. As with $L_u(0^-, \lambda)$, $E_d(0^-, \lambda)$ must be determined by extrapolation from a profile of $E_d(z, \lambda)$ over the upper few optical depths and reconciled with direct surface measurement of $E_s(\lambda)$. [Optical depth, $\tau(z, \lambda)$, in the context of this report is the integral of $K(z, \lambda)$, for either radiance or irradiance, depending on the context, from the surface to a given depth z.]

Upwelled spectral radiance $L_u(0^-, \lambda)$ is the in-water variable which, when propagated upward through the sea surface leads to the *"measured"* value of $L_W(\lambda)$. $L_W(\lambda)$ is in turn adjusted using $E_d(\lambda)$, to derive normalized water-leaving radiance, $L_{WN}(\lambda)$, for a clear-sky zenith sun at mean Earth-sun distance. Unfortunately, it is not practical to measure $L_u(0^-, \lambda)$ precisely at an infinitesimal depth below the surface. Therefore, the profile of $L_u(z, \lambda)$ must be measured over the upper few optical depths with sufficient accuracy to determine $K_L(z, \lambda)$ for $L_u(z, \lambda)$ and to propagate $L_u(z, \lambda)$ to the surface. At near-infrared wavelengths, the first optical depth is confined to the upper few tens of centimeters. Determination of $L_u(0^-, \lambda)$ in this situation is more challenging and will require special instruments and experiment designs to accommodate the effects of instrument self-shading, wave focusing, small-scale variability, possible fluorescence, Raman scattering and extremely small working volumes. Careful measurements of inherent optical properties, including $a(z, \lambda)$, $c(z, \lambda)$, and $b_b(z, \lambda)$, and spectral fluorescence may be useful, in addition to $E_d(z, \lambda)$ and $L_u(z, \lambda)$ measurements made with specially designed radiometers.

Sky radiance, is required to enable estimation of the aerosol phase function through inversion of the radiative transfer equation. It is also useful for estimating the mean cosine of the transmitted light field in the water. The sky radiance should be measured directly; however, for the latter application it need only be estimated by occulting the sun's image on a deck cell measuring the incident spectral radiance from the sun and sky. The mean cosine at the surface can be used with profile measurements of $E_d(\lambda)$, $E_u(\lambda)$ and $c(\lambda)$ to estimate $b_b(\lambda)$ (Gordon 1991). An ability to exploit this and similar relationships will greatly enhance both development and verification of bio-optical algorithms. The spectral sky radiance distribution over zenith and azimuth angles is required to determine the aerosol scattering phase functions at radiometric comparison stations during the system initialization cruises and will be very useful if measured at all validation stations throughout the mission.

Upwelled radiance distribution measurements just beneath the sea surface will be required for quantifying the

Table 1. Required observations for initialization and system calibration for satellite product verification and radiative transfer (also ongoing calibration and atmospheric algorithm validation studies) and bio-optical algorithm development and validation.

	Product Verification	Radiative Transfer	Bio-optical Algorithms
Primary Optical Measurements			
Incident Spectral Irradiance, $E_d(0^-, \lambda)$	×	×	×
Downwelled Spectral Irradiance, $E_d(z, \lambda)$	×	×	×
Upwelled Spectral Irradiance, $L_u(z, \lambda)$	×	×	×
Spectral Solar Atmospheric Transmission, $\tau_s(\lambda)$	×	×	×
Submerged Upwelled Radiance Distribution, $L(z, \theta, \phi)$	×	×	×
Spectral Sky Radiance Distribution	×	×	×
Upwelled Spectral Irradiance, $E_u(z, \lambda)$		×	×
Calculated or Derived Variables			
Water-leaving Radiance, $L_W(0^-, \lambda)$	×	×	×
Attenuation Coefficient Downwelled Irradiance, $K_E(z, \lambda)$	×	×	×
Attenuation Coefficient Upwelled Radiance, $K_L(z, \lambda)$	×	×	×
Spectral Reflectance, $R_L(z, \lambda)$	×	×	×
Ambient Properties			
Sea and Sky State Photographs	×	×	×
Wind Velocity	×	×	×
In situ Fluorescence Profiles		×	×
Aerosol Samples		×	×
Temperature and Salinity Profiles			×
Secchi Depth			×
Primary Biogeochemical Measurements			
Phytoplankton Pigments (HPLC Technique)		×	×
Phytoplankton Pigments (Fluorometric Technique)		×	×
Total Suspended Material (TSM) Concentration		×	×
Colored Dissolved Organic Material (CDOM)		×	×
Inherent Optical Properties			
Spectral Beam Attenuation Coefficient, $c(z, \lambda)$		×	×
Spectral Absorption Coefficient, $a(z, \lambda)$		×	×
Spectral Backscattering Coefficient, $b_b(z, \lambda)$		×	×
Spectral Volume Scattering Function, $\beta(z, \lambda, \theta)$		×	×
Red Beam Attenuation, $c(z, 660\ \text{nm})$		×	×
Algorithm Specific Research Measurements			
Airborne Fluorescence and Radiances		×	×
Coccolith Concentration			×
Detritus Absorption Coefficient		×	×
Humic and Fulvic Acids			×
Inorganic Suspended Material			×
Organic Suspended Material			×
Particle Absorption Coefficient		×	×
Particle Fluorescence			×
Particle Size Spectra		×	×
Particulate Organic Carbon (POC)			×
Particulate Organic Nitrogen (PON)			×
Phycobilipigments Concentration			×
Phytoplankton Species Counts			×
Primary Productivity (^{14}C)			×
Total Dissolved Organic Carbon (DOC)			×

× = Needed for the indicated effort.

angular distribution of water-leaving radiance at stations used for system calibration initialization and long-term system characterization. These measurements will also be useful in relating radiance and irradiance reflectance, and K profiles, to inherent optical properties and biogeochemical substances, e.g., chlorophyll a and colored dissolved organic material, during bio-optical algorithm development and validation.

Atmospheric transmittance spectra should be measured using a sun photometer in order to determine aerosol optical depths at each station. These data are particularly needed to verify the atmospheric corrections in direct comparisons between SeaWiFS $L_W(\lambda)$ estimates and those determined from in-water $L_u(0^-, \lambda)$.

Sea state photographs are required to document surface wave conditions during radiometric measurements. This information is essential for identifying measurements made under questionable environmental conditions.

Wind velocity is required to generate through models, estimates of the surface wave slope distribution, which will be used to calculate reflected skylight and sun glint in radiative transfer models (Cox and Munk 1954). Surface wave models driven by wind velocity may also be used to provide quantitative estimates of surface wave induced radiometric fluctuations. Qualitatively, wind velocity, and photographs or videotape recordings, of sea state will be useful for assessing station data quality.

Upwelled spectral irradiance $E_u(z, \lambda)$ is a useful measurement, in addition to E_d and Lu because there exist both empirical and theoretical relationships between inherent optical properties, phytoplankton pigments, total suspended matter, and irradiance reflectance. $L_u(0^-, \lambda)$ and $E_u(0^-, \lambda)$ are related by the factor $Q(\lambda)$, which is not well determined at present. Combined measurements of $L_u(0^-, \lambda)$ and $E_u(0^-, \lambda)$ will be extremely useful in determining $Q(\lambda)$, which will in turn, allow traceability of SeaWiFS measurements to previously derived irradiance reflectance relationships and algorithms.

Inherent optical properties, including spectral volume absorption, spectral beam attenuation, spectral backscattering, and integral moments of the volume scattering function will be useful, but not required, aids to relating normalized water-leaving radiances to chlorophyll a and other bio-optical variables. Eventually, a sufficiently complete description of inherent optical properties may provide a set of physically based bio-optical algorithms and models of water-leaving radiance. In particular, measurements of inherent optical properties may be valuable in modeling upwelled radiance spectra at near-infrared wavelengths, where the remote sensing optical depth is confined to the upper few tens of centimeters, a region where direct measurements of $L_u(0^-, \lambda)$ are especially difficult.

Red beam attenuation coefficient, $c(660)$, and *in situ* chlorophyll a fluorescence measurements are exceptionally useful in analyzing profiles of $E_d(z)$, $L_u(z)$, and $E_u(z)$ to derive profiles of $K_d(z)$, $K_L(z)$ and $K_u(z)$, respectively. If these profiles are viewed in real time, they are also useful guides for taking water samples at depths that allow the vertical structure of chlorophyll a and suspended particles to be accurately resolved in the top optical depth. Finally, the chlorophyll a fluorescence profile is used to interpolate HPLC and extracted fluorescence measurement of chlorophyll a concentrations from water samples at discrete depths. It is desirable to make these measurements simultaneously with irradiance and radiance profiles, only if it can be done in a way to avoid self-shading of the instrument (section 5.1.6).

Secchi depth measurements are required for real-time assessment of water transparency during a station and as a quality check during analysis of radiometric profiles.

Aerosol concentration samples using high volume techniques will be useful, in conjunction with aerosol optical depth spectra determined from sun photometer measurements, for chemical, size, and absorption characterization of aerosols, especially in studies of the effects of Saharan and Asian dust clouds on atmospheric corrections.

2.2 Biogeochemical Properties

Pigment concentrations will be determined, using the HPLC method and standards adopted by the JGOFS program, to develop and validate chlorophyll a algorithms and assess the effects of accessory pigment concentrations on water-leaving spectral radiances. These data will also be used to calibrate continuous profiles of chlorophyll a fluorescence (section 2.1). Phytoplankton pigment concentration will also be determined using classical chlorophyll a and phaeopigment fluorescence techniques that were used for CZCS pigment validation and algorithm development. The HPLC technique provides more accurate and precise information for a greater number of pigments, but gives different values than does the fluorescence method for various species compositions and chlorophyll a to phaeopigment ratios. While the HPLC method is the primary pigment technique required for SeaWiFS, the classical technique is still required to allow the CZCS and SeaWiFS data sets and algorithms to be compared.

Phycobilipigments, common in some cyanobacteria and prymnesiophytes, are treated separately from the HPLC fat soluble pigments. The concentration of these water soluble pigments is important due to the contribution of solar stimulated phycoerythrin fluorescence to the underwater light field and also to characterize the phytoplankton population. Phycobilipigment species at times, account for a major fraction of the primary productivity, especially at high latitudes and in oligotrophic waters, and have been difficult to quantify due to their small size. These measurements are not required, because SeaWiFS does not contain bands at their absorption or fluorescence peaks, but they are desireable, since several aircraft sensors do, e.g., the Airborne Visible/Infrared Imaging Spectrometer (AVIRIS), Airborne Oceanographic Lidar (AOL), the Mul-

tispectral Airborne Radiometer System (MARS), and future satellite sensors, e.g., the Moderate Resolution Imaging Spectrometer (MODIS) and the Medium Resolution Imaging Spectrometer (MERIS).

Total suspended material (TSM) measurements are required to assess the effect of suspended sediment on the derived products. TSM is of primary importance in coastal waters, where simple radiance ratio algorithms for TSM have accuracies equivalent to, or better than, those for estimating chlorophyll-like pigment concentration. Organic suspended matter and inorganic suspended matter concentrations are subfractions of TSM; this partitioning of TSM is particularly useful in process studies.

Particulates, both particulate organic carbon (POC) and particulate organic nitrogen (PON), are required for process studies to help characterize the adaptive state of phytoplankton and to inventory critical biogeochemical elements.

Dissolved organic carbon (DOC) has been shown to be a major oceanic carbon pool due, in part, to improvements in measuring techniques. Quantification of the transformations of this pool is crucial to understanding the marine carbon cycle. The colored fraction, CDOM, of the DOC is highly absorbent in the blue range, thus decreasing blue water-leaving radiances, and it must be taken into consideration for pigment concentration algorithms. DOC measurements are needed to develop robust relationships between CDOM and DOC, to evaluate the usefulness of ocean color observations for estimating DOC concentrations.

CDOM concentrations are required to assess the effect of Gelbstoff on blue water-leaving radiances and chlorophyll concentration. This is of primary importance in Case 2 waters, but is also relevant to phytoplankton degradation products.

Humic and fulvic acids comprise the bulk of CDOM and have different specific spectral absorption coefficients. Their concentrations are useful for determining the correction used for phytoplankton pigment concentration algorithms in Case 2 waters and for estimating CDOM from ocean color observations.

Coccolith concentration, the number density of small plates of calcium carbonate, which are produced in copious amounts by marine phytoplankton called coccolithophores, is very important to light scattering. Scattering by coccoliths is highly apparent in visible wavelength satellite imagery, because they perturb the usual relationships between water-leaving radiances and chlorophyll *a* concentration and adversely impact atmospheric corrections. Additionally, coccolith formation, sinking, and dissolution are significant factors in the ocean carbon flux budget. It is therefore necessary to measure coccolith concentration, both as number density and calcium carbonate concentration, to aid in 1) the correction of chlorophyll *a* concentration algorithms, 2) coccolith algorithm development, and 3) atmospheric correction development and validation.

Particle absorption coefficient, comprised of absorption by living, dead, and inorganic particles, is a useful variable for modeling the portion of solar energy that is absorbed by phytoplankton and bacteria.

Detritus absorption coefficient, that is, absorption of light by detritus, represents a major loss of light which would otherwise be available to the phytoplankton component of the marine hydrosol. In many cases, absorption by detritus is a significant term in the marine radiative transfer processes, and its determination is useful for phytoplankton production models and modeling the light field.

Particle size spectra are very useful for in-water radiative transfer calculations particularly if measurements include particles smaller than 1 μm.

Particle fluorescence, derived for particle scattering to fluorescence ratios using laser sources on single cell flow systems, is also very useful for evaluating the population structure of the plankton.

Phytoplankton species counts are important because species-to-species variability in optical and physiological properties represents a major source of variability in bio-optical algorithms and primary productivity models. This has been recognized, but it is generally ignored in remote sensing algorithms due to the tedious nature of species enumeration, the small sizes of many species, and the large number of species involved. However, this information at various levels of rigor is useful in evaluating the population and pigment composition. This is especially important for some groups, such as coccolithophores.

Primary productivity, ^{14}C, is not strictly required for validation of water-leaving radiances or system initialization. Furthermore, primary productivity is not a standard derived SeaWiFS product, owing to the complexity of relating ocean color to production. However, it will be extremely useful for process study applications of ocean color data if these measurements are made at the same time that the water column optical properties are determined. These data will aid in development of models of primary production using satellite ocean color observations, a goal which is central to the overall SeaWiFS science mission. Of special importance are determinations of key photo-physiological parameters derived from production measurements as functions of irradiance. If ^{14}C productivity measurements are made, they should conform to the *JGOFS Core Measurements Protocols* (JGOFS 1991).

2.3 Airborne Spectral Radiometry

Radiance measurements from aircraft can augment in-water measurements of $L_u(z, \lambda)$, made to compare directly with SeaWiFS measurements for validation of its radiometric performance and algorithms. Radiance measurements from aircraft can, if they are accurately made, contribute an additional useful constraint in defining internally consistent sun-ocean-atmosphere-sensor models that will comprise the essence of SeaWiFS radiometric valida-

tion. For this application, aircraft radiometers must meet the SeaWiFS specifications for radiometric accuracy, SNR, spectral resolution at a spatial resolution that will permit direct comparisons with in-water measurements, and through spatial averaging with SeaWiFS measurements. Conversely, aircraft radiance measurements made with less accuracy than the SeaWiFS prelaunch specifications would introduce an unacceptable error source into the validation models and cannot be used for this purpose.

Airborne ocean color data may also be used to determine spatial variability in ocean optical properties during shipboard algorithm development and validation experiments. In this context, airborne ocean color measurements will be especially valuable in productive Case 1 and Case 2 waters, where variability in ocean optical properties can be large over mesoscale and smaller distances. Synoptic maps of ocean color distributions can obviously guide sampling by ships. It can also be used to place in-water data from an individual station in context with respect to nearby variability, and thus provide a basis for spatial interpolation and averaging when comparing in-water bio-optical measurements with SeaWiFS image data. This application can be accomplished using aircraft radiometers meeting somewhat less stringent performance specifications than is demanded for direct validation comparison between SeaWiFS and aircraft radiance measurements.

Airborne measurements of fluorescence by CDOM, chlorophyll and phycoerythrin, both by laser and solar excitation, are useful to evaluate spatial and temporal variability near ship and mooring stations and to provide independent assessments of bio-optical algorithms.

2.4 Ancillary Measurements

Hydrographic data, water temperature (T), and salinity (S), derived from conductivity, temperature, and depth (CTD) profiles, are useful for characterizing the physical water mass regime in which an optical profile is measured. A T-S characterization is especially important near ocean fronts and eddies, where interleaving water masses of very different biogeochemical composition, and therefore fundamentally different bio-optical properties, can produce complex spatial and temporal patterns of near-surface optical properties. In these circumstances, T-S profiles can provide an indication of whether a station location is suitable for reliable remote sensing validation and algorithm development comparisons.

2.5 Optical Moorings

Optical moorings will be maintained in one or more regions of low optical variability to provide long-term time series comparisons between *in situ* and SeaWiFS measurements of normalized water-leaving radiance. Moored optical systems will also be extremely useful in a variety of oceanographic studies. For example, global satellite observations of ocean pigment biomass and estimates of phytoplankton production are essential to achieve the objectives of the JGOFS program (NAS 1984), and the SeaWiFS sensor will play a key role in this effort. The oceans exhibit physical and biological variability over a wide range of space and time scales. This variability, and the need to synoptically measure distributions of physical and biological properties over large areas and long time periods, has motivated recent developments utilizing contemporaneous buoy, ship, aircraft, and satellite sampling strategies (Smith et al. 1987). In addition, long-term mooring data are required to provide continuous observations and permit an optimization of the accuracy of the derived satellite products (Booth and Smith 1988).

There are two sources of systematic error in estimates of phytoplankton pigment biomass derived from satellite ocean color data. First, errors in satellite estimation of pigment biomass arises because physical forcing, biological properties, and ocean optical properties all vary systematically with depth, and the upper layer optical signal observed by satellites may not adequately represent deeper structure. In many circumstances, subsurface changes may go undetected without contemporaneous water column profile data from either shipboard or moored sensors. Second, visible wavelength sensor systems do not obtain data when the atmosphere is cloudy. Air-sea interactions giving rise to cloudiness are often closely linked to biological processes. For example, Michaelsen et al. (1988) have shown that episodic wind events, which give rise to coastal upwelling and subsequent phytoplankton production along the California coast, cause cloudiness that bias the statistics of pigment concentrations derived from ocean color imagery. Similar biases of a factor of 3–4, due to wind mixing during cloudy periods, were observed by Muller-Karger et al. (1990). In circumstances of this nature, visible and infrared satellite observations of the ocean are not random samples. Moored optical sensors can measure systematic temporal variability in the vertical distribution of pigment biomass and, at the same time, provide the continuous time series which may be used to remove the sampling bias associated with cloudiness.

The detection and verification of inter- and intra-annual fluctuations in productivity and associated bio-optical variables are key goals of programs focused on studying global change. These goals place stringent requirements for long-term accuracy and precision on the measurement systems to be employed. The monitoring of bio-optical parameters to resolve variability at global and decadal scales, as proposed by the SeaWiFS and MODIS missions, will require that moored *in situ* optical instruments be maintained to supplement and support the satellite data sets. For example, the CZCS sensor degradation and the difficulties encountered in attempting to characterize that degradation, strongly point out how valuable in-water optical measurements would have been to that program.

2.6 Drifting Optical Buoys

Drifting optical buoys, which are expendable and analogous to ARGOS sea surface temperature (SST) drifters, represent a viable, cost-effective way to obtain significant numbers of daily optical observations to validate global data sets of water-leaving radiance. There will probably never be more than a few permanent optical moorings, due to their high cost, and very few ship measurements can be obtained on any given day, again due to cost and investigator availability. Optical data from drifting buoys, while less complete than measurements from ships and fixed optical moorings, can potentially surpass both in terms of global coverage and the number of near real-time comparisons with SeaWiFS observations. Judicious seeding of *inexpensive* drifters provides one means of sampling conditions and regions critical to SeaWiFS product verification, e.g., to study regions with chronically high levels of aerosols due to dust storms, and to study possible variations in SeaWiFS performance as a function of latitude due to orbital variations in sensor performance and sun angle dependency of algorithms.

Optical drifter development activities at Halifax (M. Lewis) and the NASA/GSFC aim at instruments to measure seven and three upwelling spectral radiances, respectively, and a single downwelling irradiance. Along with temperature and barometric pressure, these data are transmitted over an ARGOS link. Storage procedures are designed to make maximum use of the limited ARGOS bandwidth. (An interrogating store and forward satellite system with greater bandwidth would be beneficial for this purpose.) The upwelling radiance data are obtained at a depth of approximately 0.5 m and must be propagated through the surface using $K_L(\lambda)$ estimated from the relative spectral shape. Therefore, these water-leaving radiance estimates will be inherently less accurate than surface reflectance observations made together with optical profiles and more complete ancillary observations.

Both of these systems are in the test and evaluation phases. High risk areas which are being examined include long-term stability, identification of biofouling effects, operating lifetime, and validation of the techniques used for calculating the water-leaving radiance from the simple drifting sensors. The accuracy of the ARGOS system for drifter location is sufficient for global area coverage (GAC), but experience needs to be gained in analysis of the data to demonstrate the feasibility of using ARGOS positioning (150 m to 1 km accuracy) for system calibration and validation work in water mass regimes where mesoscale variability is significant.

The cost of optical drifters will limit the number deployed. Proponents envision 50 such buoys adrift at any one time throughout the world—a number sufficient to provide a large enough sample size to support viable global validation. In such a scenario, typically 60% of the drifters would be obscured by clouds during a SeaWiFS pass (those in some areas will have a much greater probability for clouds). Furthermore, current divergence areas will be systematically undersampled by drifters.

The accuracy of calculated L_W derived from drifter data has been estimated to be ~15%, even though at the time they are deployed, the calibrated accuracy of the instruments will be less than 5%. This is a possibly pessimistic estimate based on:

1) the untestable possibility of drifts in radiometric responses during long-term deployment of an expendable instrument, and
2) errors associated with propagating $L_u(0.5\text{ m}, \lambda)$ through the water column and interface to estimate $L_W(\lambda)$ without benefit of measurements of $K(z, \lambda)$, surface roughness and other ancillary measurements to be carried out at corresponding ship stations.

If L_{WN} from drifters is only good to 15%, they cannot be used to verify SeaWiFS radiometry within 5%, no matter how many drifter comparisons are made. Accuracies must be less than 5% if this technology is to be used. Accuracies of 15% may, however, be useful for validating SeaWiFS and derived products, and for interpolating SeaWiFS data through periods of extensive cloud cover.

3. SPECIFICATIONS

The measurements of optical properties and other variables described in this report are those necessary for validating data obtained with the SeaWiFS sensor, and for the development of in-water and atmospheric algorithms. The specifications herein are those required of instruments used on ships, or other platforms, to acquire that optical data. In some cases the specifications have been selected to allow use of instruments that are affordable and either currently exist, or can be developed without major improvements in today's state-of-the-art. In a few cases, new or improved instruments must be developed to realize the specified performance characteristics.

The data accuracy requirements for this program are more severe than those for a general ocean survey. Here, various investigators will use a variety of instruments that will be calibrated independently at a number of facilities, and contribute data to a common database which will be used to validate SeaWiFS measurements. The resulting radiometric and bio-optical database will provide an essential means of detecting and quantifying on-orbit changes in the SeaWiFS instrument relative to its prelaunch calibration and characterization. This chapter specifies instrument characteristics and data accuracies thought by the SPSWG to be sufficient and necessary for this task. The validation analysis would be significantly degraded should calibration errors or differences of even a few percent, or wavelength errors or differences of a few nanometers, occur in (between) the instruments used to acquire the SeaWiFS bio-optical database.

3.1 In-Water Radiometers

3.1.1 Spectral Characteristics

In-water radiometers shall be capable of making measurements at the wavelengths shown in Table 2 as a minimum. The table presumes the use of properly blocked interference filters to provide the required spectral bandpass and out-of-band rejection (10^{-6} or better). Care must also be taken to avoid possible out-of-band leakage due to fluorescence by filter, or other optical component, materials. Filter radiometers should have channels with center wavelengths, as measured in the assembled instrument, matching those given in Table 2 to within ±1 nm for 410 and 443 nm, and within ±2 nm for all other spectral bands. Shifts of these magnitudes in center wavelengths will result in changes in measured radiometric values of approximately ±1% or less (C. Booth, pers. comm.) and this specification should be met if possible.

Table 2. Recommended spectral bands for discrete wavelength filter radiometers using 10 nm full-width half-maximum (FWHM) bandwidths. In addition, out-of-band blocking in the far tails of the instrument response functions should be at least 10^{-6}.

SeaWiFS Band	*Wavelengths* [nm]	E_d, E_u, L_u [nm]	E_s [nm]
1	402–422	412[1]	412
2	433–453	443, 435[2]	443
3	480–500	490	490
4	500–520	510	510
5	545–565	550[3], 560[3]	550[4]
6	660–680	665, 683	665[4]
7	745–785	[5]	780
8	845–885	[5]	875[6]

1. A preferred option is to substitute two separate 10 nm FWHM bands centered at 406 and 416 nm, for a single 412 nm channel. The two channels would allow more accurate modeling of $L_{WN}(412)$ matching SeaWiFS characteristics.

2. An optional extra band is used to improve modeling of L_{WN} radiances to match the SeaWiFS 443 nm channel.

3. The 545–565 nm range is broken into two channels to detect possible phycoerythrin fluorescence.

4. E_s deck, only one channel in this band is necessary.

5. Due to the specialized nature of infrared in-water measurements, specialized sensors will be needed.

6. Optional for E_s.

It is recognized, however, that enforcing a ±1 nm hard-and-fast specification could be prohibitively expensive, and this tolerance should be regarded as a goal. With knowledge, to less than 0.2 nm, of the actual center wavelengths and complete spectral response functions, corrections probably can be made to infer effective radiometric quantities for the SeaWiFS channels, when the spectral characteristics of SeaWiFS channels have also been measured, shortly before launch. Bandwidths must be 10 nm ±2 nm FWHM. They are made narrower than the SeaWiFS channels to reduce the skewing of the parameters derived from underwater irradiance or radiance profiles in spectral regions where absorption by natural sea water may vary rapidly with wavelength.

To maintain the above tolerances, it is anticipated that filters will be ordered to a center wavelength with a tolerance of $\lambda_0 \pm 1$ nm and a FWHM bandwidth of 8.5 ±1 nm. However, when the filter is installed in a radiometer with a 10° (half-angle) FOV, the spectral bandpass will broaden by 2–3 nm, and the center wavelength will shift. Furthermore, as a filter ages in use, its transmission curve may undergo changes to further broaden the FWHM bandpass and shift the peak. The tolerances specified above include an allowance for some degradation before expensive filter and detector changes must be done.

In a single instrument, all channels at a given nominal wavelength should match within 1 nm, if possible. Therefore, it is desirable to obtain all of the filters used by an investigator for measurements at any nominal wavelength λ_m from a single manufacturing lot when possible. If this is done, $E_s(\lambda_m)$, $E_d(\lambda_m)$, $E_u(\lambda_m)$, $L_u(\lambda_m)$, and any atmospheric radiometric quantities measured with that investigator's systems, would all have greater likelihood of being measured over the same range of wavelengths, for each nominal wavelength λ_m. In any event, the actual spectral response function of each instrument channel must be measured and known to be accurate to less than 0.2 nm.

Table 3. High resolution spectroradiometric specifications.

Optical Sensors	
Spectral Range:	380 to 750/900 nm
Spectral Resolution:	5 nm (or less FWHM)
Wavelength Accuracy:	10% FWHM of resolution (0.5 nm)
Wavelength Stability:	5% FWHM of resolution (0.25 nm)
Signal-to-Noise Ratio:	1,000:1 (at minimum)
Stray Light Rejection:	10^{-6}
Radiometric Accuracy:	3%
Radiometric Stability:	1%
FOV Maximum:	10° (for radiance)
Temperature Stability:	Specified for 0–35° C
Linearity:	Correctable to 0.1%
Ancillary Sensors	
Temperature:	0.2° C
Pressure:	0.1% (full scale)
Horizontal Inclination	1° over 40° range

High resolution monochromator-based spectroradiometers, with adequate sensitivity and stray light rejection characteristics, are also suitable instruments and are recommended for many algorithm development studies. Suitable specifications for such instruments are given in Table 3. (These instruments must also meet the specifications summarized in Tables 2 and 4.)

Table 4. Required instrument sensitivities for SeaWiFS validation and algorithm development as a function of radiometric measured variable and wavelength.

Property	*Variable*	410 nm	488 nm	665 nm	*Comment*
$E_d(z,\lambda)$, Downwelled Irradiance	$E_d(0)_{\max}$	200	200	200	Saturation Irradiance
	$E_d(3/K_d)$	1	1	1	Minimum Expected Irradiance
	$\frac{dE}{dN}$	5×10^{-3}	5×10^{-3}	5×10^{-3}	Digital Resolution (profiles)
	$\frac{dE}{dN}$	5×10^{-2}	5×10^{-2}	5×10^{-2}	Digital Resolution (surface unit)
$E_u(z,\lambda)$, Upwelled Irradiance	$E_u(0)_{\max}$	80	80	40	Saturation Irradiance (Case 2/coccoliths)
		25	15	1	Saturation Irradiance (Case 1)
	$E_u(3/K_d)$	1×10^{-2}	2×10^{-2}	1.5×10^{-3}	Minimum Expected Irradiance
	$\frac{dE}{dN}$	5×10^{-4}	5×10^{-4}	5×10^{-5}	Digital Resolution (surface unit)
	$\frac{dE}{dN}$	5×10^{-5}	5×10^{-5}	5×10^{-6}	Digital Resolution (profiles)
$L_u(z,\lambda)$, Upwelled Radiance	$L_u(0)_{\max}$	16	16	8	Saturation Radiance (Case 2/coccoliths)
		5	3	0.2	Saturation Radiance (Case 1)
	$L_u(3/K_d)$	2×10^{-3}	4×10^{-3}	3×10^{-4}	Minimum Expected Radiance
	$\frac{dL}{dN}$	5×10^{-4}	5×10^{-4}	5×10^{-5}	Digital Resolution (surface unit)
	$\frac{dL}{dN}$	5×10^{-5}	5×10^{-5}	5×10^{-6}	Digital Resolution (profiles)
E_{cal}, Source Irradiance	E_{cal}	2	5	15	Calibration Irradiance
	$\frac{dE}{dN}$	2×10^{-3}	5×10^{-3}	1×10^{-2}	Digital Resolution (E_d, E_s, E_u cal.)
L_{cal}, Source Radiance	L_{cal}	0.6	1.5	4.5	Calibration Radiance
	$\frac{dL}{dN}$	6×10^{-4}	1×10^{-3}	4×10^{-3}	Digital Resolution (L_u cal.)

Notes: 1. E_u and E_d are in units of $\mu\text{W cm}^{-2}$ nm^{-1} and L_u is in units of $\mu\text{W cm}^{-2}$ nm^{-1} sr^{-1}.
2. Responsivity resolution in radiometric units per digital count at the minimum required signal level.
3. Specified ranges should maintain a 100:1 SNR.

3.1.2 Responsivity, SNR, and Resolution

The expected operating limits for radiometric responsivities, SNR, and digital resolution are specified in Table 4, the limits for which were derived as follows:

1. An E_d saturation value of 200 $\mu\text{W cm}^{-2}$ nm^{-1} is assumed at all wavelengths.
2. Implicit, but not stated, in Table 4 is that the minimum required $E_d(0)$ is 20 $\mu\text{W cm}^{-2}$ nm^{-1}; it will not be appropriate to occupy validation stations when illumination is less.
3. A minimum $E_d(0)$ implies a minimum detectable $E_d(z)$ of 1 $\mu\text{W cm}^{-2}$ nm^{-1} at 3 optical depths $(3/K)$.
4. Digital resolution must be $\leq$ 0.5% of reading to maintain a 100:1 SNR. To permit 1% accuracy in absolute calibration, if that goal can be met, the instrument must digitally resolve 0.1% of the irradiance (radiance) produced by laboratory standards; typical irradiance (radiance) values for calibration using 1,000 W FEL standard lamps traceable to the National Institute of Standards and Technology (NIST), and required digital resolutions at these signal levels, are given in Table 4 as "Calibration Irradiance" and "Digital Resolution," respectively. An SNR of 100:1 requires $E_d(z)$ at three optical depths be resolved to 0.005 $\mu\text{W cm}^{-2}$ nm^{-1} per count or 2.5 digit resolution. At the surface, $E_d(0)$ should be resolved to 0.05 $\mu\text{W cm}^{-2}$ nm^{-1} per count.
5. The Case 1 saturation values of $E_u(0)$ represent the *Instrument Specification Sub-Working Group's* estimate of maximum reflectances to be expected in ordinary Case 1 waters: 12.5% at 410 nm, 7.5% at 488 nm and 0.5% at 670 nm. These saturation values will be too low for measurements in Case 2 waters or coccolithophore blooms. In these situations, a maximum expected reflectance of 40% for $\lambda < 660$ nm and 20% for $\lambda \geq 660$ nm is assumed. This implies that the expected maximum irradiance in $E_u(0)$

should be $80\,\mu W\,cm^{-2}\,nm^{-1}$ for $\lambda < 660$ nm and $40\,\mu W\ cm^{-2}\ nm^{-1}$ for $\lambda \geq 660$ nm.

6. The minimum required irradiances at 3 optical depths (Table 4) assumes minimum reflectances of 1% at 410 nm, 2% at 488 nm and 0.15% at 670 nm.
7. The saturation and minimum radiances, and radiance responsivity resolutions, for $L_u(0)$ and $L_u(z)$ at three optical depths are 0.2 times the corresponding specification for $E_u(0)$ or $E_u(z)$. This assumes $E_u/L_u = Q = 5$ at all wavelengths and depths.

The specifications in Table 4 are meant as guidance to interpret the following required performance requirements:

a) The instrument must maintain a 100:1 SNR at every operating range encountered, during field measurements.

b) The data for measurements obtained in the field must be recorded with a digital resolution less than or equal to 0.5% of reading.

c) The dynamic range of the instrument's linear sensitivity must extend to include the signal levels encountered during laboratory calibrations, and the calibration signals must be recorded with a digital resolution of 0.1% of reading to permit 1% accuracy in calibration.

In general, the above performance specifications do not pose exceptionally difficult engineering challenges, with the possible exception of the full dynamic range implied by Case 2 or coccolith saturation radiance $L_u(665\text{ nm})$ to minimum expected $L_u(665\text{ nm})$. This situation will require specially designed radiometers in any event (section 3.1.8). It is not necessary that every radiometer used for SeaWiFS validation operate over the full dynamic ranges given in Table 4. A radiometer is merely required to maintain the above performance specifications over the dynamic ranges of irradiance and radiance existing at locations and associated illumination conditions where it is used for SeaWiFS validation or algorithm development.

3.1.3 Linearity and Stability

Errors attributable to linearity or stability should be less than 0.5% of readings over the 104 ranges specified in Table 4. This is a challenging goal, but one which must be met if the equally challenging goal of achieving 1% accuracy in absolute calibration is to be meaningful.

3.1.4 Sampling Resolution

Sampling frequency should be compatible with the profiling technique being used. For the preferred multispectral filter radiometers and spectroradiometric (dispersion) instruments using array sensors, the minimum sampling frequencies are determined by the profiling rate and the depth resolution required. In general, five or more samples per meter should be obtained at all wavelengths. All channels of $E_d(z,\lambda)$, $E_u(z,\lambda)$, and $L_u(z,\lambda)$ at all wavelengths should be sampled to within 10 msec at each depth.

The time response of the instrument to a full-scale (saturation to dark) step change in irradiance should be ¡1 s to arrive at a value within 0.1%, or one digitizing step, whichever is greater, of steady state. In addition, the electronic e-folding time constant of the instrument must be be consistent with the rate at which the channels are sampled, i.e., if data are to be acquired at 10 Hz, the e-folding time constant should be 0.2 s to avoid aliasing. Individual data scans may be averaged to improve SNR performance, provided adequate depth resolution is maintained.

3.1.5 Angular Response Characteristics

The response of a cosine collector to a collimated source incident at an angle θ from the normal, must be such that:

1) for E_u measurements, the integrated response to a radiance distribution of the form $L(\theta) \propto 1+4\sin\theta$ should vary as $\cos\theta$ accurate to within 2%; and
2) for E_d measurement, the response to a collimated source should vary as $\cos\theta$ accurate to less than 2% for angles $0° < \theta \leq 65°$ and 10% for angles $65° < \theta \leq 85°$.

Departures from $\cos\theta$ will translate directly to approximately equal errors in E_d in the case of direct sunlight.

The in-water FOV for upwelled radiance bands should be ~10° (half-angle). The resulting solid angle FOV (~0.1 sr) is large enough to provide reasonable levels of flux, using silicon detectors, yet small enough to resolve the slowly varying (with θ, for $\theta < 30°$) field of upwelled radiance. Smaller FOV sensors are appropriate, of course, if all of the other performance specifications are satisfied.

3.1.6 Operating Depth

The instruments shall be capable of operating to depths of 200 m. Depths should be measured with an accuracy of 0.5 m and a precision of 0.2 m for profiles in bands 1–6.

3.1.7 Instrument Attitude

The orientations of the instrument with respect to the vertical shall be within ±10°, and the attitude shall be measured with orthogonally oriented sensors from 0–30° with an accuracy of ±1° in a static mode; it is not intended that this accuracy be maintained while an instrument is subject to large accelerations induced by surface waves. These data shall be recorded with the radiometric data stream for use as a data quality flag.

3.1.8 Red and Near Infrared Wavelengths

Due to the fact that the SeaWiFS red and near infrared channels–bands 6–8 at wavelengths of 665, 780, and

865 nm, respectively–have such short attenuation lengths in water, special attention must be paid to these measurements. Problems due to instrument self-shading (Gordon and Ding 1992) and very rapid attenuation of $L_u(z,\lambda)$ must be considered at these wavelengths. Large instruments, such as the standard Biospherical Instruments, Inc., MER packages, are not adaptable to these measurements.

Suggested procedures for making the measurements are to use either fiber optic probes carrying light back to a remote instrument, or very small single-wavelength discrete instruments. Each of these concepts is adaptable to deployment from a small floating platform. Care must be taken to avoid direct shading by the supporting platform, but at these wavelengths, the large attenuation coefficients of water makes shadowing by objects more than a few meters away irrelevant.

While the minimum measurement scheme would be two discrete (10 nm FWHM) channels at 780 and 875 nm, additional channels at 750 and 850 nm, or more elaborately, high resolution spectroradiometry, would be useful in determining the spectral distribution of the upwelling light field in these bands.

These measurements should be performed as part of the standard validation data acquisition, because of their importance in the atmospheric correction algorithms. It is anticipated that in the majority of cases, and particularly in most Case 1 waters, these measurements will show negligible upwelling light. In Case 2 waters, cases of extremely high productivity or in coccolithophore blooms, $L_{WN}(\lambda)$ at these wavelengths may be significant and these measurements will become very important.

When in-water measurements are performed at these wavelengths, the deck cell channels should be expanded to include bands at 750 and 875 nm (Table 2).

3.2 Spectral Surface Irradiance

The irradiance at the ocean surface shall be measured at wavelengths which correspond to the SeaWiFS spectral bands (Table 2), but with 10 nm FWHM bandwidth. A total radiation pyranometer may provide helpful ancillary information, but this is not a required instrument.

Instruments mounted aboard ships must be positioned to view the sky with minimum obstruction or reflections from the ship's superstructure, antennas, etc. Particular care must be taken to prevent sun shadows from antennas falling on the irradiance collecting surface. Gimbal mounting of the deck sensor may be helpful to keep the surface of the sensor horizontal. However, improperly designed gimbal systems can accentuate fluctuations caused by ship motion, and if there is obvious oscillation in the measured irradiance, the gimballing should be improved to eliminate the problem.

An intuitively attractive technique is to measure irradiance with a sensor floated a fraction of a meter below the sea surface, far enough away from the ship to avoid ship shadows. The floatation assembly should be designed to avoid shadowing the radiometric FOV and to damp wave induced motions. This type of arrangement has an additional potential for supporting a small sensor to also measure upwelling radiance $L_u(\lambda)$ just below the surface. Unfortunately, the community has only very limited experience with this approach for measuring $E_s(\lambda)$ (Waters et al. 1990) and the attendant difficulties with wave induced fluctuations in near-surface E_d. Additional research should be performed to evaluate the use of a floating surface unit as the potentially preferred method for measuring $E_s(\lambda)$ in future revisions to these protocols.

3.2.1 Surface Radiometer Characteristics

The specified number of channels and spectral characteristics of deck cells are the same as those for subsurface irradiance measurements (see Table 2). Saturation irradiances are the same as for $E_d(\lambda)$ (see Table 4). The dynamic operating range for these sensors needs to be 25 db, with a SNR of 100:1 but must include the nominal calibration irradiance (Table 4). Linearity must be within $\pm 0.5\%$. Sampling frequency should match the frequency of the underwater radiometer, which should be 1 Hz or faster, and all wavelengths should be sampled within ≤ 10 ms. Cosine response characteristics should give relative responsivity to a collimated source (in air) which matches $\cos\theta$, accurate within 2% for $0° \leq \theta < 65°$, and within 10% for $65° \leq \theta \leq 90°$. If a floating surface radiometer is used, its cosine response and immersion characteristics must meet the specifications for profiling irradiance meters.

For some oceanographic process studies, it may be acceptable to use a radiometer system measuring $E_s(\lambda)$ at only a single wavelength. If only a single channel deck radiometer is available, its spectral characteristic should closely match one of channels 2–5 with a 10 nm FWHM bandwidth. A broad-band, or photosynthetically available radiation (PAR), radiometer should never be used for this purpose.

3.3 Airborne Radiometer Specifications

The performance characteristics to be specified for an airborne radiometer will vary, depending on how a particular instrument is to be employed in SeaWiFS validation experiments. For radiometric comparisons with SeaWiFS and in-water measurements, the fundamental criterion to be met is that estimates of spectral normalized water-leaving radiance derived from airborne measurements must have the same accuracy specified for those derived from in-water measurements of $L_u(z,\lambda)$ (Table 4). A less accurate radiometer may be used to semi-quantitatively characterize spatial variability near ship stations.

In general, the spectral characteristics of airborne radiometers should match those specified for $L_u(\lambda)$ in Table 2. In some cases, however, it may be acceptable for a radiometer to match the SeaWiFS specifications, that

being, center wavelength within 2 nm and 20 nm FWHM bandwidth. Recalling the sensitivity of solar radiometry to the exact center wavelength and detailed spectral response function (sections 3.1.1 and 4.1.2), any use of airborne radiometers must quantitatively account for the different spectral responsivity functions of the SeaWiFS, in-water radiometer, or airborne radiometer measurements of radiance at each channel's nominal center wavelength.

A high altitude imaging radiometer must have a radiometric accuracy and SNR in all channels equal to those of the SeaWiFS instrument if its imagery is to be used for direct radiometric verification of SeaWiFS radiometric performance. In some cases, the requisite SNR may be realized through pixel averaging to a 1 km spatial resolution commensurate with that of SeaWiFS. However, direct radiometric comparisons between aircraft and SeaWiFS radiances also require that the different atmospheric path effects be carefully modeled, and that the uncertainty in those modeled adjustments be independently estimated. This can be done most effectively when the aircraft measurements are combined with the full suite of shipboard in-water, atmospheric, and ancillary measurements (Table 1). In this case, direct comparisons between the aircraft and ship radiometry may require that SNR and accuracies realized in combined analyses of the two data sets must represent a smaller spatial resolution than the SeaWiFS nominal 1 km FOV.

A radiometer's sensitivity to the polarization of aperture radiance is critical for ocean color sensing. An airborne ocean color radiometer must have a polarization sensitivity of less than 2% in all channels. The sole exception to this rule will occur in the case of instruments designed to actually measure the polarization components of aperture radiance, e.g., as in the polarization channels of the French Polarization Detecting Environmental Radiometer (POLDER) instrument.

Each application of a particular airborne radiometer system, which is proposed for SeaWiFS validation, must be evaluated on its own merits. The instrument's responsivity, accuracy, stability, FOV, and spectral characteristics must be evaluated in the context of the models to be used to compare its radiance measurements to in-water or SeaWiFS radiance measurements. The suitability of spatial averaging to improve signal-to-noise must be evaluated in terms of the spatial variability prevailing in the experiment site, particularly when in-water and aircraft radiances are to be directly compared. On the other hand, finer resolution aircraft imagery, or trackline data, will often be essential for determining the validity of attempts to directly compare in-water and SeaWiFS radiances measured at a particular site.

In summary, airborne radiometry can obviously contribute extremely valuable data for validating SeaWiFS radiometric performance and algorithms. However, there is a wide possible range of airborne radiometer characteristics that can be applied to this program, and detailed specifications of required characteristics can only be done in the context of each particular experiment's design. Only the guiding principals and desired end-to-end performance can be specified here.

3.4 IOP Instruments

The inherent optical properties (IOP) are the beam attenuation coefficient $c(z,\lambda)$ (units of m^{-1}), the absorption coefficient $a(z,\lambda)$ (units of m^{-1}), and the volume scattering function, $b(\theta,z,\lambda_0)$ (units of m^{-1} sr^{-1}). The integral of the volume scattering function over 4π sr is the total scattering coefficient, $b(z,\lambda)$ (units of m^{-1}). The integral of the volume scattering function over the back hemisphere is the backscattering coefficient, $b_b(z,\lambda)$ (units of m^{-1}).

It will be possible to measure the spectral attenuation and absorption coefficients *in situ* at the time of SeaWiFS deployment. The instruments for measuring the spectral absorption and attenuation coefficients should have, at a minimum, the characteristics given in Table 5.

Spectral resolution at more than SeaWiFS wavelengths would be desirable to deduce pigment concentrations. In the case of beam attenuation coefficients, the requirements for accuracy and precision correspond to changes in $c(\lambda)$ resulting from changes in concentration of approximately 5 and 2 $\mu g\, l^{-1}$ of suspended mass, respectively. Stability should be tested with instruments connected to the data acquisition system. Stability with time should be better than 0.005 m^{-1} between calibrations.

Table 5. Minimum instrument characteristics for the measurement of the spectral absorption and attenuation coefficients.

Instrument Characteristics	
Spectral Resolution:	410, 443, 490, 520, 510 and 670 nm
Bandwidth:	10 nm
Accuracy:	0.005 m^{-1}
Precision for $\lambda < 650$ nm:	0.002 m^{-1}
Precision for $\lambda \geq 650$ nm:	0.005 m^{-1}
Stability with Temperature:	0.005 m^{-1} over 0–25° C
Sampling Interval:	≥ 4 samples m^{-1}
Source Collimation Angle:	≤ 5 mrad
Detector Acceptance Angle:	≤ 20 mrad
Depth Capability:	200 m

The spectral total scattering coefficient cannot be measured directly. It can be obtained from $b(\lambda) = c(\lambda) - a(\lambda)$, provided $c(\lambda)$ and $a(\lambda)$ are determined with the appropriate accuracy. The spectral backscattering coefficient $b_b(\lambda)$ has the same requirements for spectral resolution, bandwidth, and linearity as $a(\lambda)$ and $c(\lambda)$. Since $b_b(\lambda)$ is not a transmission-like measurement, however, the accuracy of its determination will be approximately 10%.

The shape of the volume scattering function can, at

present, be determined *in situ* only crudely with devices like the Alpha and Scattering Meter (ALSCAT) and the General Angle Scattering Meter (GASM), which were built more than a decade ago at the Scripps Institute of Oceanography Visibility Laboratory (VISLAB). These are single angle measurement devices, which must be scanned as a function of angle and wavelength. Because measuring scattering with these instruments is a slow process, they do not lend themselves readily to incorporation into other instrument platforms. Since it will be possible to independently determine $b(\lambda)$ and $b_b(\lambda)$ at the time of deployment of SeaWiFS, the determination of the shape of the volume scattering coefficient could possibly be determined with acceptable accuracy by measuring a few moments of the scattering function. A new instrument development effort would have to be initiated to pursue this approach.

3.5 Atmospheric Aerosols

Sun photometers should be used to measure atmospheric aerosol optical thickness. These sun photometers should be in agreement with World Meteorological Organization (WMO) sun photometer specifications (Frohlich 1979). Specifically, the instruments should have a 2° FOV, temperature stabilization, and a precision of ±0.01%. The specific wavelengths of channels should correspond to the recommended WMO wavelengths of 380, 500, 675, 778, and 862 nm. For SeaWiFS validation, additional channels at 410, 440, 520, and 565 nm should be added to the WMO set.

3.6 Sky Radiance Distribution

Spectral sky radiance distribution measurements should be made using a photoelectric all-sky camera. Spectral characteristics of the sky radiance camera channels are those specified for $E_s(\lambda)$ (Table 2). Data should be in a format such that absolute radiance values can be obtained with an accuracy of 5% and sky irradiance can be determined from integrals of the data to within 10%. If the dynamic range of the camera is insufficient to capture both the sun and sky distribution, neutral density filters, or some other method, should be used so that radiance from both the sun and sky can be measured.

3.7 Phytoplankton Pigments

HPLC equipment and associated standards must conform to protocols specified for the *JGOFS Core Measurement Protocols*, Chapter 9, "Pigment and Chlorophyll." *In situ* chlorophyll fluorometers should have a resolution of at least 0.001 mg chlorophyll *a* per m^3.

3.8 Hydrographic Profiles

A calibrated CTD system should be used to make profiles to maximum depths between 200 and 500 m. The instrument should meet the minimum specifications given in Table 6.

Table 6. Minimum instrument characteristics for the measurement of hydrographic profiles.

Parameter	*Range*	*Accuracy*	*Resolution*
Pressure [dbars]	0–500	0.3%	0.005%
Temperature [°C]	-2–35	0.015° C	0.001° C
Salinity [PSU]	1–45	0.03 PSU	0.001 PSU

4. SENSOR CHARACTERIZATION

4.1 Radiometric Characterization

The characterization of radiometric instruments used for the acquisition of field data for SeaWiFS validation and algorithm development shall include the determination of those instrument characteristics that affect its calibration as used in the field environment. Thus, in addition to the obvious radiometric calibration, it is necessary to determine:

a) the spectral sensitivities of the various measurement channels;

b) the angular sensitivities of an irradiance or radiance sensor in the medium, i.e., air or water, in which it is to be used;

c) the temporal response of the system;

d) the effects on responsivity caused by water immersion; and

e) the effects of temperature and pressure on the above characteristics.

The elements of radiometer characterization and calibration are outlined schematically in Fig. 1.

For an instrument to provide suitable data for SPO use, the investigator must be certain the instrument's characterization has not changed beyond accepted limits and that the time history of the calibration is traceable. Certain attributes, e.g., angular response characteristics, typically remain constant so it is sufficient to determine them once, unless instrument modifications are performed. The exact nature of instrument modifications during maintenance will determine which characterization procedures must be repeated. On the other hand, radiometric calibrations and the assessment of system spectral characteristics of filter radiometers, must be repeated before and after each major field deployment.

4.1.1 Absolute Radiometric Calibration

Determination of the absolute radiometric responses of the irradiance and radiance sensors requires the availability of a properly manned and equipped radiometric calibration facility. Such a facility must be equipped with suitable stable sources and sensors, e.g., lamp standards of spectral irradiance and flat response radiometers, respectively.

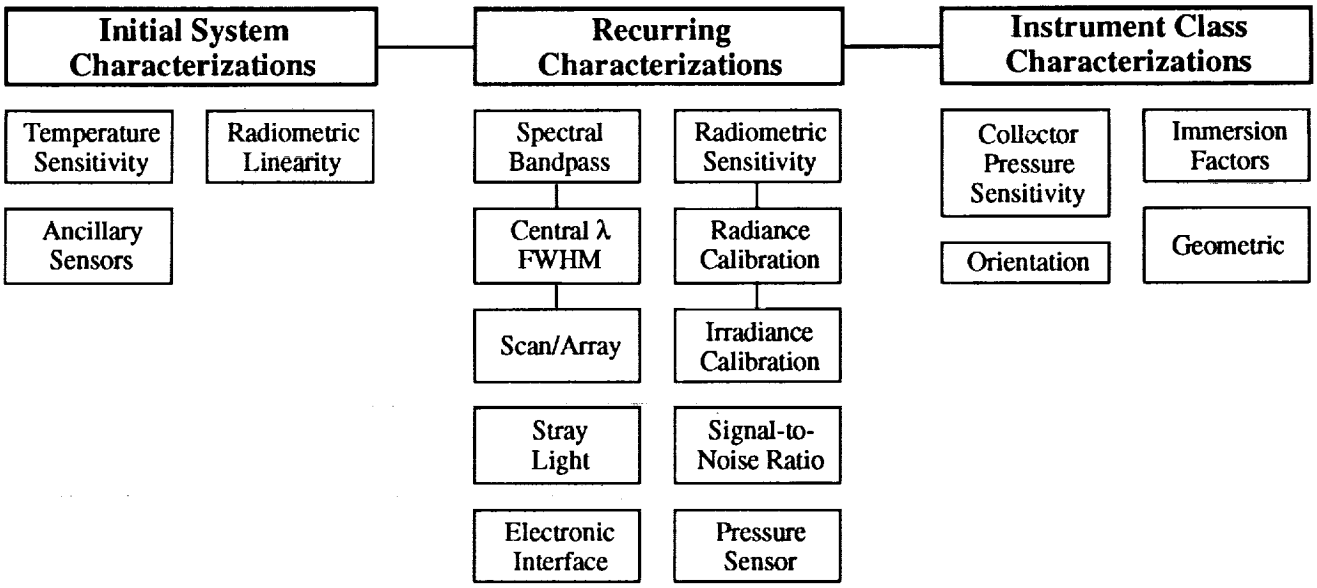

Fig. 1. Elements of radiometer characterization and calibration.

Either the sources or the sensors must have known spectral radiometric characteristics traceable to NIST (section 4.2). The calibration facility must also have a variety of specialized radiometric and electronic equipment, including reflectance plaques, spectral filters, integrating spheres, highly regulated power supplies for the operation of the lamps, and precision electronic measurement capabilities for setting and monitoring the lamp current and voltage, and for measuring the output of the radiometer.

It is not expected that every investigator will be able to perform his own radiometric calibrations. Because of this, a few centrally located facilities will be equipped and staffed to perform these calibrations as a routine service for the community. The facilities will perform frequent intercomparisons to assure the maintenance of the radiometric traceability to the NIST standard of spectral irradiance. The goal shall be to provide reproducible calibrations from 400–850 nm to within better than ±1%; the minimum requirement for radiometric data to be used in SeaWiFS validation is for repeatable calibrations within less than 5%.

Radiometric calibrations of irradiance sensors will be performed after it has been ascertained that the conformity of the sensor angular response to the required cosine function is satisfactory; the sensor linearity is satisfactory; and the spectral sensitivity, including out-of-band blocking, is known and satisfactory.

Radiometers shall be calibrated using a 1,000 W FEL Standard of Spectral Irradiance, with calibration traceable to NIST and lamp operation in accordance with Walker et al. 1987. The irradiance collector is placed normal to, and at the prescribed distance from, a working standard lamp of spectral irradiance. The lamp should be of appropriate size to provide an irradiance at the sensor which will be at least 30% and preferably above 50% of full-scale for the sensor channel being calibrated; this is not always achievable in practice (Table 4). The lamp-sensor space shall be appropriately baffled and draped so that occulting the direct path between lamp and sensor will result in a response of less then 0.1% of the response to the lamp flux.

For multispectral instruments, all channels may be calibrated simultaneously if sufficient flux is available at all wavelengths. The instrument response is recorded for all channels together with associated dark responses. Ambient and photosensor temperatures are recorded, where available. For characterization, the radiometric calibration should be performed at temperature extremes of −2° C and 40° C for in-water sensors, and at −10° C and 45° C for irradiance sensors used above the surface. If responses differ significantly at temperature extremes, responses should also be determined at intermediate temperatures.

The portable irradiance and radiance reference standard to be used to trace instrument stability during field deployments (section) should be placed in position on the sensor immediately following the calibration to establish the instrument response to this reference unit.

Radiance calibrations require a source of uniform known radiance that will fill the angular field of view of the radiance sensor. Either of two methods may be used:

Method 1: A working lamp standard of spectral irradiance is placed at the prescribed distance from a plaque of known Lambertian reflectance. The plaque is normal to, and centered on, the lamp calibration axis. The radiance sensor is positioned to view the plaque at an angle of 45° from the plaque normal (any other angle at which the diffuse reflectance of the plaque is known is acceptable also). It must be established that the plaque fills the sensor's FOV and that the presence of the sensor case

has not perturbed the irradiance on the plaque. The instrument response and dark signal is recorded. It must be verified that, the plaque fills the FOV with uniform radiance for each channel of a multichannel radiance sensor; separate calibration setups may be required for different channels and the lamps may have to be moved as much as 3 m away from the plaque to assure uniform illumination. This procedure is difficult to apply to sensors with a large FOV.

Method 2: An integrating sphere with an exit port of sufficient size to fill the FOV of the radiance sensor may be used if the radiance of the exit port, at the channel wavelengths, can be determined with sufficient accuracy.

These methods are discussed more fully in section 4.2.2.

The requirements given above for noting and controlling temperatures and for use of the portable irradiance and radiance reference standard (section 4.2.5), apply here as well.

4.1.2 Spectral Bandpass Characterization

These instruments should be characterized to define the nominal wavelengths and bandwidths, defined as the full width of the passband as measured to the FWHM intensity points. The nominal, or center wavelength, will usually be defined as the wavelength halfway between wavelengths at which the normalized response is 0.5, and the channel is characterized by this wavelength and the FWHM bandwidth. The determination of the spectral response function, i.e., the passband, will be made for each channel with a scanning monochromatic source, with a bandwidth less than 0.2 nm; the source output must be normalized to a detector of known spectral sensitivity. The response function thus measured is then normalized to the maximum (peak).

Although the results of this characterization will usually be represented by only the nominal wavelength and FWHM bandpass, the full normalized response function should be recorded for use in detailed wavelength adjustments and comparisons with SeaWiFS channel response functions, which will not be known until shortly before launch. It is further recommended that the internal instrument temperature be monitored during these tests, and that the test be repeated at two temperatures at least 15°C apart, e.g., 10° and 25°C. If a significant shift, greater than 1.0 nm, with temperature of either the center wavelength or bandwidth is detected, then additional temperature calibration points are recommended. Dark offsets must be recorded during each test.

For spectral characterizations of irradiance diffusers, the entire surface of the diffuser should be illuminated by the monochromator's output. In the case of radiance detectors, a diffuser should be used to diffuse the monochromator slit image and uniformly fill the instrument's FOV.

The wavelength response of a monochromator-based radiometer is calibrated by scanning over line sources, with sharp peaks at well known wavelengths. Suitable spectral calibration sources, such as, mercury, cadmium, and neon lamps, are provided by several vendors, together with tabulations of the wavelengths of the emission lines generated by each source.

The width of the slit function of a monochromator may be estimated by scanning over a laser line, e.g., HeNe, at a very small wavelength interval. The instrument FOV must be filled during the test.

It is anticipated that the monochromator-based spectral characterization will not be able to adequately measure leakage of broadly distributed out-of-band radiation; therefore, blocking of blue light in channels longer than 540 nm must be routinely tested. Where continuous wave (CW) argon lasers are available, out-of-band response should be measured at 488 nm. One recommended test that can be performed during the absolute calibrations at $\lambda \leq 640$ nm is the sequenced measurement of three Schott BG-18 filters, each 1 mm thick, using an FEL-type light source. The procedure is to measure the channel signal using each filter separately, then in combination, and comparing the computed and measured transmissions. If significantly higher combined transmission of the three filters in combination is measured relative to the calculated transmittance, then spectral leakage is present. At wavelengths greater than 640 nm, other filters that attenuate the wavelength of interest with a transmission of less than or equal to 0.1 and which pass shorter wavelength light with significantly greater transmission, should be substituted for the BG-18.

Consideration must also be given to unblocked fluorescence by the filters, or other optical elements, as a possible source of light leaks. Methods to test for fluorescence contamination specifically, are not well established at present.

While leakage of blue light into red channels is the most significant oceanographic optical problem, the leakage of red and infrared (IR) light into blue channels can cause significant errors when the instrument is calibrated using a red-rich source. A convenient way to measure this leakage is to place a long wavelength pass, sharp cut, absorbing glass filter that does not exhibit fluorescence, between a broad band, e.g., incandescent, source and the sensor. A non-zero response indicates unwanted out-of-band red response and the need for improved red blocking.

4.1.3 Temporal Response

The temporal response of a spectrometer may be examined by introducing a step function of near full-scale flux to the system using an electrically operated shutter and measuring the system's transient response at 0.1 s, or shorter, intervals. The response should be stable within one digitizing step, or 0.1%, whichever is greater, of the steady state value in one second or less.

4.1.4 Radiance Field-of-View

It is required that the radiance FOV of the instrument be known. The FOV should not normally enter into the absolute calibration, however, if the FOV is fully filled by a calibration source of uniform radiance. In this test, the instrument is placed on a rotational stage with the entrance aperture of the radiometer over the rotation axis. A stable light source with a small filament is placed several meters in front of the instrument, which is then scanned from $-30°$ to $+30°$ in $2°$ increments. The angle positioning should be within $\pm 0.1°$. The on-axis, $0°$, mechanical alignment is made using the window surface as reference, by adjusting to get the reflection of the lamp filament to return on axis. The error in this alignment is approximately $\pm 0.1°$. The in-air measurement angles, θ_a, are converted to corresponding angles in seawater, θ_w, using the relation $\theta_w = \theta_a / n_w$, where n_w is the index of refraction of seawater at the particular wavelength of each channel.

4.1.5 Collector Cosine Response

The directional response of cosine collectors must be characterized. The directional response of the deck cell is determined in air, and the in-water instruments are measured immersed in water. Full spectral determinations are required. For instruments measuring upwelling irradiance $E_u(z, \lambda)$, it is recommended that the cosine response of each instrument be measured individually. For downwelling irradiance $E_d(z, \lambda)$ instruments, checking a production run may be satisfactory if the vendor's material and design are demonstrated to be uniform throughout the run.

Absolute responsivity calibration is done in air with light arriving normal to the plane of the collector. To properly measure all irradiance arriving at the plane of the collector, the response should follow a cosine function such that $E(\theta) = E(0) \cos\theta$, where $E(\theta)$ is the indicated irradiance in response to flux arriving at angle θ with the normal to the plane of the collector, and $E(0)$ is the irradiance the same flux would produce if it were normal to the surface. If this requirement is met, then the on-axis calibration is sufficient and the device will correctly measure the irradiance arriving at the collector regardless of the direction, or directions, from which the light arrives.

The preferred irradiance collector design has an improved cosine response over that of a simple flat plate diffuse collector (Boyd 1951, Tyler and Smith 1979). This improvement is mostly for near-grazing angles ($\theta \sim 90°$ to the normal) and is particularly important when upwelling underwater irradiance measurements are made, i.e., with the collector facing downward. In that case, most of the light is from the sides, in the region of near-grazing angles.

Since $E_d(z, \lambda)$ measurements are to be made underwater, the testing to determine the fidelity of the instrument to the cosine function must be made with the instrument submerged. A description of the suitable experimental procedure follows Petzold and Austin (1988).

The instrument is suspended in a tank of water while supported by a fixture designed to allow rotation about an axis through the surface and center of the collector. A tungsten-halogen lamp with a small filament is enclosed in a housing with a small exit aperture and placed approximately 1 m from a large window in the tank. The collector is placed approximately 25 cm behind this window; an equivalent lamp distance of ≥ 1.25 m is required. A circular baffle should be placed immediately in front of the window to reduce stray light. The water should be highly filtered to the extent that the effects of scattered light are indiscernible.

The equivalent air path lamp distance should be approximately 1.25 m or greater. At this distance, the falloff at the outer edge of a 6 cm diameter diffuse collector would be 0.9994, or -0.06%, when the diffuser is at $\theta = 0°$ with the normal. The net effect over the entire area of the diffuser would be 0.9997 or -0.03%. When $\theta = 90°$, with the diffuser edge-on to the lamp, the distance to the lamp varies for different points on the surface. The net error over the entire surface for this condition is 0.99997 or -0.003%. All other angles fall between these limits.

The signals from the instrument are recorded for $\theta = 0°$ and at $5°$ intervals to $\theta = \pm 75°$ and $2.5°$ intervals over $75° < \theta < 90°$. The readings at $\theta = 0°$ are recorded at the beginning, the middle, and the end of each run and examined as a measure of lamp and instrument stability over the time involved. At least two runs should be made about different axes through the surface of the diffuser. All readings are normalized to 1.000 at $\theta = 0°$ and then compared with the value of the cosine of each angle. If $V(\theta)$ is the normalized measured value, relative local error at angle θ is given as $\frac{V(\theta)}{\cos\theta} - 1$.

Assuming the average response to the four measurements made at each θ (four separate azimuth angles ϕ) adequately represent the overall mean cosine response of the collector, then the error, ϵ, in measuring irradiance over the interval $\theta_n < \theta < \theta_N$ for a uniform radiance distribution is approximately

$$\epsilon = \frac{\sum_{i=n}^{N} \overline{V}(\theta_i) \sin\theta_i \, \Delta\theta}{\sum_{i=n}^{N} \cos\theta_i \sin\theta_i \, \Delta\theta} - 1, \qquad (1)$$

using a simple trapezoidal quadrature. Similarly, for a radiance distribution of the form $1 + 4\sin\theta$, to simulate upwelled irradiance

$$\epsilon = \frac{\sum_{i=0}^{N} \overline{V}(\theta_i)\,(1 + 4\sin\theta_i) \sin\theta_i \, \Delta\theta}{\sum_{i=0}^{N} \cos\theta_i\,(1 + 4\sin\theta_i) \sin\theta_i \, \Delta\theta} - 1, \qquad (2)$$

where $\theta_0 = 0$, $\theta_N = \frac{\pi}{2}$ and $\Delta\theta = \frac{\pi}{2N}$.

The asymmetry of the cosine response, δ, is equivalent to a tilt of an ideal cosine collector with respect to the instrument's mechanical axis, which can be quantified as

$$\delta = \frac{\int_{\theta_1}^{\theta_2} \cos(\theta + \theta_t) \sin\theta \, d\theta}{\int_{\theta_1}^{\theta_2} \cos(\theta - \theta_t) \sin\theta \, d\theta}, \tag{3}$$

where θ_t is the tilt angle. The measured asymmetry is computed as the ratio of sums of measurements at opposite ϕ ($\theta \geq 0$) and $-\pi$ ($\theta < 0$) in the same plane, that is,

$$\delta = \frac{\sum_{i=0}^{\theta_N = \frac{\pi}{2}} \overline{V}(\theta_i, 0) \sin\theta_i \, \Delta\theta}{\sum_{i=0}^{\theta_N = -\frac{\pi}{2}} \overline{V}(\theta_i) \sin\theta_i \, \Delta\theta} - 1, \tag{4}$$

for $\Delta\theta = \pm\frac{\pi}{2N}$.

Variations in asymmetry from channel-to-channel may be due to the placement of the individual detectors behind the diffuser. Any offset of the average asymmetry with the mechanical axis could be due to:

1) a misalignment on the rotating test fixture,
2) a tilt of the diffuser,
3) the detector array not being centered,
4) a nonuniformity of the reflectance of the internal surfaces of the instrument between the diffuser and the sensor array, or
5) a nonuniformity in the diffuser.

4.1.6 Immersion Factors

When the diffuse plastic material used in most irradiance collectors is submerged in water, the transmission through the material becomes less than the transmission in air. As light enters the diffuser a small part is reflected at the air-plastic or water-plastic interface. The relative size of this reflectance, called Fresnel reflectance, depends upon the index of refraction of the medium on either side of the interface. The change is such that the relative amount of light which enters through the interface is larger in water than in air. After entering the plastic diffusing material some of the light will, due to scattering, arrive back at the interface where some gets reflected back into the material and some will exit into the air or water. More of this light is able to leave the plastic and reenter the external medium in water than in air. Thus this mechanism decreases the transmission when the diffusing material is submerged relative to the transmission in air. The net result is a loss of transmission when the diffusing material is submerged. Since the instrument is calibrated in air, an error due to this change in transmission will result when measurements are made with the instrument submerged, unless a correction is made for this immersion effect.

To measure this effect, a suggested and acceptable procedure is as follows: The instrument is placed in a tank of water with the irradiance collector level and facing upward. A tungsten-halogen lamp with a small filament, powered by a stable power supply, is placed at some distance above the water surface. The depth of the water is lowered in steps and readings are recorded for all wavelengths from each carefully measured depth. A final reading is taken with the water level below the collector, i.e., with the collector in the air. The amount of energy arriving at the collector varies with the water depth and is a function of:

a) the attenuation at the air-water interface, which varies with wavelength,
b) the attenuation over the water path, which varies with depth and wavelength, and
c) the change in solid angle of the light leaving the source and arriving at the collector, caused by the light rays changing direction at the air-water interface, which varies with wavelength and water depth.

Using Fresnel reflectance equations, the transmittance through the surface is

$$T_s(\lambda) = \frac{4 n_w(\lambda)}{\left(1 + n_w(\lambda)\right)^2}, \tag{5}$$

where $n_w(\lambda)$ is the index of refraction of the water at wavelength λ. The transmittance through the water path, $T_w(\lambda)$, is

$$T_w(\lambda) = e^{-K(\lambda) z}, \tag{6}$$

where $K(\lambda)$ is an attenuation coefficient of the water and z is the path length in corresponding units.

The change in solid angle with water depth z is given by the factor

$$G(z, \lambda) = \left[1 - \frac{z}{d}\left(1 - \frac{1}{n_w(\lambda)}\right)\right]^{-2}, \tag{7}$$

where d is the distance of the lamp source from the collector surface. The immersion correction factor $F_i(\lambda)$ for irradiance is then calculated for each depth z as

$$F_i(\lambda) = \frac{E_a(\lambda)}{E_w(z, \lambda)} T_s(\lambda) T_w(z, \lambda) G(z, \lambda), \tag{8}$$

where $E_a(\lambda)$ and $E_w(z, \lambda)$ are the irradiance in air and the irradiance underwater at depth z, respectively.

There are two unknowns in Eqs. (5) through (8): the attenuation coefficient of the water $K(\lambda)$ and the immersion factor $F_i(\lambda)$. A minimum of three measurements must be made to solve for $F_i(\lambda)$: one in air to get $E_a(\lambda)$, and two at different water depths for $E_w(z, \lambda)$. The recommended method is to take readings of $E_w(z, \lambda)$ at many depths. Then, using the exact form of (8), a least-squares

regression is solved for the $F_i(\lambda)$ and $K(\lambda)$ terms giving the best fit. The complete derivation of Eqs. (5) through (8) is given in Petzold and Austin (1988).

The absolute calibration for the spectral radiance channels is found by viewing a surface of known radiance in air in the laboratory. When the instrument is submerged in water, a change in responsivity occurs and a correction must be applied. This change in responsivity is caused by the change in the indices of refraction of the different media, in this case air and water. Two optical changes occur, both of which are caused by the change in refractive index. The two effects to be corrected are:

1) the transmission change through the air-window interface during calibration and the water-window interface during data measurement, and
2) the change in the solid angle included in the underwater FOV relative to that in air.

Since $n_w(\lambda)$ is a function of wavelength the correction factor $F_i(\lambda)$ will also be a function of wavelength.

If the refractive index of air is assumed to be 1.000 at all wavelengths, and if $n_g(\lambda)$ is the index of regraction for the window, then, as shown in Austin (1976), the correction for the change in transmission through the window is

$$T_g(\lambda) = \frac{\left(n_w(\lambda) + n_g(\lambda)\right)^2}{n_w(\lambda)\left(1 + n_g(\lambda)\right)^2}, \tag{9}$$

and the correction for the change in the FOV, F_v, is

$$F_v(\lambda) = \left(n_w(\lambda)\right)^2. \tag{10}$$

The index of refraction for a plexiglass window, $n_g(\lambda)$, may be computed using an emperical fit to the Hartmann formula, i.e.,

$$n_g(\lambda) = 1.47384 + \frac{7.5}{\lambda - 174.71}, \tag{11}$$

where λ is the wavelength in nanometers (Austin 1976). The index of refraction for seawater $n_w(\lambda)$ may be similarly computed using an emperical fit of the data from Austin and Halikas (1976),

$$n_w(\lambda) = 1.325147 + \frac{6.6096}{\lambda - 137.1924}. \tag{12}$$

The immersion factor $F_i(\lambda)$ is then obtained as

$$F_i(\lambda) = T_g(\lambda)\, F_v(\lambda) = \frac{n_w(\lambda)\left(n_w(\lambda) + n_g(\lambda)\right)^2}{\left(1 + n_g(\lambda)\right)^2}. \tag{13}$$

4.1.7 Linearity and Electronic Accuracy

The linearity of the radiometric channels must be determined over their expected range of use. The above-surface (deck cell) and underwater irradiance sensors intended for the measurement of downwelling irradiance have full-scale (saturation) values that are not readily obtained with the usual incandescent blackbody sources, such as 1,000 W 3,200 K tungsten-halogen projection lamps. The linearity at the high end of the calibrated range may be determined by using 900–2,000 W high pressure xenon arc lamps, which provide a small, stable source of high intensity, (~6,000 K) radiation. With such lamps, irradiance levels approximating full sunlight can be attained. Using such sources for the high end, and the more easily managed tungsten-halogen lamps over the range below 20–30% of full scale, the linearity of the response characteristic of the radiometric channels can be assessed. The flux should be changed in 5 db (0.5 log) or less steps using a proven and accepted procedure for controlling irradiance such as inverse square law, or calibrated apertures. These suggested procedures for testing linearity at the higher levels are not well established in practice, and research is needed to determine the precision which can be attained.

If departures from linearity are found, they must be incorporated into the calibration function for the instrument and be properly applied to the raw level-1 data to obtain calibrated level-2 irradiance and radiance data. Level-1 and level-2 data are defined in section 6.1.

Ancillary sensors, such as, transmissometers, should be characterized for the linearity and accuracy of the measurement covering the full output range of the sensor. Instruments with manual or automatic range dependent gain changing should be tested annually (at a minimum) for scale offset and linearity in each range. Errors exceeding 0.1% of reading over the normal range must be corrected.

Other characteristics of electronic sensor systems may adversely affect measurement accuracy. During the design and engineering prototype development of a radiometer, the design and implementation must be analyzed to characterize, and correct as needed, possible effects of hysteresis, overload, recovery times, cross talk between either optical transducers or electronic channels, and sensitivity to orientation in the Earth's magnetic field, which is particularly likely with photomultiplier tubes.

4.1.8 Temperature Characterization

Two major types of temperature-induced variation may be seen in an optical radiometric instrument: 1) offset or *dark* changes, and 2) scale *responsivity* changes. Each underwater instrument must be individually characterized over the range -2–40° C. In the case of deck cells, the temperature range for testing should be extended to -10–45° C. If sensors exhibit temperature coefficients greater than 0.01% per degree-Centigrade over this temperature range, they should be fully characterized over their respective ranges to establish the means and precision with which post-acquisition processing can be used to correct for temperature dependency. Although knowledge of the zero, or dark current, drift is essential for working at the lowest radiances or irradiances, more significant near-surface errors

may be induced by temperature variations in responsivity. These possible responsivity changes must be individually determined across the spectrum.

In the above discussion, the temperatures cited are *environmental* temperatures, but any correction must use the temperature of the affected element, which is normally in the interior of the instrument. This is best accomplished by routinely using temperature sensors placed at critical locations within the instrument. For highest precision, dynamic temperature testing involving temporal transients, as well as possible temperature gradients within an instrument, may be appropriate.

4.1.9 Pressure Effects

Pressure can cause radiometric measurement errors by deforming irradiance collectors. Pressure coefficients associated with Teflon-based irradiance diffusers are known to exist, but they are not uniform and there may be hysteresis effects. It is recommended that each type of irradiance detector be examined for variations in responsivity with pressure. If a significant effect is observed, then pressure-dependent responsivity coefficients should be determined separately for each instrument and collector. The pressure characterization should also test for, and quantify, hysteresis and temporal transients in responsivity under a time varying pressure load. The characterization of pressure effects has not previously been common practice, and the requisite procedures are therefore poorly defined; new protocols must be developed.

4.1.10 Pressure Transducer Calibration

The radiometer's pressure transducer, which is used to measure instrument depth during profiles, should be tested and calibrated before and after each major cruise.

4.2 Radiometric Standards

4.2.1 Lamp Irradiance Standards

The options available for radiometric calibration standards are limited to standard sources or standard detectors. Lamp standards of spectral radiance and irradiance are provided by NIST and various commercial standardizing laboratories and manufacturers who furnish NIST traceable secondary standards. The uncertainty cited for these standards by NIST is at best 1% in the visible and 3% is a more realistic estimate of absolute accuracy attainable using lamp standards alone. Over the calibration range from 250–2,500 nm, the uncertainty is approximately 6% at the endpoints.

The lamp standard of spectral irradiance is traditionally used for radiometric calibration, mainly because of its ease of use compared to the spectral radiance lamp. NIST publishes guidelines for the setup, alignment, and use of these standards. The vendors that manufacture and calibrate these lamps also issue guidelines for their use.

4.2.2 Radiance

Spectral radiance may be obtained by using an irradiance standard lamp and a Lambertian reflecting plaque. The standard lamp is positioned on-axis and normal to the center of the plaque at the calibrated distance. The instrument or detector package to be calibrated is nominally positioned to view the plaque at 45° measured from the axis. The radiance, then, is given by

$$L(\lambda) = \frac{\rho(\lambda)E(\lambda)}{\pi}, \tag{14}$$

where $\rho(\lambda)$ is the bidirectional reflectance of the plaque for 0° incidence and 45° viewing, $E(\lambda)$ is lamp irradiance, and the total FOV of the instrument being calibrated is filled by the illuminated plaque.

The known radiance of the plaque provides an accuracy comparable with that of the irradiance standard lamp, i.e., $\leq 3\%$, for calibrating a radiance detector with a very narrow FOV ($\sim 1°$. Large plaques, e.g., 40×40 cm, have been successfully used to calibrate radiance sensors having up to 25° full-angle FOVs. Intercomparisons of calibrations, made using this technique at different laboratories, of MER-series radiance sensors (full-angle FOVs ranging from 20–24° in air) have generally agreed within ~5%.

A better approach to calibrating multispectral radiance sensors is to view an integrating sphere that is uniformly illuminated by stable, appropriately baffled lamps, and which has an exit port large enough to completely fill the sensor's FOV. The sphere and exit port must be large enough to place the radiance sensor far enough away to prevent significant secondary illumination of the sphere walls due to retro-reflection off the sensor's entrance optics; if the sensor is too close, the retro-reflected light will both increase and distort the uniformity of the radiance distribution within the sphere. Traditionally, the calibration of an integrating sphere radiance source has been accomplished by appropriately transferring the known output from a standard lamp irradiance source.

Method 1: The approach used at NASA/GSFC is to view the irradiance output of the lamp, initially, and then the sphere, with a spectrometer equipped with integrating input optics (McLean and Guenther 1989; Walker, Cromer, and McLean 1991). The spectral irradiance responsivity of the radiometer is calibrated using the lamp data, and the (assumed) Lambertian radiance of the sphere is determined by dividing the measured spectral irradiance output of the sphere by π.

Method 2: An alternative method is to calibrate a stable narrow FOV radiometer by viewing the standard lamp output reflected from a plaque, as

described above. The output from the sphere's exit port is then viewed within this radiometer. The radiometer should also be used, at this point, to map the angular distribution of radiance in the sphere as viewed through the exit port. This important verification of a uniform radiance distribution is not possible when Method 1 is used to calibrate sphere radiance. A promising variant of Method 2 is to calibrate the sphere using a self-calibrating radiometer (Palmer 1988).

4.2.3 Radiance Standardization

Detectors of the type embodied in the United Detector Technology QED-200 radiometer are 99.99% quantum efficient. Palmer (1988) shows how such a detector may be combined with precision apertures and well-characterized filters to measure self-calibrated spectral radiance with an absolute accuracy less than 1%. A calibration approach based on such radiometer standards is essential to achieve 1% internal consistency in the radiometric *accuracy* of measurements made for SeaWiFS radiometric validation.

It is worth emphasizing here that the essential objective is to achieve internal consistency in the SeaWiFS optical database through uniform application of calibration techniques based on a common radiometric standard with precision approaching 1%, or less if possible. An important, but not essential, goal is to establish NIST traceable absolute accuracy of less than 1% with this standard.

A self-calibrating radiometer may be used directly to calibrate and map the radiance distribution of integrating sphere sources (Method 2 in section 4.2.2 above). The self-calibrating radiometer standard of radiance may be transferred to a stable lamp source of irradiance through the reversal of the reflectance plaque technique, described above for calibrating radiance sensors with a standard lamp irradiance source.

These ideas, as yet, have not been incorporated into a practical and widely accepted set of procedures for calibrating oceanographic or airborne radiometers using self-calibrating radiometric standards. A significant level of laboratory work must be done to establish the repeatability of results attainable through these techniques under a variety of conditions, and to codify that experience into calibration protocols. The spectral responsivity of the QED-200 type detector is known, for example, to vary systematically with temperature (Kohler et al. 1990), and the spectral transmission functions of the filters in a self-calibrating radiometer must be re-characterized at a frequency that will guarantee the accuracy of the calculated radiance. This frequency must be established through experience, but a reasonable first guess is that filter transmission functions should be remeasured every few months.

One SeaWiFS goal is to base radiometric validation on shipboard, moored, and airborne radiometry with 1% accuracy. If that goal is to be substantially achieved, then the work described above to establish *new* calibration standards and protocols must be pursued vigorously over the next two years.

4.2.4 Traceability and Comparisons

The variety of instruments available for validation measurements makes it imperative that some common calibration traceability exists. Recognizing that it would be impractical to characterize and calibrate all oceanographic and aircraft radiometers at GSFC, several remote calibration facilities should be established, and working standards and protocols used at these facilities should all be traced directly to those at the GSFC calibration facility. This organizational structure is shown schematically in Fig. 2. Methods of standards intercomparison may include use of NIST calibrated filter radiometers to track and document the operation of each facility (radiometer wavelengths to be determined). Round-robin *blind* calibration comparisons of a *standard* instrument would also be implemented to benchmark the internal consistency of calibrations performed at the various facilities.

4.2.5 Portable Standards

Stable lamp sources in rugged, fixed geometric configurations should be used to track instrument performance in between radiometric calibrations. Irradiance channels can be monitored with irradiance sources at fixed distances from the collectors, while radiance sources can be monitored by filling the FOV with diffuser plates placed in front of the irradiance sources, or by using integrating cavity sources. In each case, careful attention must be given to fixing specific geometries of source and detector in each use. The stability of the lamp output and the repeatability of measurement must be sufficient to detect 2% variations in an instrument's performance. An instrument should be connected to the portable standard and its response recorded daily, keeping a record of instrument responsivity throughout an experiment since, these sources would provide an essential warning of problems if they appear.

The portable field reference source must be available when the complete radiometric calibrations are performed so that a baseline may be established and maintained for each sensor channel (section 4.1.1). These sources are not a substitute for complete calibrations. However, the temporal record they provide will be invaluable in cases where the pre- and post-cruise calibrations disagree or if the instrument is disturbed, e.g., opened between calibrations, or the data quality are otherwise suspect. These portable standards are an important part of the recommended instrument package.

Although several manufacturers offer somewhat portable irradiance and radiance sources, there has been very little previous work to validate and use portable radiometric standards to test oceanographic radiometers in the field. Therefore, detailed hardware specifications and procedural

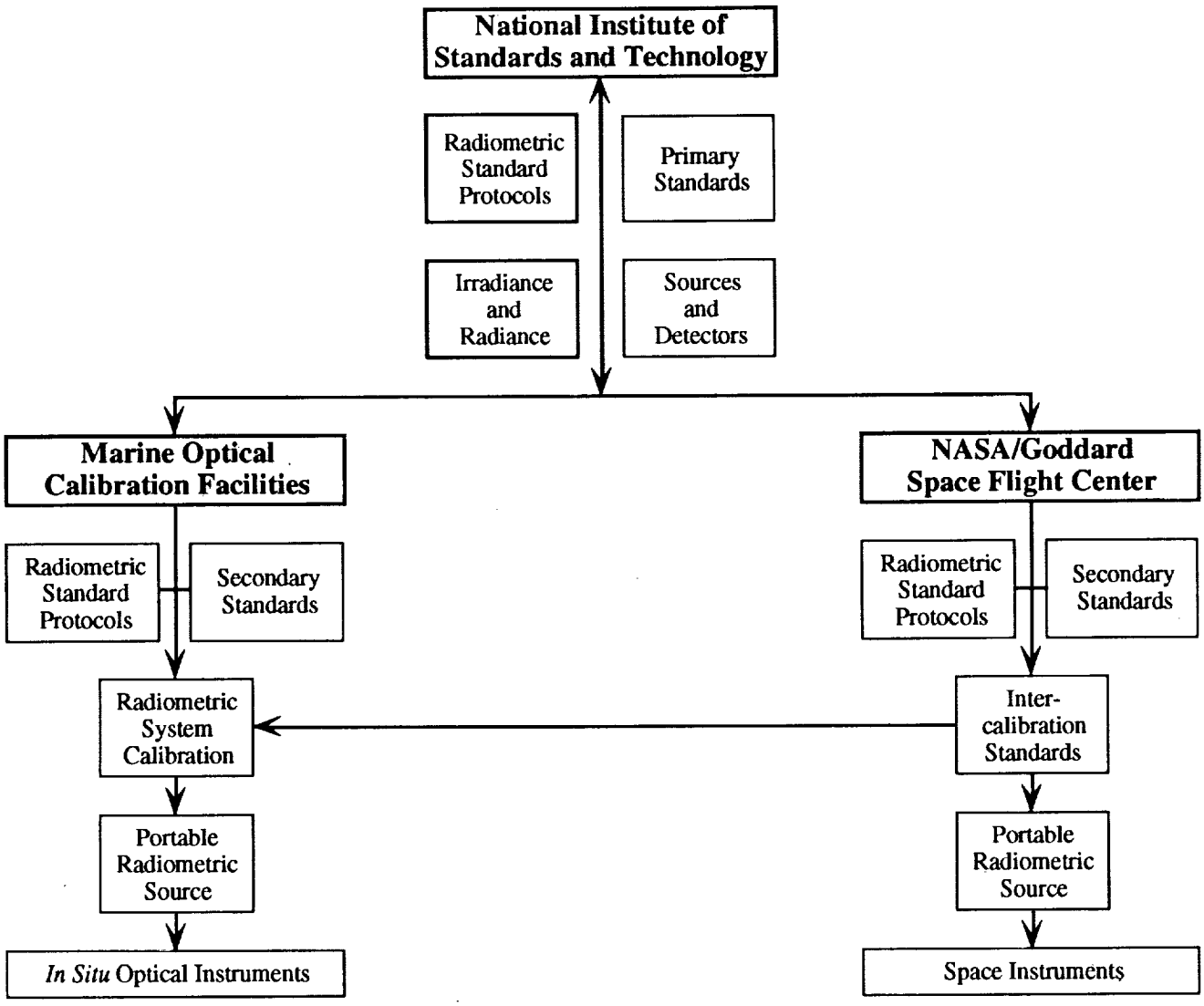

Fig. 2. Organizational structure for optical instrumentation characterization and calibration.

protocols must be developed through a series of laboratory and field tests using candidate equipment and standards.

4.3 Airborne Radiometers

In general, the protocols specified in section 4.1 for oceanographic radiance sensors are applicable for characterizing and calibrating airborne radiometers. Obvious exceptions are that immersion and underwater FOV characterizations are not appropriate for aircraft sensors.

Polarization sensitivity is more critical in airborne than underwater radiometry. If a radiometer measures polarization components of radiance, then its responsivity and rejection of cross-polarization radiance must be characterized for each component channel. For aircraft radiometers, as with SeaWiFS, sensitivity to linear polarization must be less than 2%, and the actual degree of polarization sensitivity must be characterized for each channel.

A generalized protocol for characterizing a radiometer's polarization sensitivity is given here. The instrument should view a source of linearly polarized radiance, and its apparent radiance response $L_1(\lambda)$ should be recorded. The instrument should then be rotated 90° about its FOV axis, still viewing the linearly polarized radiance source, and the apparent radiance response $L_2(\lambda)$ should be recorded. The instrument's polarization sensitivity will be calculated as

$$P(\lambda) = \left| \frac{2(L_1(\lambda) - L_2(\lambda))}{L_1(\lambda) + L_2(\lambda)} \right|. \quad (15)$$

As required for the SeaWiFS sensor, airborne radiometers must satisfy $P(\lambda) < 0.02$.

A very simple, semi-quantitative test of a radiometer's polarization sensitivity can be performed outdoors on a cloud- and haze-free day. The instrument should be pointed at the sky in the zenith-sun plane at an angle of approximately 90° from the sun, and its response $L_1(\lambda)$ recorded. Since singly-scattered Rayleigh radiance

is 100% polarized at a scattering angle of 90°, if aerosol scattering is small, the sky radiance viewed at this angle will be strongly polarized. If the instrument is then rotated 90° about its FOV axis to measure $L_2(\lambda)$, an approximate estimate of $P(\lambda)$ may be computed, as above.

Specification of detailed protocols for laboratory characterization of a radiometer's polarization sensitivity will require more attention than is available here. In particular, protocols should be developed which describe in detail:

1) laboratory setups for producing a stable, uniform, extended source of linearly polarized radiance; and
2) laboratory procedures for measuring the actual degree of polarization of the polarized radiance source and for determining the accuracy of the polarization sensitivity estimate achieved using a particular experimental setup.

Temperature dependence of an airborne radiometer's polarization sensitivity should initially be characterized at 5° and 30° C. If significant differences in $P(\lambda)$ exist at these extremes of instrument operating temperatures, then polarization sensitivity measurements should be made at several additional temperatures in that range.

4.4 Calibration of IOP Meters

Calibration of beam transmissometers has traditionally been carried out by means of measurements in air with a subsequent adjustment for changes in the Fresnel reflections of the windows upon submergence into water. The 660 nm transmissometers produced by Sea Tech are independently calibrated at the factory against particle-free water of measured transmittance, after which calibration is maintained via frequent air calibrations. This approach is adequate until a pure water standard, using water generated by reverse osmosis, has been developed and proven reliable for shipboard use. It is anticipated that the pure water standard will be proven by the time of the SeaWiFS deployment. The pure water standard will be particularly useful for pump-through devices, such as the spectral absorption and attenuation devices now being developed, as they can be connected to the pure water system after each cast to provide frequent calibration, and make it possible to closely track any deterioration of the instruments. Daily air calibrations of systems without pumps are desired.

Calibration of the scattering devices must be handled on a case-by-case basis and calibration standards need to be developed along with the instruments.

4.5 Calibration of Sun Photometers

Sun photometer calibrations should be performed at least annually, when used consistently, through a Langley calibration procedure. In this procedure, the solar signal transmitted through the atmosphere is measured over different air masses, i.e., at different solar zenith angles, throughout the course of the day. The validity of using these measurements as *calibration* of a sun photometer hinges strongly on the assumption that aerosols are uniformly distributed and do not vary throughout the day. Therefore, these Langley calibrations should be performed in areas of atmospheric stability with low aerosol loading. Suitable locations include the astronomical observatories at Mauna Loa, Hawaii, and Kitt Peak, Arizona. In between these calibrations, radiance calibrations with standard lamps may be used as a stability check (Shaw 1976).

Temperature stability should be characterized for each instrument. Linearity and spectral calibrations should be performed with the same frequency as the absolute calibration; this work must be done in the laboratory.

4.6 Radiance Distribution Cameras

Absolute and spectral calibrations should be performed on the radiance distribution camera before and after each cruise. A full characterization of the instrument should be performed initially, including camera lens roll-off characteristics for each camera (Voss and Zibordi 1989). If attenuation devices are used to prevent solar saturation, these should be calibrated frequently to track drift. Linearity calibrations should also be performed with the same frequency as the absolute and spectral calibration. Procedures for characterizing this class of instruments are essentially the same as for other radiance detector systems. Each individual detector element in the detector array is essentially regarded as an independent radiometer.

4.7 Pigment Calibrations

HPLC equipment used to measure phytoplankton pigment concentrations is to be calibrated using standards distributed under the auspices of the U.S. JGOFS Program (JGOFS 1991). Bench fluorometers used to measure concentrations of extracted chlorophyll *a* and phaeopigments should be calibrated using authenticated standard chlorophyll *a* adopted for HPLC (JGOFS 1991). *In situ* fluorometers should be calibrated against extracted chlorophyll *a* from concurrent bottle samples.

4.8 CTD Calibrations

The conductivity probe, temperature probe, and pressure transducer of the CTD should be re-calibrated before and after each major cruise by a properly equipped physical oceanographic laboratory, including those maintained by many CTD manufacturers. In addition, the conductivity probe should be independently calibrated during the course of each cruise by obtaining salinity water samples (section 5.2.3) simultaneous with CTD readings. These salinity samples are to be analyzed, either at sea or ashore, with a laboratory salinometer calibrated with International Association for the Physical Sciences of the Ocean (IAPSO) Standard Seawater.

If simultaneous deployment of the CTD with optical instruments having independent pressure transducers is practical, the two depths measured by the different instruments should be compared over the range of the cast. If depth measurements disagree significantly, these comparisons may be used to correct whichever transducer is found to be in error through analysis of pre- and post-cruise pressure transducer calibrations.

5. MEASUREMENT PROTOCOLS

5.1 Spectral Irradiance and Radiance

Determinations of E_d, E_u, and L_u, both near the surface and as profiles, are required for calibration and validation of satellite sensed water-leaving radiances. Near-surface measurements through at least the top three optical depths are needed to reliably extrapolate to $z = 0$; a profile through at least the top optical depth is essential. To better characterize the water column for remote sensing applications, e.g., primary productivity estimation, deeper profiles should be made to 200 m or seven optical depths whenever possible. Sea bed reflection influences on L_u and E_u should be avoided for SeaWiFS validation and algorithm development by collecting data only from water deeper than six optical depths for $E_d(490)$; remote sensing applications for optically shallow situations where bottom reflectance is present are not within the scope of these protocols.

The two primary error sources in the determination of these optical parameters are: the perturbation of the in-water radiance field by the ship (Gordon 1985, Smith and Baker 1986, Voss et al. 1986, and Helliwell et al. 1990), and atmospherically induced variability in radiance incident on the sea surface during in-water measurements (Smith and Baker 1984). The influence of ship shadow on profiles of E_d, E_u, and L_u is dependent upon: solar zenith angle, the spectral attenuation properties of the water column, cloud cover, ship color and size (length, beam, draft, and freeboard), and instrument deployment geometry. Atmospheric variability depends primarily upon sun elevation and cloud cover. The near surface in-water data also show variability caused by wave focusing, which can be minimized at a fixed depth by averaging over several wave periods, but which can pose severe problems in profiles when the instrument descends at speeds of 0.5–1 m s^{-1}. Raman scattering and fluorescence result in second-order errors near 490 nm (CDOM fluorescence); at longer wavelengths, contributions from phycoerythrum and chlorophyll *a* fluorescence and water Raman scattering are significant.

5.1.1 Ship Shadow Avoidance

The complete avoidance of ship shadow, or reflectance, perturbations is a mandatory requirement for all radiometric measurements to be incorporated into the SeaWiFS validation and algorithm database. The influence of ship shadow is best characterized in terms of attenuation length $1/K_d(\lambda)$ (Gordon 1985). Because L_W is required with an accuracy of 5% or better, the protocol requires that vertical profiles collect data outside the effects of ship perturbation to the radiant energy field. To accomplish this, the instrument must be deployed from the stern, with the sun's relative bearing aft of the beam.

Estimates of the minimum distance away from the ship, expressed in attenuation lengths to minimize error, under conditions of clear sunny skies, are given below. For $E_d(\lambda)$ measurements, the general equation for distance away, ξ, in meters is given as

$$\xi = \frac{\sin(48.4^\circ)}{K_d(\lambda)}. \tag{16}$$

The distance from the ship is required to be $3/K_u(\lambda)$ m for $E_u(\lambda)$ and $1.5/K_L(\lambda)$ m for $L_u(\lambda)$ measurements. These distances should be increased if the instrument is deployed off the beam of a large vessel.

A variety of methods have been used to deploy optical instruments beyond the influence of the ship. During CZCS algorithm development, floating plastic frames were equipped with small winches to obtain near surface optical profiles some distance away from the ship. An umbilical cable provided power and data transfer. These platforms, while being somewhat difficult to deploy, worked well at avoiding ship shadow. Alternatively, extended booms can be used to deploy the instrument away from the ship which has the advantage of allowing relatively rapid deployment and simultaneous rosette bottle sampling. As a point of caution, however, long booms may accentuate unwanted vertical motions due to ship pitch and roll.

Waters et al. (1990) used an optical free-fall instrument (OFFI) that allows optical data to be obtained outside the influence of ship perturbation. In addition, the OFFI approach allows optical data to be obtained independently from violent ship motion, which may be transmitted to the instrument via the hydrowire, especially on a long boom. Yet another method for the deployment of optical sensors is via a remotely operated vehicle (ROV). Smith et al. (R. Smith, pers. comm.) have deployed a spectrometer on an ROV and obtained data completely free of ship influences.

The above criteria for ship shadow avoidance are admittedly very conservative. Unfortunately, the above cited models and observations provide only approximate guidance on minimum distances at which ship reflectance and shadow effects become insignificant under all circumstances. Therefore, the SPSWG has adopted relatively extreme distance criteria, recognizing that in many specific combinations of lighting conditions, ships and optical properties, ship shadow, and reflection effects may become unimportant much closer to the ship.

The essential requirement is that each investigator establish that his measurements of E_d, E_u, and L_u submitted for SeaWiFS validation and algorithm development are

free from ship induced errors. The simplest way to do this is to adhere to the above distance criterion, which is not difficult when using either a tethered free-fall system, or instruments mounted on an ROV. In other cases, it is incumbent upon the investigator to otherwise demonstrate the absence of ship effects, e.g., through analysis of a series of profiles at increasing distance.

At wavelengths where attenuation lengths are the same order of magnitude as, or less than, the size of the instrument package, e.g., in the ultraviolet-B (UVB) or red and near IR spectral regions, care must be taken to consider possible perturbation of the radiance field by the instrument package. Methods of accounting for *self-shadowing* by the instrument are not well established and new measurement approaches must be developed (section 5.1.6).

5.1.2 Depth Resolution in Profiles

The instrument sampling rate and the speed at which the instrument is lowered or raised through water should yield at least 2 and preferably 6–8 samples per meter.

5.1.3 Instrument Dark Readings

The dark current of optical sensors is frequently temperature dependent. Consequently, accurate radiometric measurements require careful attention be given to dark current variability. It is recommended that each optical measurement be accompanied by a dark current measurement. When there is a large difference between the temperature on deck and the water temperature, the instrument should be allowed to equilibrate with the water at the start of each cast.

Deep casts, e.g., 500 m, may permit the determination of the dark current in each optical channel at the bottom of each cast. However, many instruments are not designed to be safely lowered to 500 m, and this approach is usually not feasible. Furthermore, there is some intrinsic uncertainty over possible contamination by bioluminescence when dark readings are obtained in this way. If the instrument is equipped with a shutter, dark currents can be measured at any depth in the cast. If the dark current is not determined during the cast, it should be determined as soon as possible after the instrument is returned to the deck.

Temperature effects on sensor responsivity can be significant and should not be ignored. Therefore, sensors should be equipped with thermistors on detector mounting surfaces to monitor temperatures for data correction. Otherwise, deck storage should be under thermally protected conditions prior to deployment and on-deck determination of dark voltages.

5.1.4 Surface Incident Irradiance

Atmospheric variability, especially under cloud cover, leads directly to variability of the in-water light field and must be corrected to obtain accurate estimations of optical properties from irradiance or radiance profiles. First order corrections for this variability can be made using above water (on deck) measurements of downwelling spectral irradiance, $E_s(\lambda) = E_d(0^+, \lambda)$. Smith and Baker (1984) and Baker and Smith (1990) theoretically computed the irradiance just below the air-water interface, $E_d(0^-, \lambda)$, from deck measurements to correct in-water profile data.

The deck sensor must be properly gimballed to avoid large errors in $E_s(\lambda)$ due to ship motion in a seaway. However, improper gimballing can actually accentuate sensor motion under some circumstances, and this aspect of a shipboard radiometer system must be engineered with care.

Waters et al. (1990) demonstrated a method to more directly determine $E_d(0^-, \lambda)$ by deploying an Optical Surface Floating Instrument (OSFI) to obtain continuous optical data just below the air-water interface. These $E_d(0^-, \lambda)$ are used as a normalization factor to correct for variations in irradiance during a vertical profile, or over the period of a day for a series of profiles. Research is needed to determine whether this should be the preferred approach for SeaWiFS validation measurements.

5.1.5 Instrument Attitude

An instrument's vertical attitude is a critical factor in measurements of $E_d(z, \lambda)$ and $E_u(z, \lambda)$ and is only slightly less so for $L_u(z, \lambda)$. Therefore, roll and pitch sensors must be installed in the underwater radiometers used for the SeaWiFS project. The data from the attitude sensors are to be recorded concurrently with the radiometric data and are to be used as a quality control indicator. It is not deemed necessary to determine or control attitude determination errors resulting from surface wave-induced accelerations at very shallow depths.

5.1.6 Instrument Self-Shading

Gordon and Ding (1992) modeled the errors introduced by an instrument's own shadow in direct measurements of $L_u(\lambda)$ and $E_u(\lambda)$. For this error to be less than 5%, without modeled corrections, the instrument radius r must satisfy $r \leq \left(40a(\lambda)\right)^{-1}$ for $E_u(\lambda)$ and $r \leq \left(100a(\lambda)\right)^{-1}$ for $L_u(\lambda)$. They calculate for $\lambda = 865$ nm in pure water, as an example, that the instrument radius must be approximately 0.3 cm to measure $E_u(865)$ with $\leq 5\%$ error; the instrument radius must be significantly smaller for direct measurement error in $L_u(865)$ to be $\leq 5\%$.

Gordon and Ding (1992) also propose a simple model for correcting $L_u(\lambda)$ and $E_u(\lambda)$ for self-shadowing. They write

$$\hat{L}_u(\lambda) = \frac{\tilde{L}_u(\lambda)}{1 - \varepsilon(\lambda)} \tag{17}$$

and

$$\varepsilon(\lambda) = 1 - e^{-k' a(\lambda) r}, \tag{18}$$

where $\hat{}$ is the true value, $\tilde{}$ is the measured value, $k' = y/\tan\theta_{0w}$, θ_{0w} is the refracted solar zenith angle and y is

an empirical factor for which they give values determined by fitting their model results ($y \sim 2$). A similar correction, with a different table of values for y applies to $E_u(\lambda)$.

When the above geometric corrections are applied, Gordon and Ding (1992) estimate errors $\leq 5\%$ in $L_u(\lambda)$ could be determined from measurements with instruments having diameters $\leq 24\,\mathrm{cm}$ for $\lambda \leq 650\,\mathrm{nm}$, and with instruments of diameter $\leq 10\,\mathrm{cm}$ for $650 < \lambda \leq 700\,\mathrm{nm}$ at solar zenith angles $\theta_0 \geq 20°$ and chlorophyll concentrations $\leq 10\,\mathrm{mg\,m^{-3}}$. To measure $L_u(\lambda)$ correctable to less than 5% error at $\theta_0 = 10°$ (chlorophyll concentrations $\leq 10\,\mathrm{mg\,m^{-3}}$), instrument diameters must be $\leq 12\,\mathrm{cm}$ for $\lambda \leq 650\,\mathrm{nm}$ and $\leq 5\,\mathrm{cm}$ for $650 < \lambda \leq 700\,\mathrm{nm}$. Even with these corrections, however, instrument diameters $\leq 1\,\mathrm{cm}$ must be used to assure self-shading $L_u(\lambda)$ errors $\leq 5\%$ at 780 and 875 nm.

Experimental tests are needed to confirm the accuracy in $L_u(\lambda)$ and $E_u(\lambda)$, which can be obtained using corrections of the form proposed by Gordon and Ding (1992). These experiments should be carried to completion prior to SeaWiFS launch. In the interim, until confirming experimental results are available for fine tuning, corrections should be made using the coefficients and procedures recommended by Gordon and Ding (1992) on the basis of their Monte Carlo simulations.

5.2 Ancillary Profiles

Beam transmittance, CTD profiles, and chlorophyll *a* fluorescence should be measured at the same stations as the irradiance and radiance measurements. Preferably, these auxiliary profiles should be measured simultaneously with, or otherwise immediately before or after, the radiometer profiles. If possible, these profiles should be made in conjunction with bottle samples. For the verification of the satellite sensor, these data will be used as a guide to the uniformity of the first optical depth and to determine water bottle sampling depths.

The IOP, fluorescence, and CTD profiles will also be used as a guide for, and constraints on, the smoothing of $K(z)$ from the radiometric profiles. The location of maxima and other features in the structure of these profiles identify inflection points for segmenting the optical profiles into finite depth elements (layers) for the analysis described by Mueller (1991) or Petzold (1988). Both of these techniques use multiple segments for the statistical fit of analytic functions to the measured profiles. These data will also be used to develop and validate pigment and primary productivity algorithms.

5.2.1 Beam Transmittance

The windows on the beam transmissometer must be cleaned with lens cleaner or a mild detergent solution, and a soft cloth or tissue, rinsed with distilled water, and finally rinsed with isopropyl alcohol and wiped dry. An approximate *air calibration* reading should be made before every cast to verify the windows are clean. A transmissometer *dark voltage* should also be measured at this time. These *on-deck air calibrations* are not very reliable measures of temporal drift or degradation in the instrument's source or detector, however. In the humid, or even wet, environment on the deck of a ship, the windows are often quickly obscured by condensation, and the glass tends to absorb enough water to affect transmission slightly (J.R. Zaneveld, pers. comm.). A very careful air calibration shall be performed before and after each cruise under dry laboratory conditions. During an extended cruise, the instrument should be moved to a dry location in a shipboard laboratory, and after allowing several hours for the windows to dehydrate, a careful air calibration should be performed. Only the laboratory air calibrations should be used in the final processing of beam transmissometer data.

Both the laboratory condition air calibration and dark voltages, and the factory calibration voltages, assume the data acquisition system measures instrument response as true volts. It is imperative, therefore, to calibrate the end-to-end analog-to-digital (A/D) data acquisition system and characterize its response to known input voltages. Corrections of the form

$$\widehat{V} = a(T) + b(T)\widetilde{V}, \tag{19}$$

where T is temperature, must usually be applied to external voltage inputs recorded with the A/D circuits of CTDs or profiling radiometer systems. The range dependent A/D bias coefficients should be determined at approximately 5° C intervals over the range from 0°–25° C to characterize the temperature sensitivity of the data acquisition system.

For the development of bio-optical algorithms describing the inherent and apparent optical properties of the water, and for algorithms estimating primary productivity, more stringent requirements are recommended for transmissometer calibration and characteristics. Spectral measurements of beam transmittance should be made with absolute accuracies of 0.1% transmittance per meter, or 0.001 $\mathrm{m^{-1}}$ beam attenuation coefficient $c(\lambda)$. These accuracies may be achieved using new calibration techniques, which include a clean-water standard such as a continuous flow of reverse osmosis water, but methods and protocols suitable for use at sea are presently under study (J.R. Zaneveld, pers. comm.).

5.2.2 Chlorophyll *a* Fluorescence

An *in situ* fluorometer should be employed to measure a continuous profile of chlorophyll *a* fluorescence. The fluorometer should be mounted on the same underwater package as the transmissometer, CTD, and water sampler, if one is employed. If possible, the radiometer should also be on this package.

The A/D channel used to acquire and record signal voltages from the *in situ* fluorometer must be calibrated,

and its temperature-dependent response to known voltage inputs characterized. During processing, a correction of the form given in (19), must usually be applied to values recorded with the A/D circuits of CTDs and profiling radiometer systems. As in beam transmittance, the range dependent A/D bias coefficients should be determined at approximately 5° C intervals over the range from 0–25° C to characterize the temperature sensitivity of the data acquisition system.

Zero fluorescence offsets should be measured on deck before and after a cast; the optical windows should be shaded to avoid contamination of the zero offset value by ambient light. Before each cast, the fluorometer windows should be cleaned following the manufacturer's instructions.

For chlorophyll *a* determinations, fluorescence measurements should be compared to HPLC and extracted pigment measurements from discrete water samples, for comparison with JGOFS standard measurements and historical databases. *In situ* fluorescence measurements will be used to provide continuous vertical profiles of interpolated pigment concentration using bottle samples as tie points.

5.2.3 CTD Profiles

Vertical profiles of CTD should be measured to at least the depth of the deepest bio-optical profile. If the station schedule will permit it, sections of CTD casts extending to 500 m, or deeper, will be useful for computing relative quasi-geostrophic currents and shear, which may affect the advection and mixing of bio-optical properties during a cruise. A real time analysis and display of the CTD profile, together with displays of $c(660)$ and *in situ* fluorescence profiles, should be available as a guide in choosing the depths at which water sampling bottles will be closed.

If possible, a few deep ($\geq$ 1500 m) CTD and bottle sample profiles should be made during each cruise to obtain data for calibrating the CTD's conductivity probe. During these *CTD calibration casts*, water samples should be taken at depths where the vertical gradient of salinity is very small. This practice will minimize errors in the conductivity calibration resulting from the spatial separation of the water bottle and CTD profile. The bottled salinity samples may be stored for post-cruise analyses ashore at a laboratory equipped with an accurate salinometer and IAPSO Standard Seawater, if suitable equipment and standard water are not available aboard the ship.

5.3 Atmospheric Measurements

5.3.1 Sun Photometry

Measurements of the direct solar beam, using the sun photometer, should be performed during the optical stations. If sky radiance distribution measurements are performed, it is important that these measurements are performed contemporaneously. While the preferred method of determining the optical thickness of the atmosphere is by measuring the solar transmission as a function of solar zenith angle, rarely are the atmospheric conditions stable enough at sea for this method to work. Thus a stable, well calibrated photometer can be used with measurements at a single zenith angle to obtain the solar transmission and thus the aerosol optical depth.

Atmospheric measurements should be performed only when no clouds, including high cirrus, obstruct the solar disc. Careful documentation of sky conditions are important, as are accurate recordings of time of day and station location. The latter data are important in determining the true solar zenith angle and, hence, the air mass in the solar path. It should also be obvious that care should be taken to avoid ship perturbations (stack gas) from interfering with the measurements. Ancillary measurements such as barometric pressure are important in separating Rayleigh scattering from the aerosol scattering.

5.3.2 Sky Radiance Distribution

Complete sky radiance distributions should be measured with a radiance distribution camera during the SeaWiFS radiometric initialization and validation optical stations. For this purpose, it is critically important that these measurements be obtained whenever totally clear sky conditions persist. Coincident with these measurements, sun photometer measurements should be obtained. When locating the camera system for these measurements, it is important the FOV be as unobstructed as possible. While it would be optimum to have a completely unobstructed FOV, this is often not practical. Therefore, during measurements, at least one hemisphere, defined by the sun-zenith plane, should be unobstructed; through symmetry, this should yield a complete radiance distribution.

Ship perturbations must be avoided. It is important to document where the instrument is located and what possible perturbations might exist, even though these effects may be obvious in the data.

It would also be highly desirable to add sky radiance measurements to every SeaWiFS algorithm development and validation cruise. Gordon (1989) rigorously demonstrated the importance of determining $\overline{\mu}_d$, the mean cosine for downwelling radiance (Morel and Smith 1982), for the bio-optical interpretation of $K_d(\lambda, z)$. Gordon (1989) also showed for cloud-free skies how a reasonable estimate of $\overline{\mu}_d(0^+)$ can be obtained from spectral irradiance deck cell measurements with and without the sun blocked from the irradiance collector's view. This procedure should be done routinely, whenever it is practical to do so. Unfortunately, the collective scientific experience is that cloud-free skies rarely occur at ocean optical stations.

If a calibrated spectral radiance distribution camera is available, then $L_{\mathrm{sky}}(\lambda, \theta, \phi)$ should be measured several times during each spectral radiometer cast and used to compute $\overline{\mu}_d(0^+, z)$. Radiance distribution cameras are ex-

pensive to build, however, and one is not likely to be available aboard every SeaWiFS validation vessel. A recommended alternative approach is to acquire:

1) all-sky photographs taken either with a conventional camera or, preferably, a digitally recorded camera system (some research must be done to develop procedures for attenuating, or blocking, the sun's image and for using filters);
2) measurements, with a narrow FOV spectral radiometer of $L_{\mathrm{sky}}(\lambda, \theta_i, \phi_i)$ at several discrete angles θ_i and ϕ_i; and
3) $E_s(\lambda)$ measurements of $E_{\mathrm{sun}}(\lambda) + E_{\mathrm{sky}}(\lambda)$ with the sun's image blocked by shadowing the deck cell irradiance collector (Gordon 1989).

During the prelaunch experiments, $\overline{\mu}_d(0^+, \lambda)$ estimated from measurements of these types should be compared with $\overline{\mu}_d(0^+, \lambda)$ determined from direct measurements of sky radiance using a spectral radiance distribution camera system.

5.4 Water Samples

Duplicate samples should be taken at each of 12 depths, including at least three depths within the first attenuation length $1/K(490)$, however, in coastal areas with short attenuation lengths, this may not be possible. Samples should also be taken in the *in vivo* fluorescence and beam attenuation maxima. The remaining samples should be spaced throughout the water column using beam attenuation, *in situ* fluorescence, and CTD profiles as a guide.

5.4.1 Pigment Analysis

Water samples should be taken at the site of, and simultaneously with, the surface in-water upwelled radiance and reflectance measurements, and at depth increments sufficient to resolve variability within the top optical depth. The $K(z, \lambda)$ profiles over this layer will be used to compute optically weighted, near-surface pigment concentration for bio-optical algorithm development (Gordon and Clark 1980).

When possible, samples should be acquired at several depths distributed throughout the upper 200 m of the water column [or in turbid water, up to seven optical depths, $\ln((E(0)/E(z)) = 7$], to provide a basis for relating chlorophyll *a* fluorescence signals to pigment mass concentration.

For high accuracy determinations of chlorophylls *a*, *b*, and *c*, as well as carotenoid pigments, it is recommended that HPLC techniques be used (Mantoura and Llewellyn 1983, Gieskes and Kraay 1986). The protocols to be employed in the SeaWiFS validation program for HPLC pigment analyses are prescribed in the JGOFS Core Measurement Protocols (JGOFS 1991). These protocols include:

1) pre-filtering to remove large zooplankton and particles,
2) use of Whatman glass fiber filters (GFF) (approximately 0.7 μm pore size),
3) extraction in 90% acetone, and
4) calibration with authenticated standards.

In addition to HPLC analyses, it is also recommended that the *standard* fluorometric method (Yentsch and Menzel 1963, Holm-Hansen et al. 1965, and Strickland and Parson 1972) for measuring chlorophylls and phaeopigments also be applied to the same extracted pigment samples (section 6.5.2) used for HPLC analysis. This additional analysis by the standard fluorometric method will enable a direct link to the historical bio-optical algorithms and database developed during the CZCS validation experiments.

5.4.2 CDOM and DOC

The measurement of the absorption coefficient due to dissolved organic matter (DOM) should follow the general procedures prescribed in Bricaud et al. (1981). In addition, it is important to remove particles down to 0.2 μm using, e.g., 0.2 μm Nuclepore or aluminum oxide filters, to minimize scattering contributions to the quasi-diffuse attenuation measurements made by typical spectrophotometers, especially for ultraviolet spectra; laboratory work is needed in this area to verify that commercially available 0.2 μm filters do not leach organics into the sample.

Spectrophotometric measurements should be made immediately if possible. If they cannot be performed immediately after sample collection, intermediate storage of the filtrate as frozen samples in dark, clean, glass bottles is permissible in current practice. However, the effects of storing frozen samples before DOM and DOC analyses are not yet documented in the literature, and laboratory tests should be carried out before such data are used in SeaWiFS algorithm development. Nevertheless, the DOM and DOC data from such samples will be valuable, even if they are only qualitative. Spectrophotometry should be performed with a double-beam instrument using a 10 cm or longer cuvette, with monochromatic light to minimize fluorescence effects. Scans should be made on multiple replicates from 300–800 nm to minimize photobleaching.

For waters with low values of absorption coefficient due to DOM, logarithmic extrapolation from ultraviolet wavelengths into the visible may be required. The spectral slope needed for these extrapolations is dependent on both the spectral region in question and the humic/fulvic acid fraction (Carder et al. 1989). Concentrations of marine humus can be eluted onto XAD-3 resin columns, or equivalent, using methanol concentrated by evaporation, diluted (10:1) in deionized water buffered to pH 8.3, and measured spectrophotometrically, which is a procedure similar to that of Carder et al. (1989), except for separation and drying into the humic and fulvic acid fractions. The retention factor for the columns can be examined by comparing

the absorption coefficients in the 300–370 nm region. This method of concentrating CDOM to measure absorption in the visible can be accomplished using small resin volumes (< 50 ml). Data should be log-transformed and smoothed with a multiple-point (< 20 nm range) running average and reported for at least the following wavelengths: 300, 320, 340, 370, 400, 450, 490, and 520 nm.

5.4.3 Absorption by Particles

The absorption spectrum of suspended particles should be determined at sea using GFF and a dual-beam spectrophotometer. A known volume of water is filtered, and the combined transmission spectrum of the wetted filter and particulates is measured with the spectrophotometer. Empirically derived algorithms are then used to calculate the absorption spectrum of the particles in suspension from the transmission spectrum of the filter plus particles (Mitchell and Kiefer 1984).

An aliquot (1–2 liters) of seawater sample is filtered through a Whatman GFF (24 or 25 cm diameter, effective pore size 0.7 μm) at low vacuum. Pre-filtered seawater, using a Millipore GS filter with 0.22 μm pore diameter, is filtered again through a second GFF filter, and this wetted filter is used as a blank. Thorough saturation of both filters is necessary (Mitchell and Kiefer 1988). Filters are affixed, sample side up, to a quartz slide with a drop of pre-filtered seawater. The sample-side of the filter should face the spectrophotometer's light source, with the glass facing the detector. Spectra should be measured as soon as possible, because pigment decomposition may occur (Stramski 1990). Optical density spectra, $\mathrm{OD}_{\mathrm{filt}}(\lambda)$ (which are dimensionless), are scanned from 760 to 390 nm and to 350 nm if possible. Values of $\mathrm{OD}_{\mathrm{filt}}(\lambda)$ greater than 0.4 should be avoided because algorithms correcting for multiple scattering in the filter have been limited to this range (Mitchell 1990). Optical density of the particles in suspension, $\mathrm{OD}_{\mathrm{susp}}(\lambda)$, is calculated from $\mathrm{OD}_{\mathrm{filt}}(\lambda)$ using an algorithm of the form suggested by Mitchell (1990)

$$\mathrm{OD}_{\mathrm{susp}}(\lambda) = C_1 \mathrm{OD}_{\mathrm{filt}}(\lambda) + C_2 \left(\mathrm{OD}_{\mathrm{filt}}(\lambda)\right)^2. \qquad (20)$$

Previously determined coefficients C_1 [0.396 (J. Cleveland, pers. comm.) and 0.392 (Mitchell 1990)] and C2 [0.496 (J. Cleveland, pers. comm.) and 0.665 (Mitchell 1990)] are in general agreement.

Particulate absorption coefficient spectra, $a_p(\lambda)$ (units of m^{-1}), are then calculated from optical density spectra as

$$a_p(\lambda) = \frac{2.3}{X}\left(\mathrm{OD}_{\mathrm{susp}}(\lambda) - \mathrm{OD}_{\mathrm{susp}}(750)\right), \qquad (21)$$

where X, is the volume of water filtered divided by the clearance area of the filter (Mitchell 1990). Ongoing investigations are evaluating uncertainties involved in this methology, including non-zero absorption at 750 nm, variability between filter lots, and differences between filter types (G. Mitchell and J. Cleveland, pers. comm.).

5.4.4 Total Suspended Matter

All suspended particulate material (SPM) dry weight ($\mathrm{mg\,l^{-1}}$) will be determined gravimetrically as outlined in Strickland and Parsons (1972) and specified in the JGOFS protocols (JGOFS 1991). In general, samples are filtered through 0.4 μm preweighed polycarbonate filters, washed with three 2.5–5.0 ml aliquots of distilled water, and immediately dried, either in an oven at 75° C, or in a dessicator. The filters are then reweighed in a laboratory ashore, on an electrobalance with seven-place precision.

5.5 Ancillary Observations

Ancillary observations are often important in flagging and interpreting apparently aberrant data. A minimal set of ancillary supporting observations must include:

1) date and time [Greenwich Mean Time (GMT) and local];
2) geographic location, using the Global Positioning System (GPS) if possible, before and after each cast and at times of satellite and aircraft overpasses;
3) solar azimuth and zenith angles, as calculated from position, date, and time;
4) position of the optical cast in relation to the ship orientation and position of the ship relative to the sun (sketch in the field notes is recommended);
5) sea state (photographed if possible) with approximate swell height, direction, and notes on presence and density of white caps;
6) quantitative measurements of surface wire angles during deployments of the instrument package;
7) time of cast (begin and end), as well as time and depth of water samples collected;
8) percent cloud cover and cloud type, and solar occlusion conditions; and
9) wind direction and velocity.

Desirable additional ancillary measurements include:

a) for radiometric stations, an all-sky photograph and a photographed time history of sea surface is advised; and
b) Secchi depth.

5.6 Moorings

5.6.1 Prototype Optical Buoy System

A prototype optical measurement system designed for long-term buoy deployment with a satellite data telemetry capability is presently under development and is focused on satisfying the SeaWiFS optical data requirements. The

concept is constrained by the requirement that the instrument be capable of maintaining measurement integrity while being unattended for long periods of time. This constraint has lead to a design that minimizes the number of moving parts to one, and has resulted in the spectrographic application of concave holographic diffraction gratings. These holographic gratings provide an approximate flat focal field to the degree that planar silicon photodiode arrays may be used as detectors. Inherent within this technology are the features of simplicity, compactness, durability, and stability.

The optical system utilizes two spectrographs with a dichroic *water* mirror in order to measure radiometric properties with high spectral resolution and stray light rejection. The dichroic mirror is designed to transmit the red (630–900 nm) and reflect the blue portions (380–600 nm) of the spectrum, making the transition from reflectance to transmittance between 600 and 640 nm. The potential for stray light is greatly reduced by splitting the visible spectrum at the beginning of the water absorption region since most of the short wavelength energy is diverted from the entrance slit of the long wavelength spectrograph. The splitting also allows the spectrographs, i.e., gratings and sampling periods, to be optimized for the two distinctive spectral domains. A further reduction of stray light for the long wave spectrograph will be achieved by utilizing a minus blue filter.

The optical system will be deployed on a slack-line moored wave rider buoy that has a 10–20 m *optical bench* attached. Apparent optical properties will be measured by a series of remote collectors that are coupled to the instrument with fiberoptics. Data will be compressed, stored, and forwarded through a NOAA/Geosynchronous Orbital Environmental Satellite (GOES) and an ARGOS telemetry link.

This type of optical mooring represents a new and challenging technology. Detailed protocols for deploying and maintaining this type of mooring, and for evaluating its data quality, must be developed in light of the experience to be gained over the next 2–3 years. Current practice is to apply OMP-8, or similar compounds, to prevent growth of marine organisms on the windows of moored radiometer systems. This approach is less satisfactory for IOP instruments, because for collimated light, transmission characteristics of the optical windows can be adversely affected by the layer of the anti-fouling material.

5.7 Drifting Optical Buoys

Drifting optical instruments are a recent development and there is almost no history of their quantitative application to problems in ocean color algorithm development and remote sensing radiometric validation. It is probable that significant experience in the uses and limitations of such instruments will be gained in SeaWiFS related experiments during the prelaunch period. The critical questions about these instruments, which should be answered during prelaunch work include:

1. How accurately can $L_W(\lambda)$ be estimated from $L_u(z,\lambda)$ at a single near surface depth, using only an estimate of $K_L(\lambda)$ obtained from ocean color ratios? Is 5% accuracy feasible?
2. How accurately can $L_{WN}(\lambda_1)$:$L_{WN}(\lambda_2)$ ratios be estimated with these instruments using only a single channel $E_d(\lambda)$ measurement for normalization? (Which is contemplated for both instruments currently being developed, as described in section 2.6.) Are the L_{WN} ratios from clear sky and overcast conditions comparable enough that the drifter data can provide a basis for interpolating SeaWiFS data through cloudy periods?

When answers to these fundamental questions are in hand, it will be possible to draft and implement more detailed protocols for the use of optical drifters in SeaWiFS radiometric validation and algorithm development.

Many potential applications of optical drifters in oceanographic research using SeaWiFS data are more obvious, but from a radiometric standpoint are less stringently demanding. Protocols for those applications are, however, beyond the scope of this report.

5.8 Sampling and Bio-optical Validation

Spatial and temporal variability in bio-optical properties will profoundly affect the validity of comparisons between SeaWiFS and in-water optical measurements. A single SeaWiFS instantaneous FOV measurement will integrate $L_W(\lambda)$ over approximately a square kilometer, or larger off nadir viewing angles. Furthermore, the location accuracy of a single pixel may be several kilometers, except in near-shore areas where image navigation can be improved by using land-navigated anchor points. Bio-optical profiles measured at a single station are representative of a spatial scale that is only a small fraction of a kilometer.

Data from a grid of several station locations may be required to estimate the spatial averages of optical properties represented by a SeaWiFS pixel, or a block of pixels. Because the ship measurements over the grid are not instantaneous, temporal variability in bio-optical properties can add additional uncertainty to the comparisons. Aircraft radiometric observations can, conceptually, be used both to locate comparison sites away from areas of strong spatial variability and to document changes in the pattern of spatial variability over the period required for a ship to occupy all stations in a comparison grid.

5.8.1 Initialization and Sampling

Data intended for direct comparisons between observed $L_u(\lambda)$ and SeaWiFS $L_W(\lambda)$ estimates should usually be acquired in areas where bio-optical variability is known

to be very small. This will ordinarily dictate that such data be acquired from optically clear, persistently oligotrophic water masses. Potentially suitable sites include the northeastern Pacific central gyre off Baja, California (to the southwest), and the central Sargasso Sea. When planning validation cruise locations and timing, seasonal and regional cloud cover statistics should also be considered, to maximize the likelihood of simultaneous SeaWiFS and shipboard observations. An oligotrophic site in the northeast Pacific, near Hawaii, is the prime candidate for placing a moored radiometer for continuous time-series radiometric comparisons with SeaWiFS $L_W(\lambda)$ estimates.

Another set of radiometric comparisons between surface or near surface, and SeaWiFS measurements, should be made to detect any thermally induced perturbations in responsivity of the SeaWiFS channels. The spacecraft and instrument will be heated by sunlight throughout the descending (daylight) data acquisition segment of each orbit and will be cooled by thermal radiation while in the Earth's shadow throughout the remainder of the orbit. This cycling is likely to induce transient thermal gradients in the instrument, as well as a time varying cycle in the temperatures of its detectors and other components; these thermal variations could affect spectral bandpass and responsivity of one or more SeaWiFS channels.

A series of radiometric comparison stations should be made over a wide range of latitude in both the northern and southern hemispheres, to look for evidence of cyclic thermal sensitivity. Unfortunately, a set of stations covering the full range of latitudes cannot all be sited in regions where mesoscale variability in ocean optical properties can be neglected. As when acquiring data for developing and validating bio-optical algorithms (section 5.8.2), a significant effort must be exerted to quantify spatial variability in normalized water-leaving radiance. Airborne radiometer data, in combination with careful characterization of atmospheric aerosol and cloud conditions, should be employed to augment shipboard radiometry at the stations selected for this aspect of the validation.

5.8.2 Validation Sampling

For SeaWiFS algorithm development and validation, measurements must be made in Case 1 and 2 water masses spanning wide ranges of optical properties and phytoplankton pigment concentration. In optically transparent, low chlorophyll, oligotrophic water masses, spatial variability is usually small and a station location and sampling strategy much like that discussed above for SeaWiFS radiometric validation is appropriate.

In turbid, high chlorophyll, eutrophic water masses, mesoscale and smaller scale variability is often significant. In very productive Case 1 water masses, station placement and other aspects of sampling schemes are identical with those for Case 2 water masses (below). At algorithm development stations, where measurements need neither be coincident with, nor matched to, SeaWiFS observations, it will be necessary to characterize spatial and temporal variability only over the relatively short scales separating the separate in-water radiometric, optical, and pigment measurements. Airborne ocean color or lidar characterizations of spatial variability in the vicinity of these stations will not usually be essential, although such additional information will be very helpful.

At stations where data are acquired for algorithm validation, and where a match to contemporaneous SeaWiFS measurements is required, it will be necessary to determine the patterns of spatial variability over a domain extending approximately 20 × 20 km centered at the station, and to center the ship in a 2 × 2 km domain over which $K(490)$ and chlorophyll concentration vary < 35% about the mean. In some cases it may be possible to determine spatial variability adequately from ship station data and along track measurements alone. In regions of strong mesoscale variability, however, concurrent aircraft ocean color or lidar measurements should be used both as a guide for selecting the ship's location, and for providing a basis for spatially extrapolating the in-water measurements to match the much coarser resolution of the SeaWiFS measurements.

Although coastal and continental shelf areas comprise only 10% of the total ocean area, they provide roughly half of the oceanic new production and most of the sequesterable DOC (Walsh et al. 1991). These areas are typically higher in phytoplankton pigment concentration and may include colored terrigenous constituents such as DOM and suspended sediments (Morel Case 2 waters). Precise locations where offshore Case 1 waters merge into Case 2 waters can neither be determined *a priori*, or from space-derived data alone. To rectify this uncertainty and to obtain data to develop Case 2 algorithms for chlorophyll *a* and DOC, new protocols for sampling such waters need to be established.

To achieve valid comparisons between the ship and satellite, sharp horizontal gradients and sub-pixel patchiness must be avoided, and image navigation must have land anchor points near the study site. Measurements used to calculate normalized water-leaving radiance must be made under cloud-free conditions and within five minutes of the satellite overpass. These conditions are difficult to meet in Case 2 water masses, where mesoscale and sub-mesoscale variability is typically very strong. Sub-pixel variations of no more than ±35% of the mean pixel chlorophyll will be tolerated. To improve the chances of achieving this criterion, attempts should be made well before the overpass to place the ship away from fronts and sharp gradients.

Accurate aircraft ocean color radiometry can be especially valuable for SeaWiFS algorithm validation in Case 2 waters. High altitude, well navigated (< 250 m) aircraft radiance imagery contemporaneous with a satellite overpass can be used to assess sub-pixel patchiness and horizontal gradients in the vicinity of ship measurements. Similarly, flights prior to the overpass can be used to place

the ship in a low gradient environment. Imaging spectrometers such as the Airborne Ocean Color Imager (AOCI) or AVIRIS can be used the previous day to direct the ship to the general low gradient study area, while near real-time information from low altitude airborne radiometers or laser fluorometers, e.g., Ocean Data Aquisition System (ODAS), MARS, and AOL, measured a few hours before an overpass can be used to improve ship placement.

Through flow-through pumping systems or towed systems outside the ship wake, fluorometry can be used to assess chlorophyll patchiness if frequent, i.e., every 10–15 minutes depending upon gradients, chlorophyll fluorescence-yield calibration measurements are performed. Towed absorption, scattering, reflectance, and c meters can also be used to characterize spatial variability when a high degree of covariance exists between these parameters and chlorophyll a concentration in a study area.

5.9 Vicarious Calibrations

An important obligation of any flight project is the production of a high quality calibrated Earth-located (level-1) data set. Consequently, it is the recommendation of this workshop to produce a calibrated set of SeaWiFS radiances that have been verified through direct, or vicarious, calibration techniques.

One potentially useful technique follows the approach currently in use to verify the responsivity of the AVHRR's Television and Infrared Observation Satellite (TIROS) satellite instruments. Twice a year, an aircraft instrument, which has been recently calibrated directly to the laboratory based NIST traceable standards, should be used to obtain simultaneous views of a particular ocean scene. The aircraft scene must be obtained from a high altitude aircraft, such as the NASA ER-2, and flown at an altitude above most of the terrestrial atmosphere. Existing AVHRR-NASIC (NASA Aircraft Satellite Instrument Calibration) Project data sets demonstrate a capability to limit the uncorrected trend in the AVHRR data sets to under 2% over two years. This concept may allow an independent verification of the atmospheric radiative transfer models used to compute ocean biological quantities when the aircraft data are used in conjunction with the surface truth campaign measurements of those ocean biological quantities. However, the SeaWiFS absolute accuracy requirements are more stringent than those associated with the AVHRR, and a correspondingly more accurate airborne radiometer system (sections 3.3 and 4.3) must be used (also section 2.3).

6. METHODS OF ANALYSIS

6.1 In-Water Radiometric Profiles

Measurements of upwelling radiance $L_u(z,\lambda)$, spectral surface irradiance $E_s(\lambda)$, downwelling irradiance $E_d(z,\lambda)$, and upwelling irradiance $E_u(z,\lambda)$, should be recorded and archived at five levels:

Level-0 Raw instrument digital output.

Level-1 Instrument output in volts, or frequency if appropriate, and depth.

Level-2 Calibrated irradiance and radiance, ancillary measurements in appropriate geophysical or biological units, and depth corrected for dark/zero offsets.

Level-3 Smoothed profiles of $K_E(z,\lambda)$ and $E_d(z,\lambda)$ or $L_u(z,\lambda)$ with irradiance and radiance normalized by measured surface irradiance.

Level-4 Level-3 data normalized to clear-sky, zenith sun at mean Earth-sun distance, and spectrally adjusted to match the actual reference wavelengths and FWHM bandwidths.

The formats of these data sets will vary somewhat between individual instruments. The SPO will promulgate suitable standard format specifications, or guidelines, to facilitate database management and interchanges of level-1 through level-4 data, inclusive. These data files should each contain a header record identifying as a minimum:

1) date and time, i.e., GMT, of the station;
2) geographic location (latitude and longitude in decimal degrees to nearest 0.001);
3) cloud cover and sky conditions;
4) identification of each variable, including units and wavelengths, for radiometric channels;
5) source of dark/zero-offset data;
6) calibration date and file identification;
7) instrument identification;
8) method of K-determination (level-3);
9) normalization algorithm (level-4);
10) Secchi depth; and
11) depths of associated water samples, if any.

In addition to profile files, each data set should contain:

a) calibration files used to compute level-2 data;
b) level-0 and level-1 dark files, and an average dark voltage file used to compute the corresponding level-2 files (in some cases a dark value may be extracted from the deep portion of a profile);
c) files with data from comparisons with a portable irradiance and radiance reference standard made in the field and used to track the instrument's stability during a deployment; and
d) anecdotal and environmental information about each profile, either in the header, or in an accompanying ASCII text file.

The data should be retained at full resolution, but with contaminated records removed, through level-2. If the data

are binned prior to K-determination, as is sometimes done in the derivative method (section 6.1.4), the binned representations should be recorded as a level-2a file, in addition to the full resolution level-2 file.

6.1.1 Instrument Calibration Analysis

The data from pre- and post-deployment calibrations should be compared with: 1) each other, 2) the long-term history of an instrument's calibrations, and 3) the record of comparisons with a portable field irradiance and radiance standard, to be made frequently during a cruise. Based on this analysis of the instrument's history, a calibration file should be generated and used to transform the data from level-1 to level-2. This analysis, and the rationale for adopting a particular set of calibration coefficients, both for responsivity and wavelength, should be fully described in documentation accompanying the data set, preferably in an ASCII file to be retained on-line with each data set.

6.1.2 Raman Corrections

Marshall and Smith (1990), and references therein, show transpectral Raman scattering contributes significantly to measured irradiance between 500 and 700 nm. At a given wavelength, the Raman contribution is excited by ambient irradiance at a wavenumber shift of 3,400 cm^{-1}, e.g., Raman scattering at 500 nm (20,000 cm^{-1}), is excited by light at 427 nm (23,400 cm), and at 700 nm (14,286 cm^{-1}) by light at 565 nm (17,686 cm^{-1}). Marshall and Smith (1990) give a transverse Raman scattering cross section (at 90°) of 8.2×10^{-30} cm^{-2} $molecule^{-1}$ sr^{-1}, a value within the range of other published observations. By integration, they derive a total Raman scattering coefficient

$$b_r(488) = 2.6 \times 10^{-4}\,m^{-1}. \tag{22}$$

The wavelength dependence of the Raman scattering cross section is theoretically similar to Rayleigh scattering

$$b_r(\lambda) \equiv \left(\frac{\lambda}{488}\right)^{-4} b_r(488), \tag{23}$$

although, this has not yet been experimentally confirmed.

A method for applying Raman corrections to radiance profiles is suggested and applied to homogeneous clear-water profiles by Marshall and Smith (1990). A robust Raman scattering correction model for general application in more turbid and vertically stratified water masses is needed. The relative magnitude, and thus importance, of the Raman signal at each wavelength in the upper three attenuation lengths should also be investigated more thoroughly than has been done to date.

6.1.3 Normalization by Surface Irradiance

The dominant errors in measured $K(z,\lambda)$ profiles result from changes in cloud cover causing strong variations in incident surface irradiance, $E_s(\lambda,t)$, measured at time t, during the time required to complete a radiometric cast. In present use, $E_s(\lambda,t)$ refers to incident spectral irradiance measured with a deck cell aboard a ship. Smith and Baker (1984, 1986) discuss a method for propagating $E_s(\lambda)$ through the sea surface to estimate $E_d(0^-,\lambda)$; they also present a model for adjusting $E_d(0^-,\lambda)$ to compensate for solar zenith angle.

An alternative, and conceptually better, scheme for estimating $E_d(0^-,\lambda)$ is to measure $E_d(z_r,\lambda)$ using a radiometer floated away from the ship and held at a shallow depth, z_r, during a cast (Waters et al. 1990). In either case, the record of $E_s(\lambda,t)$ or $E_d(z_r,t)$ is recorded together with profiles of $E_d(z,\lambda,t)$, $E_u(z,\lambda)$, and $L_u(z,\lambda)$. Assuming that transmission of $E_s(\lambda,t)$ through the surface does not vary with time, then a simple and effective normalization of the profiles is obtained as

$$E_d'(z,\lambda) = \frac{E_d(z,\lambda)E_s(0^-,\lambda)}{E_s(\lambda,t)}, \tag{24}$$

where $E_s(\lambda,t)$ is the deck cell irradiance measured at the time t when the radiometer was at depth z and $E_s(0^-,\lambda)$ is the measurement when the radiometer was at the surface.

Some previous investigators have used $E_s(\lambda,t)$ at a single reference wavelength, e.g., 550 nm, to normalize profiles, and have thus ignored the usually small spectral variations in incident irradiance. For SeaWiFS validation and algorithm development, however, the recommended protocol is to use multispectral $E_s(\lambda,t)$, or possibly near-surface $E_d(z_r,\lambda,t)$, to determine $E_d(z,\lambda,t)$ at each wavelength.

Because of spatial separation between the surface and underwater radiometers, cloud shadow variations are not measured either identically or in phase, by the two instruments. Therefore, the $E_s(\lambda,t)$ or $E_d(z_r,\lambda,t)$ profiles should be smoothed to remove high frequency fluctuations while retaining variations with periods of 15 seconds or greater. The smoothed $E_s(0^-,\lambda)/E_s(\lambda,t)$ profiles should then be applied as a normalizing function to the irradiance and radiance profiles.

6.1.4 K-Analysis

Normalized and Raman corrected profiles of $E_d(z,\lambda)$, $E_u(z,\lambda)$, and $L_u(z,\lambda)$ should be fit to the equations

$$E_d(z,\lambda) = E_d(0^-,\lambda)\, e^{-\int_0^z K_d(z',\lambda)dz'}, \tag{25}$$

$$E_u(z,\lambda) = E_u(0^-,\lambda)\, e^{-\int_0^z K_u(z',\lambda)dz'}, \tag{26}$$

and

$$L_u(z,\lambda) = L_u(0^-,\lambda)\, e^{-\int_0^z K_L(z',\lambda)dz'}, \tag{27}$$

respectively. The vertical profiles of attenuation coefficients $K_d(z,\lambda)$, $K_u(z,\lambda)$, and $K_L(z,\lambda)$, in conjunction

with the respective surface values $E_d(0^-,\lambda)$, $E_u(0^-,\lambda)$, and $L_u(0^-,\lambda)$ provide complete specifications of smoothed irradiance and radiance profiles.

If the natural logarithm of (25), (26), and (27) is taken, equations of the following form are obtained

$$-\int_0^z K(z)dz = \ln(E(z)) - \ln(E(0^-)), \tag{28}$$

so that

$$K(z) = -\frac{d\ln(E(z))}{dz}\bigg|_z. \tag{29}$$

The traditional method of K analysis, e.g., Smith and Baker (1984 and 1986), is to estimate $K(z)$ as the local slope of measured $\ln(E(z))$ in an interval of a few meters centered at depth z_m, i.e., at depths near depth z_m,

$$\ln(E(z)) \cong \ln(\widehat{E}(z_m)) - K(z_m)(z - z_m). \tag{30}$$

The unknowns $\ln(\widehat{E}(z_m))$ and $K(z_m)$ are determined as the intercept and (negative) slope of a least-squares regression fit to measured $\ln(E(z))$ data within the depth interval $z_m - \Delta z \leq z < z_m + \Delta z$. The half-interval Δz is somewhat arbitrary. Smith and Baker (1984 and 1986) suggest a Δz of approximately 4 m, but for noisy profiles a Δz as large as 10 m may be needed to smooth over incident irradiance fluctuations left as residuals by the deck cell normalization.

When this method is used, the shallowest possible values in the smoothed $\widehat{E}(z)$ and $K(z)$ profiles are at depth Δz m, and the deepest values are Δz m above the deepest measurements in the profile. If obvious ship shadow effects are present in the data, the shallowest valid smoothed data point will be at depth $z_s + \Delta z$, where z_s is the depth to which the data are regarded as contaminated and are excluded from the analysis.

It is often convenient, although not necessary, to preaverage radiometric data into, e.g., 1 m, bins prior to performing the least-squares analysis. If this is done, the data should be pre-filtered to remove any noise spikes and then averaged before it is log-transformed.

A corollary to having a large database, is the need to facilitate its manipulation and analysis in order to make its application to various tasks feasible. For example, in the proposed SeaWiFS effort, radiometric measurements from many oceanographic stations will be examined. Each station will require one or more vertical profiles from the surface to depths of up to 200 m of downwelling irradiance, upwelling radiance, and upwelling irradiance in at least 5–8 spectral bands. Using a multispectral radiometer during a profile, such as the MER class of instruments, the data in all channels will be sampled contemporaneously and recorded digitally 2–10 times per meter. These are level-1 data and are stored in files for subsequent processing and analysis.

Level-2 through level-4 data give increasingly refined processed information in each successive level, thereby requiring various amounts of intervention from the analyst. After appropriate editing to remove artifacts such as the effects of ship shadow, vertical profiles of K are computed from the logarithmic decrement with depth of the radiometric profiles. Direct derivative method calculations of Ks using computer techniques (see above) require the use of a depth interval so large, frequently 20 meters, that information about the slope and, hence, about K near the top and bottom of the profile is lost, and averaging over such a large interval causes the slopes in sharply defined layers, e.g., regions of high gradients, to be poorly represented. Attempts to reduce these effects by using a significantly smaller depth interval results in unacceptably noisy K profiles.

An improved approach, suggested by Petzold (1988), is to fit a series of analytic functions to the radiometric data using non-linear least-squares regression fitting techniques. The profiles are broken up into as many layers as required, and functions are fit to each layer with the constraint that the functions and the derivatives of the functions be everywhere continuous and finite. It is found that the logarithm of the radiometric data versus the depth can be fit by a series of hyperbolic tangents superimposed on straight lines using this technique. The data for a profile consisting of two layers can be matched by using the analytic expression together with the values of five parameters derived from the regression fitting procedure. In analyses of 2,100 profiles, the most complicated profiles encountered required 20 parameters—most required 5 or 10.

With the analytic form of the curve fitting the data, it is a simple matter to differentiate the function to determine the slope of the radiometric profile and obtain noise-free profiles of K. Using this technique, Petzold is able to store a very large database in a very compact form, storing only the parameters and the program for reconstructing the data. Additional analyses can be easily performed using the analytic representation of the data in lieu of the original large discrete data files.

The basic functional form of the expression used to fit the data is

$$Y = P_1 + P_2 B + P_3 \frac{A - \frac{1}{A}}{A + \frac{1}{A}}, \tag{31}$$

where $B = P_4 - X$, $A = e^{B/P_5}$, P_1 through P_5 are coefficients to be determined in the analysis, X is the depth in meters, Y is the base 10 logarithm of the radiometric measurement, *i.e.*, the downwelling irradiance (E_d), upwelling irradiance (E_u) or upwelling radiance (L_u). The form of (31) is a hyperbolic tangent superimposed upon a straight line. It has a point of inflection at $X = P_4, Y = P_1$ and approaches the asymptote $Y = P_1 + P_2 B \pm P_3$ as X becomes larger or smaller than P_4.

The first derivative is

$$\frac{dY}{dX} = -P_2 - \frac{P_3}{P_5}\left(\frac{2}{A+\frac{1}{A}}\right)^2 \tag{32}$$

When $X = P_4$, $B = 0$ and $Y = P_1$

$$\frac{dY}{dX} = -P_2 - \frac{P_3}{P_5}. \tag{33}$$

K may be defined as the slope of the plot of the natural logarithm of the measured radiometric variable against depth, or

$$K = 2.3026\frac{dY}{dX}. \tag{34}$$

At the point of inflection ($X = P_4$ and $Y = P_1$)

$$K = 2.3026\left(P_2 + \frac{P_3}{P_5}\right). \tag{35}$$

In the limit, $K \rightarrow 2.3026P_2$ and K will not exceed some finite value.

The method described above was applied to radiometric profile data from six cruises covering a wide variety of ocean regimes and latitudes from 24.0–77.4° N. Approximately 2,100 profiles were fitted, and typically, the standard deviation of the ratio between the function derived from the regression method and the original radiance and irradiance data was 6% or less. For a large fraction of the fitted profiles the standard deviations were between 1–3%.

An alternative method of determining K-profiles has been recently developed by Mueller (1991). Radiometric profiles are represented in terms of optical depth τ, which from (25), (26), and (27) is

$$\tau(z,\lambda) = \int_0^z K(z',\lambda)dz' = \ln\left(\frac{E(0^-,\lambda)}{E(z,\lambda)}\right). \tag{36}$$

The K-profile is represented analytically by Hermitian cubic polynominals $\gamma_{ij}(\xi)$ over finite depth elements. The argument ξ is a local coordinate such that $\xi = 0$ at the center of a finite depth element, $\xi = -1$ at the shallow end-point (node) of the element and $\xi = 1$ at the deep node. Hermitian cubic polynomials are defined in any text on finite element modeling, e.g., Pinder and Gray (1977).

At depth z, $K(z,\lambda)$ is expressed as

$$\begin{aligned} K(z,\lambda) = {} & \overline{K}_0(\lambda)\gamma_{01}(\xi) + \partial_z\overline{K}_0(\lambda)\gamma_{11}(\xi) \\ & + \overline{K}_1(\lambda)\gamma_{02}(\xi) + \partial_z\overline{K}_1(\lambda)\gamma_{12}(\xi), \end{aligned} \tag{37}$$

where $\overline{K}_0$ and $\overline{K}_1$ are values of K, and $\partial_z\overline{K}_0$ and $\partial_z\overline{K}_1$ are its vertical derivatives, at the two nodes of the depth element containing z. With this representation of $K(z,\lambda)$, it is possible to write (36) for each measured depth z_m as the weighted sum

$$\tau(z_m,\lambda) = \sum_{n=0}^{N}(h_{m,n}\overline{K}_n + h_{m,n+N}\partial_z\overline{K}_n \tag{38}$$

for the $n = 0, 1, \ldots N$ nodes dividing the water column into N depth elements. The coefficients h_{ij} are obtained as analytic integrals over the Hermitian polynominals γ_{ij} for the finite elements above and including depth z; $h_{ij} = 0$ for elements below the one containing z. Since such an equation may be written for every measured optical depth, the profile may be represented in matrix form as

$$\vec{\tau} = \underset{\sim}{H}\vec{K}, \tag{39}$$

where $\vec{\tau}$ is the vector of measured optical depths, $\underset{\sim}{H}$ is the matrix of coefficients h_{ij} and $\vec{K}$ is the vector of $\overline{K}_n$ and $\partial_z\overline{K}_n$ at the N nodes. The least-squares solution for the unknown vector $\vec{K}$ is obtained as

$$\vec{K} = \left[\underset{\sim}{H}^T\underset{\sim}{H}\right]^{-1}\underset{\sim}{H}^T\vec{\tau}, \tag{40}$$

which with (37) yields the complete profile $K(z)$.

The surface boundary condition assumed by Mueller (1991) is that $K(z)$ is constant between the sea surface (node 0) and the first subsurface node (node 1). If obvious or suspected ship shadow effects are present in the upper profile, the depth of node 1 is set immediately below the affected area and the data in that top element are excluded from the fit; the solution to (40) at nodes 0 and 1 are, in this case, determined entirely by the data from depths below node 1.

The solution at the deepest node is not constrained and depends only on the observations in the depth element immediately above it. The one-sided solution to (40) is often unstable at this node. If two nodes are placed close together at the bottom of the cast, then the unstable solution is confined to only the bottom node, which may be discarded after (40) is solved.

In order to solve (40), the surface values of $E_d(0^-,\lambda)$, $E_u(0^-,\lambda)$, and $L_u(0^-,\lambda)$ must be independently determined or specified. At present, this is done iteratively by requiring the solution to closely approximate the mean value of measurements in the top 1–2 m of the profile. Data from this near-surface layer are usually not significantly affected by ship shadow, but they may be severely affected by irradiance fluctuations associated with light focusing by surface waves. Additional research is needed to develop a more objective method of determining these surface values.

Currently, the placement of nodes is largely subjective, even when guided by structure in accompanying $c(660)$ and chlorophyll fluorescence profiles (Mueller 1991). Qualitatively, the integral solutions mimic the structure in the $c(660)$ and fluorescence profiles more faithfully than do the derivative solutions; they also do a better job of filtering irregularities that are apparently associated with large fluctuations in deck cell irradiance. Quantitative evaluation of sensitivity to exact node placement is in progress. Development of objective criteria for node placement will require further research.

6.1.5 Finite Bandwidth Correction

Siegel et al. (1986) and Marshall and Smith (1990) discuss the effects of finite spectral FWHM bandwidth, and the normalized response function, on determination of the attenuation coefficient $K(\lambda)$ for a vertically homogeneous water column. Given a channel's nominal wavelength λ' and normalized response function $h(\lambda)$, the apparent attenuation coefficient measured in a homogeneous water column is approximately

$$K_s(z,\lambda') = \frac{\int_0^\infty K(\lambda)h(\lambda)e^{-K(\lambda)z}d\lambda}{\int_0^\infty h(\lambda)e^{-K(\lambda)z}d\lambda}. \quad (41)$$

Marshall and Smith (1990) applied a correction for this effect to clear-water profiles of $E_d(z, 589)$. In general, correction of $K(z,\lambda')$ for finite bandwidth effects associated with K for pure water is straightforward. Additional research will be needed to model, from the spectral irradiance data itself, additional bandwidth effects associated with attenuation by phytoplankton and other particles, and to correct $K(z,\lambda)$ accordingly.

6.1.6 Extrapolation to the Sea Surface

Because of surface waves, it is rarely possible to measure E_d, E_u, or L_u at depths that closely approximate $z \cong 0^-$. The shallowest reliable readings typically occur at depths ranging from 0.5–2 m, and the data from this zone usually exhibit strong fluctuations (associated with surface waves) and require some form of smoothing or averaging. It is almost always necessary to apply some means of extrapolating the data upward to the sea surface. Whatever method is used should reconcile extrapolated $E_d(0^-,\lambda)$ with deck measurements $E_s(\lambda)$.

If $K(z)$ profiles are determined using the derivative method, the shallowest smoothed estimates will occur at depth $z_0 = \Delta z$, if there are no ship shadow effects. The usual procedure is to extrapolate values to $z = 0^-$ as

$$E_d(0^-,\lambda) = E_d(z_0,\lambda)e^{K_d(z_0,\lambda)z_0}, \quad (42)$$

$$E_u(0^-,\lambda) = E_u(z_0,\lambda)e^{K_u(z_0,\lambda)z_0}, \quad (43)$$

and

$$L_u(0^-,\lambda) = L_u(z_0,\lambda)e^{K_L(z_0,\lambda)z_0}. \quad (44)$$

If ship shadow is present, z_0 may be 20 m or more, and the extrapolation becomes somewhat tenuous.

If the integral method is used to determine $K(z)$ profiles, then $E_d(0^-,\lambda)$, $E_u(0^-,\lambda)$, and $L_u(0^-,\lambda)$ are automatically determined as part of the fitting procedure. The surface values thus obtained are not necessarily superior to those obtained by extrapolating the derivative method solutions, but they do have the advantage of representing an internally consistent fit to the entire profile beneath the surface boundary layer.

By either method, extrapolation of measured $E_d(z,\lambda)$, $E_u(z,\lambda)$, and $L_u(z,\lambda)$ to $z = 0^-$ becomes very difficult at $\lambda \geq 670$ nm. At these wavelengths, the rapid decrease in daylight over an extremely shallow first attenuation length may compete with an increase in flux with depth due to chlorophyll fluorescence. Additional research is needed to address measurement and estimation of $E_d(0^-,\lambda)$ and $L_u(0^-,\lambda)$ at these wavelengths, especially in chlorophyll-rich Case 2 waters.

6.1.7 Spectral Adjustments

New methods must be developed to reconcile in-water measurements $L_u(\lambda_0 + \Delta\lambda_1, 0^-)$ integrated over a sensor response function $h_1(\lambda)$ with SeaWiFS measurements of $L_t(\lambda_0 + \Delta\lambda_2)$ integrated over a wider sensor response function $h_2(\lambda)$. The challenge is to account for differing radiometric sensitivities to fine-scale Fraunhofer structure in extraterrestrial solar spectral flux $F(\lambda)$, as modified by atmospheric spectral transmittance $t(\lambda)$ and oceanic spectral reflectance $R_L(\lambda)$. By assuming $F(\lambda)$ is exactly known, and that over the wavelength range defined by $h_2(\lambda)$ and $h_1(\lambda)$, $t(\lambda)$ and $R_L(\lambda)$ vary slowly with wavelength, it should be possible to adjust the $L_W(\lambda_0 + \Delta\lambda_1)$ derived directly from the in-water instrument, to estimate the water-leaving radiance $L_W(\lambda_0 + \Delta\lambda_2)$. This will be transmitted through the atmosphere and contribute to $L_t(\lambda_0 + \Delta\lambda_2)$ measured by SeaWiFS. At the very least, this type of correction should be practical for a given atmosphere. Prelaunch radiative transfer model sensitivity studies and experimental verifications should be done to determine the magnitudes and accuracies of such corrections for the various SeaWiFS bands.

6.1.8 Normalized Water-Leaving Radiance

To standardize the in-water SeaWiFS algorithms, it is necessary to normalize measured $L_W(\lambda)$ to those that would be measured were the sun at the zenith, at the mean Earth-sun distance and with the effects of the atmosphere removed. Following Gordon (1988), normalized water-leaving radiance may be defined as

$$L_{WN}(\lambda) = \frac{L_W}{t(\lambda,\theta_0)\,(1-\rho(\theta_0))\cos\theta_0}\left(\frac{r}{\bar{R}}\right)^2, \quad (45)$$

where θ_0 is the solar zenith angle, $\rho(\theta_0)$ is the air-water Fresnel reflectance for incident angle θ_0, $t(\lambda,\theta_0)$ is the atmospheric transmittance and $\bar{R}$ is the mean Earth-sun distance. The Earth-sun distance on the day of the measurement, r, is given by

$$r = \frac{\bar{R}}{1 + 0.0167\cos\left(\frac{D-3}{365}\right)}, \quad (46)$$

where D is the sequential day of the year.

The $(r/\bar{R})^2$ adjustment was not employed by Gordon and Clark (1981) or Gordon (1988) because it cancels in ratio algorithms, and the measurements they used were all taken within the span of a few months, so this source of variation was very small in their data. The range of variation in $(r/\bar{R})^2$ is approximately 6% over a full annual cycle. This adjustment should be made, nevertheless, for it becomes important in algorithms predicting absolute values of $L_W(\lambda)$, as in the clear-water radiance model of Gordon and Clark (1981), and in algorithms for either estimating or detecting anomalously high water reflectances in, for example, a coccolithophore bloom.

6.2 Moored Radiometry

Methods are not highly developed for analyzing data from moored radiometers to calculate $L_{WN}(\lambda)$. The principles of this analysis are well understood, but the community has had little experience with moored measurements of $L_u(z,\lambda)$, determination of $K_L(z,\lambda)$, and extrapolation to $L_u(0^-,\lambda)$. The moored optical system being developed by D. Clark of NOAA's National Environmental Satellite Data Information Service (NESDIS) for SeaWiFS/MODIS is the first system to be specifically engineered to address this problem.

Smith et al. (1991) successfully acquired a nine-month time series of spectral $E_d(z,\lambda,t)$ and $L_u(z,\lambda,t)$ at three depths (33, 52, and 72 m); they placed an additional above-water radiometer on a surface float, but this unit failed and provided no data. Smith et al. (1991) analyzed the $K_d(441)$ time series over 0–32 m, using a broad-band irradiance measurement to estimate $E_d(0^-,441)$ and 32–52 m depth intervals. They did not, however, estimate $K_L(\lambda)$ for $L_u(\lambda)$. They also developed and evaluated algorithms for estimating phytoplankton pigment concentrations from spectral reflectance and from chlorophyll fluorescence at $L_u(683)$ stimulated naturally by incident daylight; they demonstrate that continuous time series of $K_d(\lambda,t)$ and pigment concentration may be measured using this type of moored system.

Smith et al. (1991) and Dickey et al. (1991) together illustrate methods that can be used to specify protocols for oceanographic analyses of bio-optical time series measured using moored optical systems. Such protocols would be very valuable for planning and executing oceanographic studies using data from moored systems together with SeaWiFS time series data; they are not, however, directly relevant to SeaWiFS validation. It is anticipated that optical protocols for U.S. and International JGOFS will be published by working groups convened by these programs.

6.3 Aerosol Optical Depth

If multiple measurements of the solar beam are obtained during stable atmospheric conditions, then the *Langley method* can be used to obtain the atmospheric transmittance. This method consists of plotting the natural logarithm of the voltage from the sun photometer versus the inverse of the cosine of the solar zenith angle. The slope of this straight line is the total optical depth of one atmosphere. If only single measurements are obtained, the instrument calibration is applied to determine radiance, which can be combined with the extraterrestrial solar irradiance to calculate the atmospheric optical depth.

To obtain the aerosol optical depth, total optical depth must be used with computed optical depths due to molecular scattering (Rayleigh optical depth), and absorption by ozone and other important gases (NO_2 for some spectral bands). By subtracting the optical depths of these well-mixed gases from the total measurements, the aerosol optical depth can be determined.

6.4 Sky Radiance Distributions

Sky radiance distributions L_{sky} measured with a calibrated radiance distribution camera, and perhaps augmented by sun photometry or narrow FOV L_{sky} discrete measurements in the zenith-sun plane, will be used to estimate the aerosol phase function (Voss and Zibori 1989). Development of detailed protocols and methods of analysis, including new inverse modeling techniques, for estimating aerosol optical depths and phase functions will require new research. The spectral mean cosine $\overline{\mu}_d(0^+,\lambda)$ for downwelling radiance at the sea surface will be calculated directly from radiance distribution camera data, when available. Under cloud-free conditions, $\overline{\mu}_d(0^+,\lambda)$ can also be estimated by measuring $E_{\mathrm{sky}}(\lambda)+E_{\mathrm{sun}}(\lambda)$ with an irradiance deck cell; the algorithm for these computations is given by Gordon (1989).

When a spectral radiance distribution camera system is not available and skies are not cloud free, it may be possible to estimate $\overline{\mu}_d(0^+,\lambda)$ from some combination of deck cell unshaded $E_{\mathrm{sky}}(\lambda)+E_{\mathrm{sun}}(\lambda)$ and shaded $E_{\mathrm{sky}}(\lambda)$ measurements, all-sky photographs and measurements of $L_{\mathrm{sky}}(\lambda,\theta_i,\phi_i)$ made at discrete angles with a hand-held radiometer. Additional research will be required to develop and test viable protocols for $\overline{\mu}_d(0^+,\lambda)$ estimation from these types of measurements.

6.5 Phytoplankton Pigments

6.5.1 HPLC Pigment Concentration

The JGOFS protocols and standards for HPLC pigment concentration analysis (JGOFS 1991) will be the primary method of determining pigment concentrations for all SeaWiFS algorithm development and validation activities.

6.5.2 Fluorometric Determination

Protocols for fluorometric determination of the concentrations of chlorophyll and phaeopigments were developed initially by Yentsch and Menzel (1963) and Holm-Hansen

et al. (1965) and are described in detail by Strickland and Parsons (1972). These measurements have been shown to contain errors, as compared to HPLC determinations, e.g., Trees et al. (1985), the CZCS photoplankton pigment concentration algorithms were based on them entirely. The SeaWiFS protocols for this analysis will be those given in Strickland and Parsons (1972) as updated by Smith, Baker, and Dustan (1981).

6.5.3 *In situ* Chlorophyll *a* Fluorescence

In situ fluorometers produce nearly continuous profiles of artificially stimulated chlorophyll *a* fluorescence. Level-1 fluorometer data (in volts) should be converted to level-2 simply by subtracting an offset, determined by shading the instrument on deck. For qualitative guidance in K-profile analysis, level-2 (or even level-1) fluorometer profiles are adequate.

To produce vertical profiles of pigment concentration, HPLC derived pigment concentrations from water samples at discrete depths should be interpolated with the aid of *in situ* fluorescence profiles, for SeaWiFS bio-optical algorithm development. These *fluorescence interpolated* profiles should then be used with $K_d(z,\lambda)$ profiles to compute optically weighted pigment concentration over the top attenuation length (Gordon and Clark 1980).

6.6 Beam Attenuation Coefficient

Raw beam transmissometer voltage profiles $\widetilde{V}(z)$ are first corrected for any range-dependent bias of the A/D data acquisition system (section 5.2.1). The corrected voltages $\widehat{V}(z)$ are then further adjusted for instrument drift (since factory calibration) with the equation

$$V(z) = \big(\widehat{V}(z) - V_{\text{dark}}\big)\frac{V'_{\text{air}}}{V_{\text{air}}}, \tag{47}$$

where V_{dark} is the instrument's current dark response with the light path blocked, and V'_{air} and V_{air} are, respectively, the current air calibration voltage (section 5.2.1) and the air calibration voltage recorded when the instrument was calibrated at the factory. $V(z)$ is then converted to transmittance $T(z,\lambda)$ over the transmissometer's path length, r, following the manufacturer's instructions for the particular instrument.

The beam attenuation coefficient $c(z,\lambda)$ is then computed as

$$c(z,\lambda) = -\frac{1}{r}\ln\big(T(z,\lambda)\big) \tag{48}$$

which has units of m^{-1}. The apparent values of $c(z,\lambda)$ should be further corrected, again following the manufacturer's instructions, for the finite acceptance angle of the instrument's receiver; this is usually a small, but significant, correction. Finally, the beam attenuation coefficient due to particles is computed as

$$c_p(z,\lambda) = c(z,\lambda) - c_w(\lambda), \tag{49}$$

where $c_w(\lambda)$ is the beam attenuation coefficient, i.e., the sum of absorption $a_w(\lambda)$ and scattering $b_w(\lambda)$, for pure water. Smith and Baker (1981) tabulate $a_w(\lambda)$ and $b_w(\lambda)$ over the spectral range of interest here.

6.7 Hydrographic Analyses of CTD Files

Each CTD profile should be pre-filtered to remove any depth reversal segments resulting from violent ship or hydrowire motions. This will remove many instances of *salinity spiking*, an artifact which occurs when water temperature changes at a rate faster than the conductivity probe can follow. The CTD data should be processed to profiles of potential temperature (° C), salinity (Practical Salinity Units [PSU] based on the Practical Salinity Scale of 1978, PSS78), and density ($\text{Kg}\,\text{m}^{-3}$) using the algorithms endorsed by the UNESCO/SCOR/ICES/IAPSO Joint Panel on Oceanographic Tables and Standards and SCOR Working Group 51 (Fofonoff and Millard 1983).

At this stage, each set of CTD profiles should be carefully examined to detect any significant static instability artifacts resulting from salinity spiking. After any such major artifacts are removed by editing, the data should be further smoothed by averaging temperature and conductivity data into 2 m depth bins, and the final profiles of salinity, density, and other derived parameters should be recomputed using the smoothed CTD profile.

At each station, depictive hydrographic analyses should include T-S profile characterizations of water masses and features in the density profile, which appear to be related to physical mixing and stability, should be compared with features in the corresponding bio-optical profiles. CTD profiles from horizontal transects, or two-dimensional grids, of stations should be used to compute two-dimensional sections, or three-dimensional gridded arrays, of geostrophic currents, temperature, salinity, and σ_t. These analysis products, together with corresponding 2-D or 3-D representation of bio-optical variability, can be used to estimate the relative importance of advection and isopycnal mixing in redistributing or modifying upper ocean optical properties during a cruise.

ACKNOWLEDGMENTS

The authors thank all of the workshop participants for their help in defining and preparing the protocols presented in this document:

Workshop Co-chairs

Mr. Roswell Austin San Diego State University
Dr. James Mueller San Diego State University

Workshop Participants

Mr. Robert Arnone NOARL
Mr. Rocky Booth Biospherical Instruments, Inc.
Dr. Kenneth Carder University of Miami
Mr. Dennis Clark NOAA/NESDIS
Dr. Donald Collins Jet Propulsion Laboratory
Dr. Wayne Esaias NASA/GSFC
Dr. Howard Gordon University of Miami
Dr. Bruce Guenther NASA/GSFC

Workshop Participants Cont'd

Mr. Ron Holyer	NOARL
Mr. Robert Kirk	NASA/GSFC
Dr. Charles McClain	NASA/GSFC
Mr. James McLean	NASA/GSFC
Dr. Gregory Mitchell	NASA Headquarters
Mr. Don Montgomery	Office Ocean. of the Navy
Dr. Raymond Smith	Univ. of Calif. at Santa Barbara
Dr. Charles Trees	San Diego State University
Dr. Kenneth Voss	University of Miami
Dr. Alan Weidemann	NOARL
Dr. Ronald Zaneveld	Oregon State University

Administrative Logistic Support

Ms. Meta Frost	Westover Consultants

Several participants proofread the document at various stages of completion and their assistance is particularly appreciated by the editors.

Glossary

A/D	Analog-to-Digital
ALSCAT	Alpha and Scattering Meter (Note: the symbol α corresponds to $c(\lambda)$, the beam attenuation coefficient, in present usage).
AOCI	Airborne Ocean Color Imager
AOL	Airborne Oceanographic Lidar
ARGOS	Name given to the data collection and location system on the NOAA Operational Satellites (not an acronym)
ASCII	American Standard Code Information Interchange
AVHRR	Advanced Very High Resolution Radiometer
AVIRIS	Advanced Visible and Infrared Imaging Spectrometer
CDOM	Colored Dissolved Organic Material
CPU	Central Processing Unit
CTD	Conductivity, Temperature, and Depth
CW	Continuous Wave
CZCS	Coastal Zone Color Scanner
DOC	Dissolved Organic Carbon
DOM	Dissolved Organic Matter
ER-2	Earth Resources-2
FOV	Field-of-View
FWHM	Full-Width Half-Maximum
GAC	Global Area Coverage
GASM	General Angle Scattering Meter
GFF	Glass Fiber Filter by Whatman
GMT	Greenwich Mean Time
GOES	Geosynchronous Orbital Environmental Satellite
GPS	Global Positioning System
GSFC	Goddard Space Flight Center
HPLC	High Performance Liquid Chromatography
IAPSO	International Association for the Physical Sciences of the Ocean
ICES	International Council on Exploration of the Seas
I/O	Input/Output
IOP	Inherent Optical Properties
IR	Infrared
JGOFS	Joint Global Ocean Flux Study
MARS	Multispectral Airborne Radiometer System
MERIS	Medium Resolution Imaging Spectrometer
MODIS	Moderate Resolution Imaging Spectrometer
NAS	National Academy of Science
NASA	National Aeronautics and Space Administration
NASIC	NASA Aircraft/Satellite Instrument Calibration
NESDIS	National Environmental Satellite Data Information Service
NIST	National Institute of Standards and Technology
NOAA	National Oceanic and Atmospheric Administration
NOARL	Naval Oceanographic and Atmospheric Research Laboratory
OCTS	Ocean Color and Temperature Sensor (Japanese)
ODAS	Ocean Data Acquisition System
OFFI	Optical Free-Fall Instrument
OSFI	Optical Surface Floating Instrument
PAR	Photosynthetically Available Radiation
POC	Particulate Organic Carbon
POLDER	Polarization Detecting Environmental Radiometer (French)
PON	Particulate Organic Nitrogen
PSU	Practical Salinity Units
QED	Quantum Efficient Device
ROSIS	Remote Ocean Sensing Imaging Spectrometer, also known as the Reflecting Optics System Imaging Spectrometer
ROV	Remotely Operated Vehicle
SCOR	Scientific Committee on Oceanographic Research
SeaWiFS	Sea-viewing Wide Field-of-view Sensor
SNR	Signal-to-Noise Ratio
SPM	Suspended Particulate Material
SPO	SeaWiFS Project Office
SPSWG	SeaWiFS Prelaunch Science Working Group
SST	Sea Surface Temperature
T-S	Temperature-Salinity
TIROS	Television Infrared Observation Satellite
TSM	Total Suspended Material
UNESCO	United Nations Educational, Scientific, and Cultural Organizations
UVB	Ultraviolet-B
VISLAB	Visibility Laboratory (Scripps Institute of Oceanography)
WMO	World Meteorological Organization
WOCE	World Ocean Circulation Experiment

Symbols

$a(z,\lambda)$	Spectral absorption coefficient
a_p	Particulate absorption coefficient spectra
$b(z,\lambda)$	Total scattering coefficient
$b(\theta,z,\lambda_0)$	Volume scattering coefficient
$b_b(z,\lambda)$	Spectral backscattering coefficient
$b_r(\lambda)$	Total Raman scattering coefficient
$c(z,\lambda)$	Spectral beam attenuation coefficient
$c(z,660)$	Red beam attenuation (at 660 nm)
C_p	Beam attenuation coefficient due to particles
$E_a(\lambda)$	Irradiance in air
$E_{\rm cal}$	Calibration source irradiance
$E_d(0^+,\lambda)$	On-deck spectral irradiance
$E_d(0^-,\lambda)$	Incident spectral irradiance
$E_d(z,\lambda)$	Downwelled spectral irradiance
$E_s(\lambda)$	Surface irradiance
$E_{\rm sky}(\lambda)$	Spectral sky irradiance distribution
$E_{\rm sun}(\lambda)$	Spectral sun irradiance distribution
$E_u(z,\lambda)$	Upwelled spectral irradiance
$E_w(z,\lambda)$	Irradiance in water

$F_i(\lambda)$ Emersion correction factor
$F_v(\lambda)$ Field-of-view coefficient
$G(z,\lambda)$ Solid angle dependence with water depth
$K(z,\lambda)$ Diffuse attenuation coefficient
$K_E(\lambda)$ Attenuation coefficient downwelled irradiance
$K_L(z,\lambda)$ Attenuation coefficient upwelled radiance
$L(z,\theta,\phi)$ Submerged upwelled radiance distribution
L_{cal} Calibration source radiance
$L_{\text{sky}}(\lambda)$ Spectral sky radiance distribution
L_t Radiance at top of atmosphere
$L_u(z,\lambda)$ Upwelled spectral radiance
$L_W(\lambda)$ Water-leaving radiance
$L_{WN}(\lambda)$ Normalized water-leaving radiance
$n_g(\lambda)$ Index of refraction of Plexiglass
$n_w(\lambda)$ Index of refraction of water
$OD_{\text{filt}}(\lambda)$ Optical density spectra of filtered particles
$OD_{\text{susp}}(\lambda)$ Optical density spectra of suspended particles
$P(\lambda)$ Polarization sensitivity
$Q(\lambda)$ $L_u(0^-,\lambda)$ to $E_u(0^-,\lambda)$ relation factor (theoretically equal to π)
$R_L(z,\lambda)$ Spectral reflectance
$T_g(\lambda)$ Transmittance correction through glass
$T_s(\lambda)$ Transmittance through the surface
$T_w(\lambda)$ Transmittance through a water path
$\beta(z,\lambda,\theta)$ Spectral volume scattering function
δ Cosine response asymmetry
ϵ Cosine collector response error
λ_0 Center wavelength
λ_n Any nominal wavelength
$\overline{\mu}_d(0^+,\lambda)$ Spectral mean cosine for downwelling radiance at the sea surface
$\xi(\lambda)$ Minimum ship-shadow avoidance distance
$\rho(\lambda)$ Bidirectional reflectance
$\tau(z,\lambda)$ Spectral optical depth
$\tau_s(\lambda)$ Spectral solar atmospheric transmission

References

Austin, R.W., 1976: Air-water radiance calibration factor, *Tech. Memo. ML–76–004t,* Scripps Inst. of Oceanogr., 8 pp.

——, and G. Halikas, 1976: The index of refraction of seawater, *SIO Ref. 76–1,* Scripps Inst. of Oceanogr., La Jolla, CA, 64 pp.

——, and T.J. Petzold, 1981: The determination of diffuse attenuation coefficient of sea water using the Coastal Zone Color Scanner, *Oceanography from Space,* J.F.R. Gower, Ed., Plenum Press, 239–256.

Baker, K.S. and R.C. Smith, 1990: Irradiance transmittance through the air/water interface, *Ocean Optics X,* R.W. Spinrad, Ed., SPIE, **1302,** 556–565.

Booth, C.R.B. and R.C. Smith, 1988: Moorable spectroradiometer in the Biowatt Experiment, *Ocean Optics IX,* SPIE **925,** 176–188.

Boyd, R.A., 1951: The development of prismatic glass block and the daylight laboratory, *Eng. Res. Bull. No. 32,* Eng. Res. Inst., Univ. of Mich., 88 pp.

Bricaud, A., A. Morel, and L. Prieur, 1981: Absorption by dissolved organic matter of the sea (yellow substance) in the UV and visible domains, *Limnol. and Oceanogr.,* **26,** 43–53.

Brown, O.B., and R.H. Evans, 1985: Calibration of Advanced Very High Resolution Radiometer infrared observations, *J. Geophys. Res.,* **90,** 11667–11677.

Carder, K.L., G.R. Harvey, R.G. Steward, and P.B. Ortner, 1989: Marine humic and fulvic acids: their effects on remote sensing of ocean chlorophyll, *Limnol. and Oceanogr.,* **34,** 68–81.

Clark, D.K., 1981: Phytoplankton algorithms for the Nimbus-7 CZCS, *Oceanography from Space,* J.F.R. Gower, Ed., Plenum Press, 227–238.

Cox, C. and W. Munk, 1954: Measurements of the roughness of the sea surface from photographs of the sun's glitter: *J. Optical Soc. of Am.,* **44,** 838–850.

Dickey, T., J. Marra, T. Granata, C. Langdon, M. Hamilton, J. Wiggert, D. Siegel, and A. Bratkovich, 1991: Concurrent high-resolution bio-optical and physical time series observations in the Sargasso Sea during the spring of 1987, *J. Geophys. Res.,* **96,** 8643–8663.

Esaias, W., G. Feldman, C.R. McClain, and J. Elrod, 1986: Satellite observations of oceanic primary productivity, *Eos, Trans., Amer. Geophys. Union,* **67,** 835–837.

Feldman, G., N. Kuring, C. Ng, W. Esaias, C. McClain, J. Elrod, N. Maynard, D. Endres, R. Evans, J. Brown, S. Walsh, M. Carle, and G. Podesta, 1989: Ocean Color: Availability of the global data set, *Eos, Trans., Amer. Geophys. Union,* **70,** 634.

Fofonoff, N.P. and R.C. Millard, Jr., 1983: Algorithms for computation of fundamental properties of seawater, *UNESCO Tech. Papers in Marine Science,* **44,** UNESCO, 53 pp.

Frohlich, C., 1979: WMO/PMOD Sunphotometer: Instructions for manufacture, *World Meteorol. Organ.,* 3 pp. (plus tables and drawings).

Gieskes, W.W.C. and G.W. Kraay, 1986: Analysis of phytoplankton pigments by HPLC before, during, and after mass occurrence of the microflagellate corymbellus during the spring bloom in the open north North Sea in 1983, *Mar. Biol.,* **92,** 45–52.

Gordon, H.R., 1981: Reduction of error introduced in the processing of coastal zone color scanner-type imagery resulting from sensor calibration and solar irradiance uncertainty, *Appl. Opt.,* **20,** 207–210.

——, 1985: Ship perturbations of irradiance measurements at sea, 1: Monte Carlo simulations, *Appl. Opt.,* **24,** 4,172–4,182.

——, 1987: Calibration requirements and methodology for remote sensors viewing the ocean in the visible, *Remote Sens. Environ.,* **22,** 103–126.

——, 1988: Ocean color remote sensing systems: radiometric requirements, *Recent Advances in Sensors, Radiometry, and Data Processing for Remote Sensing,* P.N. Slater, Ed., SPIE, **924,** 151–167.

——, 1989: Can the Lambert-Beer law be applied to the diffuse attenuation coefficient of ocean water? *Limonol. and Oceanogr.,* **34,** 1,389–1,409.

——, 1991: Absorption and scattering estimates from irradiance measurements: Monte Carlo simulations, *Limnol. and Oceanogr.,* **36,** 769–777.

——, J.W. Brown, O.B. Brown, R.H. Evans, and D.K. Clark, 1983: Nimbus-7 CZCS: Reduction of its radiometric sensitivity with time, *Appl. Opt.,* **24,** 3,929–3,931.

——, and D.K. Clark, 1980: Remote sensing optical properties of a stratified ocean: an improved interpretation, *Applied Optics,* **19,** 3,428–3,430.

——, and ——, 1981: Clear water radiances for atmospheric correction of Coastal Zone Color Scanner imagery, *Appl. Opt.*, **20,** 4,175–4,180.

——, and K. Ding, 1992: Self shading of in-water optical instruments, *Limnol. and Oceanogr.*, **37,** 491–500 (in press).

Groom, S.B., and P.M. Holligan, 1987: Remote sensing of coccolithophorid blooms, *Adv. Space Res.*, **7,** 73–78.

Helliwell, W.S., G.N. Sullivan, B. Macdonald, and K.J. Voss, 1990: Ship shadowing: model and data comparison, *Ocean Optics X,* R.W. Spinrad, Ed., SPIE, **1302,** 55–71.

Holm-Hansen, O., C.J. Lorenzen, R.W. Holmes, and J.D.H. Strickland, 1965: Fluorometric determination of chlorophyll, *J. Cons. Int. Explor. Mer.*, **30,** 3–15.

Hovis, W.A., J.S. Knoll, and G.R. Smith, 1985: Aircraft measurements for calibration of an orbiting spacecraft sensor, *Appl. Opt.*, **24,** 407–410.

Joint Global Ocean Flux Study, 1991: JGOFS Core Measurements Protocols, *JGOFS Report No. 6,* Scientific Committee on Oceanic Research, 40 pp.

Kohler, R., R. Pello, and J. Bonhoure, 1990: Temperature dependent nonlinearity effects of a QED-200 detector in the visible, *Applied Opt.*, **29,** 4,212–4,215.

Mantoura, R.F.C., and C.A. Llewellyn, 1983: The rapid determination of algal chlorophyll and carotenoid pigments and their breakdown products in natural waters by reverse-phase high-performance liquid chromatography, *Analytical Chim. Acta,* **151,** 297–314.

Marshall, B.R., and R.C. Smith, 1990: Raman scattering and in-water optical properties, *Appl. Opt.*, **29,** 71–84.

McLean, J.T., and B.W. Guenther, 1989: Radiance calibration of spherical integrators, *Optical Radiation Measurements II,* SPIE, **1109,** 114–121.

Michaelsen, J., X. Zhang, and R.C. Smith, 1988: Variability of pigment biomass in the California Current system as determined by satellite imagery, *J. Geophys. Res.*, **93,** 10,883–10,896.

Mitchell, B.G., 1990: Algorithms for determining the absorption coefficient for aquatic particulates using the quantitative filter technique, *Ocean Optics X,* R.W. Spinrad, Ed., SPIE, **1302,** 137–148.

——, and D.A. Kiefer, 1984: Determination of absorption and fluorescence excitation spectra for phytoplankton, *Marine Phytoplankton and Productivity,* O. Holm-Hansen, L. Bolis, and R. Gilles, Eds., Springer-Verlag, 157–169.

——, and ——, 1988: Chlorophyll-*a* specific absorption and fluorescence excitation spectra for light-limited phytoplankton, *Deep-Sea Res.*, **35,** 639–663.

Morel, A., and R.C. Smith, 1982: Terminology and units in optical oceanography, *Mar. Geod.*, **5,** 335–349.

Mueller, J.L., 1985: Nimbus-7 CZCS: confirmation of its radiometric sensitivity decay rate through 1982, *Appl. Opt.*, **24,** 1,043–1,047.

——, 1991: Integral method for irradiance profile analysis, San Diego State Univ., *CHORS Tech. Memo. 007-91,* 10 pp.

Muller-Karger, F.E., C.R. McClain, R.N. Sambrotto, and G.C. Ray, 1990: A comparison of ship and Coastal Zone Color Scanner mapped distribution of phytoplankton in the southeastern Bering Sea, *J. of Geophys. Res.*, **95,** 11,483–11,499.

National Academy of Sciences, 1984: *Global Ocean Flux Study, Proceedings of a Workshop,* National Acad. Press, Wash., D.C., 360 pp.

Palmer, J.M., 1988: Use of self-calibrated detectors in radiometric instruments, *Recent advances in sensors, radiometry, and data processing for remote sensing,* P.N. Slater, Ed., SPIE, **924,** 224–231.

Petzold, T.J., 1988: A method for obtaining analytical curve fits to underwater radiometric measurements, *Tech. Memo. Oc Op/TJP-88-06t,* Scripps Inst. of Oceanogr., 20 pp.

——, and R.W. Austin, 1988: Characterization of MER-1032, *Tech. Memo. EV-001-88t,* Scripps Inst. of Oceanogr., 56 pp.

Pinder, G.F., and W.G. Gray, 1977: *Finite Element Simulation in Surface and Subsurface Hydrology,* Academic Press, 295 pp.

Shaw, G.E., 1976: Error analysis of multiwavelength sun photometry, *Pure and Appl. Geophys.*, **114,** 1–14.

Siegel, D.A., C.R. Booth, and T.D. Dickey, 1986: Effects of Sensor Characteristics on the Inferred Vertical Structure of the Diffuse Attenuation Coefficients Spectrum, *Ocean Optics VIII,* M. Blizard, Ed., SPIE, **637,** 115–124.

Smith, R.C., and K.S. Baker, 1981: Optical properties of the clearest natural waters (200–800 nm), *Appl. Opt.*, **20,** 177–184.

——, and ——, 1984: Analysis of ocean optical data, *Ocean Optics VII,* M. Blizard, Ed., SPIE, **478,** 119–126.

——, and ——, 1986: Analysis of ocean optical data, *Ocean Optics VIII,* P.N. Slater, Ed., SPIE, **637,** 95–107.

——, ——, and P. Dustan, 1981: Fluorometric techniques for the measurement of oceanic chlorophyll in the support of remote sensing, *SIO Ref. 81-17,* Scripps Inst. of Oceanogr., 14 pp.

——, R. Bridigare, B. Prezelin, K. Baker, and J. Brooks, 1987: Optical Characterization of Primary Productivity Across a Coastal Front, *Marine Biology,* **96,** 575–591.

——, K.J. Waters, and K.S. Baker, 1991: Optical variability and pigment biomass in the Sargasso Sea as determined using deep-sea optical mooring data, *J. Geophys. Res.*, **96,** 8665–8686.

Stramski, D., 1990: Artifacts in measuring absorption spectra of phytoplankton collected on a filter, *Limnol. and Oceanogr.*, **35,** 1,804–1,809.

Strickland, J.D.H., and T.R. Parsons, 1972: *A Practical Handbook of Sea Water Analysis,* Fish. Res. Board. Canada, 310 pp.

Trees, C.C., M.C. Kennicutt II, and J.M. Brooks, 1985: Errors associated with the standard fluorometric determination of chlorophylls and phaeopigments, *Marine Chemistry,* **17,** 1–12.

Tyler, J.E., and R.C. Smith, 1979: *Measurements of Spectral Irradiance Underwater,* Gordon and Breach, 103 pp.

Viollier, M., 1982: Radiance calibration of the Coastal Zone Color Scanner: a proposed adjustment, *Appl. Opt.*, **21,** 1,142–1,145.

Voss, K.J., J.W. Nolten, and G.D. Edwards, 1986: Ship shadow effects on apparent optical properties, *Ocean Optics VIII,* M. Blizard, Ed., SPIE, **637,** 186–190.

——, and G. Zibordi, 1989: Radiometric and geometric calibration of a spectral electro-optic "fisheye" camera radiance distribution system, *J. of Atmos. and Oceanic Tech.*, **6,** 652–662.

Walker, J.H., C.L. Cromer, and J.T. McLean, 1991: Technique for improving the calibration of large-area sphere sources, *Ocean Optics,* B.W. Guenther, Ed., SPIE, **1493,** 224–230.

——, R.D. Saunders, J.K. Jackson, and D.A. McSparron, 1987: Measurement Services: Spectral Irradiance Calibrations, *NIST Special Publications 250-20,* 116 pp.

Walsh, J.J., G.T. Rowe, R.L. Iverson, and C.P. McRoy, 1991: Biological export of shelf carbon is a sink of the global CO_2 cycle, *Nature,* **291,** 196–201.

Waters, K.J., R.C. Smith, and M.R. Lewis, 1990: Avoiding ship induced light field perturbation in the determination of oceanic optical properties, *Oceanography,* **3,** 18–21.

Weinreb, M.P., G. Hamilton, S. Brown, and R.J. Koczor, 1990: Nonlinear corrections in calibration of Advanced Very High Resolution Radiometer infrared channels, *J. Geophys. Res.,* **95,** 7,381–7,388.

Yentsch, C.S. and D.W. Menzel, 1963: A method for the determination of phytoplankton, chlorophyll, and phaeophytin by fluorescence, *Deep-Sea Res.,* **10,** 221–231.

REPORT DOCUMENTATION PAGE

Form Approved
OMB No. 0704-0188

1. AGENCY USE ONLY *(Leave blank)*	2. REPORT DATE	3. REPORT TYPE AND DATES COVERED
	July 1992	Technical Memorandum

4. TITLE AND SUBTITLE
SeaWiFS Technical Report Series
Volume 5, Ocean Optics Protocols for SeaWiFS Validation

5. FUNDING NUMBERS
Code 970.2

6. AUTHOR(S)
James L. Mueller and Roswell W. Austin

Series Editors: Stanford B. Hooker and Elaine R. Firestone

7. PERFORMING ORGANIZATION NAME(S) AND ADDRESS(ES)
Laboratory for Hydrospheric Processes
NASA Goddard Space Flight Center
Greenbelt, Maryland 20771

8. PERFORMING ORGANIZATION REPORT NUMBER
92B00097

9. SPONSORING/MONITORING AGENCY NAME(S) AND ADDRESS(ES)
National Aeronautics and Space Administration
Washington, D.C. 20546-0001

10. SPONSORING/MONITORING AGENCY REPORT NUMBER
TM 104566, Vol. 5

11. SUPPLEMENTARY NOTES
James L. Mueller and Roswell W. Austin: San Diego State University, San Diego, California.
Stanford B. Hooker: NASA-GSFC, Greenbelt, Maryland; Elaine R. Firestone: General Sciences Corporation, Laurel, Maryland

12a. DISTRIBUTION/AVAILABILITY STATEMENT
Unclassified - Unlimited
Subject Category 48

12b. DISTRIBUTION CODE

13. ABSTRACT *(Maximum 200 words)*

This report presents protocols for measuring optical properties, and other environmental variables, to validate the radiometric performance of the Sea-viewing Wide Field-of-view Sensor (SeaWiFS), and to develop and validate bio-optical algorithms for use with SeaWiFS data. The protocols are intended to establish foundations for a measurement strategy to verify the challenging SeaWiFS accuracy goals of 5 percent in water-leaving radiances and 35 percent in chlorophyll α concentration. The protocols first specify the variables which must be measured, and briefly review rationale. Subsequent chapters cover detailed protocols for instrument performance specifications, characterizing and calibration instruments, methods of making measurements in the field, and methods of data analysis. These protocols were developed at a workshop sponsored by the SeaWiFS Project Office (SPO) and held at the Naval Postgraduate School in Monterey, California (9-12 April, 1991). This report is the proceedings of that workshop, as interpreted and expanded by the authors and reviewed by workshop participants and other members of the bio-optical research community. The protocols are a first prescription to approach unprecedented measurement accuracies implied by the SeaWiFS goals, and research and development are needed to improve the state-of-the-art in specific areas. The protocols should be periodically revised to reflect technical advances during the SeaWiFS Project cycle.

14. SUBJECT TERMS
Oceanography, Ocean Optics, Coastal Zone Color Scanner (CZCS), Sensor, Bio-optics, Protocols, Calibration/Validation

15. NUMBER OF PAGES
46

16. PRICE CODE

17. SECURITY CLASSIFICATION OF REPORT	18. SECURITY CLASSIFICATION OF THIS PAGE	19. SECURITY CLASSIFICATION OF ABSTRACT	20. LIMITATION OF ABSTRACT
Unclassified	Unclassified	Unclassified	Unlimited